**Elucidation of an intricate surveillance network
for cellular U snRNP homeostasis**

**Identifizierung eines komplexen Überwachungssystems für die
Aufrechterhaltung der zellulären U snRNP-Homöostase**

Doctoral thesis for a doctoral degree
at the Graduate School of Life Sciences,
Julius-Maximilians-Universität Würzburg,
Section: Biomedicine

**submitted by**

Rajyalakshmi Meduri

**from**

Ongole, India

Würzburg, 2016

**Submitted on:**


**Members of the *Thesis committee:***

**Chairperson:**



**Primary Supervisor:**
Prof. Dr. Utz Fischer
Department of Biochemistry
Biocenter, University of Würzburg
Am Hubland
97074 Würzburg
mail: utz.fischer@biozentrum.uni-wuerzburg.de

**Supervisor (Second):**
Prof. Dr. Alexander Buchberger
Department of Biochemistry
Biocenter, University of Würzburg
Am Hubland
97074 Würzburg
mail: alexander.buchberger@biozentrum.uni-wuerzburg.de

**Supervisor (Third):**
Prof. Dr. Markus Engstler
Department of Cell and Developmental Biology
Biocenter, University of Würzburg
Am Hubland
97074 Würzburg
mail: markus.engstler@biozentrum.uni-wuerzburg.de


**Date of Public Defence:**


**Date of Receipt of Certificates:**

**Identifizierung eines komplexen Überwachungssystems für die Aufrechterhaltung der zellulären U snRNP-Homöostase**

**Elucidation of an intricate surveillance network for cellular U snRNP homeostasis**

**Dissertation zur Erlangung des naturwissenschaftlichen Doktorgrades der Graduate School of Life Sciences, Julius-Maximilians-Universität Würzburg, Klasse Biomedizin**

**Vorgelegt von**

Rajyalakshmi Meduri

**aus**

Ongole, Indien

Würzburg, 2016

**Eingereicht am:**


**Mitglieder des Promotionskomitees:**

**Vorsitzende/r:**




**1. Betreuer:**
Prof. Dr. Utz Fishcer
Lehrstuhl für Biochemie
Theodor-Boveri-Institut für Lebenswissenschaften
Biozentrum der Universität Würzburg
Am Hubland
97074, Wuerzburg
mail: utz.fischer@biozentrum.uni-wuerzburg.de

**2. Betreuer:**
Prof. Dr. Alexander Buchberger
Lehrstuhl für Biochemie
Theodor-Boveri-Institut für Lebenswissenschaften
Biozentrum der Universität Würzburg
Am Hubland
97074, Wuerzburg
mail: alexander.buchberger@biozentrum.uni-wuerzburg.de

**3. Betreuer:**
Prof. Dr. Markus Engstler
Lehrstuhl für zell- und entwicklungsbiologie
Theodor-Boveri-Institut für Lebenswissenschaften
Biozentrum der Universität Würzburg
Am Hubland
97074, Wuerzburg
mail: markus.engstler@biozentrum.uni-wuerzburg.de


**Tag des Promotionskolloquiums:**

**Doktorurkunden ausgehändigt am:**

**Affidavit**

I hereby confirm that my thesis entitled 'Elucidation of an intricate surveillance network for cellular U snRNP homeostasis' is the result of my own work. I did not receive any help or support from commercial consultants. All sources and/or materials applied are listed and specified in the thesis.

Furthermore, I confirm that this thesis has not yet been submitted as part of another examination process neither in identical nor in similar form.

Place, Date:
Signature:

**Eidesstattliche Erklärung**

Hiermit erkläre ich an Eides statt, die Dissertation 'Identifizierung eines komplexen Überwachungssystems für die Aufrechterhaltung der zellulären U snRNP-Homöostase' eigenständig, d.h. insbesondere selbständig und ohne Hilfe eines kommerziellen Promotionsberaters, angefertigt und keine anderen als die von mir angegebenen Quellen und Hilfsmittel verwendet zu haben.

Ich erkläre außerdem, dass die Dissertation weder in gleicher noch in ähnlicher Form bereits in einem anderen Prüfungsverfahren vorgelegen hat.

Ort, Datum:
Unterschrift:

# *Acknowledgements*

# Summary

Spliceosomal U-rich small ribonucleoprotein particles (U snRNPs) are the major building blocks of the nuclear pre-mRNA splicing machinery. The core composition of U snRNPs includes the name giving U snRNA and a set of seven common (Sm) proteins termed Sm B/B', D1, D2, D3, E, F and G. These Sm proteins are arranged in the form of a toroidal ring on the single stranded conserved sequence element in the snRNA to form the Sm core domain. Even though U snRNPs assemble spontaneously *in vitro*, their assembly *in vivo* requires an amazingly large number of trans-acting assembly factors united in the Protein Arginine Methyltransferase 5 (PRMT5) and the Survival Motor Neuron (SMN) complexes. The cytoplasmic assembly pathway of U snRNPs can be divided into the early and the late phase. The early phase is dominated by the assembly chaperone, pICln, a subunit of the PRMT5 complex. This factor binds to Sm proteins and delivers them in a pICln-bound form to the PRMT5 complex. The early assembly phase then segregates into two lines. In one assembly line, a stable hexameric ring intermediate (6S complex) composed of pICln and the five Sm proteins D1, D2, F, E and G, is formed. This intermediate forms at the PRMT5 complex but dissociates from the latter upon completion of its assembly. Within the 6S complex, these Sm proteins are pre-organized into respective spatial positions adopted in the assembled U snRNP. The other assembly line forms a protein trimer composed of pICln, Sm B/B' and D3, which unlike the 6S complex is not released from the PRMT5 complex. As a consequence of their association with pICln, Sm proteins are kinetically trapped and fail to proceed in the assembly pathway. The late phase of the U snRNP formation is dominated by the SMN complex, which resolves this kinetic trap by dissociating pICln from the pre-organized Sm proteins and, subsequently catalyzes the loading of the Sm proteins on the U snRNA.

Even though basic principles of U snRNP assembly have been understood in some detail, the question arises as to why cells employ sophisticated assembly machinery for the assembly despite the reaction occurring spontaneously *in vitro*. A few studies have shown that the system works towards rendering specificity to the assembly reaction. However, Sm proteins in their free form expose hydrophobic surfaces to the cytosolic solvent. Hence, I reasoned that the assembly machinery of snRNPs might also prevent Sm protein aggregation.

In this thesis, I describe the work that leads to the discovery of a multi-layered regulatory network for Sm proteins involving post-transcriptional and post-translational surveillance mechanisms. Here, I show that the reduced level of SMN (a key assembly factor of the late phase) leads to the initial tailback of Sm proteins over pICln followed by the transcriptional down regulation of Sm protein encoding mRNAs. In contrast, depletion of pICln, a key factor of the early phase, results in the retention of Sm proteins on the ribosomes followed by their degradation via autophagy. Furthermore, I show that exceeding levels of Sm proteins over pICln caused by overexpression results in aggregation and mis-localization of Sm proteins. Thus, my findings uncover a complex regulatory network that helps to maintain the cellular U snRNP homeostasis by either preventing or clearing the unassembled Sm protein aggregates when they are not faithfully incorporated into the U snRNPs.

# Zusammenfassung

Eukaryontische mRNA Moleküle werden häufig als Vorläufer (prä-mRNAs) hergestellt, und durch diverse Prozessierungschritte zur reifen Form umgewandelt. Ein wichtiger Schritt ist hierbei die Spleißreaktion, welche das Herausschneiden von Introns und die Ligation der Exons zur reifen mRNA katalysiert. Dieser Prozess wird durch das sog. Spleißosom ermöglicht, einer makromolekularen Maschinerie, deren wichtigste Bausteine Uridin-reiche kleine Ribonukleoproteinpartikel (U snRNPs) sind.

Die spleißosomalen U snRNPs bestehen aus kleinen nicht-codierenden RNAs (U snRNA) sowie spezifischen und allgemeinen Proteinen. Während die spezifischen Proteine definierte Funktionen im Spleißprozess vermitteln, haben die allgemeinen Proteine, auch Sm Proteine genannt, primär strukturelle Funktion und vermitteln wichtige Schritte der U snRNP Biogenese. Jedes U snRNP Partikel enthält sieben Sm-Proteine (Sm B/B′, D1, D2, D3, E, F, G), die sich ringförmig an einen einzelsträngigen Bereich der U snRNPs anlagern und so eine toroidale Sm Corestruktur ausbilden. Obwohl die Zusammenlagerung dieses Sm Cores *in vitro* spontan erfolgt, werden hierfür *in vivo trans*-agierende Assemblierungsfaktoren benötigt. Diese agieren im Kontext zweier miteinander kooperierender Einheiten, die als PRMT5- und SMN-Komplex bezeichnet werden. Die initiale Phase wird vom Assemblierungs-Chaperon pICln dominiert, welches eine Untereinheit des PRMT5-Komplexes darstellt. Dieser Faktor stabilisiert die Sm-Proteine in höhergeordneten oligomeren Einheiten, die als Bausteine für die spätere Zusammenlagerungsreaktion dienen. pICln-assoziierte Sm-Proteine sind jedoch kinetisch gefangen und können daher nicht spontan auf die snRNA geladen werden. Diese Funktion übernimmt der SMN-Komplex, indem er die pICln-Sm Proteinkomplexe bindet und gleichzeitig pICln dissoziiert. Der SMN-Komplex fügt dann im letzten Schritt die Sm Proteine und die snRNA zum Sm Core zusammen.

Es stellte sich die prinzipielle Frage, weshalb Zellen für die U snRNP Biogenese eine komplexe Maschinerie ermöglichen, wenn dieselbe Reaktion *in vitro* auch spontan erfolgen kann. Eine Hypothese, die dieser Arbeit zu Grunde lag, war, dass das PRMT5/SMN System *in vivo* notwendig ist, um die unspezifische Aggregation der hydrophoben Sm Proteine zu vermeiden und deren spezifische Zusammenlagerung mit den snRNAs zu ermöglichen.

In der vorliegenden Arbeit werden Experimente geschildert, die diese Hypothese bestätigen und ein vielschichtiges regulatorisches post-transkriptionelles und post-translationales Netzwerk für die Sm-Proteine aufdeckten. Es wird gezeigt, dass eine verringerte Menge an SMN, dem Schlüsselfaktor der späten Zusammenlagerungs-Phase, zu einem anfänglichen Rückstau der Sm-Proteine an pICln zur Folge hat. Dieser Rückstau führt in einer späteren Phase zur Herunterregulierung der mRNAs, die für die Sm-Proteine codieren. Im Gegensatz dazu resultiert das Fehlen von pICln darin, dass die Sm-Proteine nicht in den Zusammenlagerungsweg eintreten können und statt dessen durch Autophagie degradiert werden. Wird die Degradation der Sm Proteine unterdrückt, komm es zu deren Delokalisation in der Zelle und Aggregation in unphysiologischen Strukturen. Die Daten offenbaren ein komplexes Regulationsnetzwerk, das die zelluläre U snRNP-Homöostase aufrechterhält und Zellen vor potentiell toxischer Proteinaggregation bewahrt.

# Table of contents

# List of figures

## List of tables

# 1 Introduction

## 1.1 Spliceosomes

The central dogma of biology involves the flow of genetic information from DNA to proteins via a semi-stable messenger RNA intermediate. In eukaryotes, mRNAs are synthesized as precursors (pre-mRNAs) that do not allow their immediate conversion into proteins. This is because, in their immature form they contain non-coding regions (introns) interspersed between coding regions (exons)(Sakharkar et al., 2004). These non-coding introns are removed from the pre-mRNAs by a process called 'splicing' that generates the open reading frame. With the evolution of complex cellular architecture, splicing strictly became a nuclear and co-transcriptional process. Although evolutionarily conserved, it is a highly dynamic process and is linked to proteome diversity. Splicing, in general, involves two trans-esterifications that are catalyzed in a sequential order by 'Spliceosomes' resulting in the generation of translatable mature mRNAs. Spliceosomes are nuclear macromolecular machines that are highly dynamic in their structure and composition enabling the catalytic removal of introns with high fidelity. One can distinguish two types of spliceosomes: the major and highly abundant spliceosomes (U2- type) responsible for processing the vast majority of introns and the less abundant minor spliceosomes (U12-type) that splice a rare class of introns (Patel and Steitz, 2003).

Major and minor spliceosomes consist of several U snRNPs (Uridine-rich small nuclear ribonucleoproteins) and many other non-snRNP splicing factors. The U snRNPs form the major building blocks of the spliceosomes. While the major spliceosomes consists of U1, U2, U4, U5, U6 snRNPs, the minor spliceosomes include U11, U12, U4atac, U5, U6atac snRNPs. The U snRNPs consist of the name giving U snRNA loaded with a set of seven common Sm proteins denoted as Sm B/B', D1, D2, D3, E, F and G. The Sm proteins have a Sm motif with two evolutionary conserved Sm domains (Seraphin, 1995). The Sm domain features characteristic anti-parallel β strands that are involved in mutual Sm protein - protein interactions (Hermann et al., 1995; Kambach et al., 1999b). As a result of this, Sm proteins form specific heteromeric entities in the cytoplasm that include Sm D1/D2, Sm B/D3 and Sm F/E/G. The U snRNAs are a class of non-coding RNAs with an average length between 100-180 nucleotides. They usually possess a unique 'Sm site' ($PuAU_{4-6}GPu$) to which the Sm

proteins bind in the form of a ring-like structure called, the Sm core (Figure 1.1) (Urlaub et al., 2001). Each of the U snRNPs further comprises of a set of specific proteins, for example, U1 snRNP-specific proteins: U1-70K, U1C, U1A (Figure 1.1). The snRNP specific proteins along with numerous other non-snRNP splicing factors contribute to the formation of functionally active spliceosomes. Unlike the Sm protein containing U snRNPs, U6 and U6atac snRNPs associate with like-Sm (LSm) proteins 2-8 instead of Sm proteins (Achsel et al., 1999). LSm proteins also assemble to form a ring-like structure that functions similar to Sm core but at the 3' end of the U6/U6atac snRNA. The Sm/LSm proteins mostly assist in overcoming the electrostatic repulsion between the RNA components during splicing (Kambach et al., 1999b) and in providing a structural basis for many proceeding steps of the pathway and recruitment of other U snRNP factors (Thore et al., 2003).
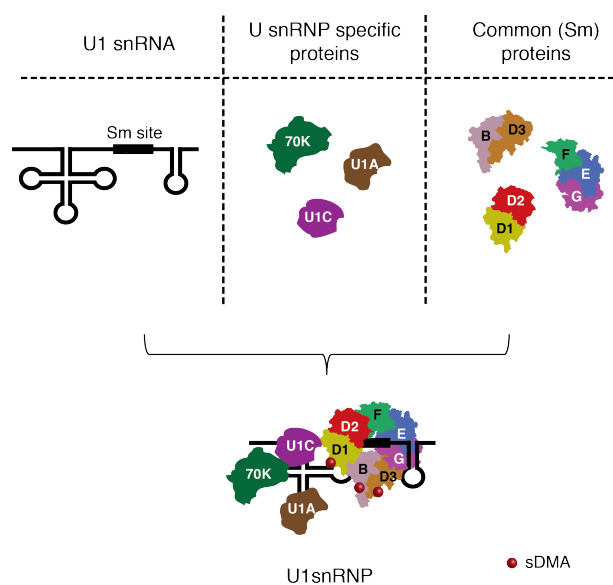


**Figure 1.1 Composition of U1 snRNP**

U1 snRNP consists of U1 snRNA, the Sm core and the U1 specific proteins- U1-70K, U1A, U1C. The Sm core is formed by the ring-like arrangement of a set of seven common Sm proteins namely, Sm B/B', D1, D2, D3, E, F and G on the Sm site of the U1 snRNA. Red spheres represent symmetrically dimethylated arginines (sDMA) on Sm proteins.

## 1.2    The mechanism of splicing

The basic architecture of the vast majority of the introns that are spliced by major spliceosomes consists of invariable GU and AG sequences within the less highly conserved

sequences at the 5′ and 3′ splice sites (ss), respectively. Also, 18-40 nucleotides upstream to the 3′ ss is the branch point site consisting of Adenine (A) followed by a polypyrimidine tract. Splicing is initiated by the recognition of these 5′ and 3′ splice sites (ss) of the introns by U1 and U2 snRNPs respectively, forming pre-spliceosomal complex. Following this, the U4/U6.U5 tri-snRNP is recruited resulting in structural rearrangements that catalyze first trans-esterification reaction after releasing U1 and U4 snRNPs. The first trans-esterification includes attack of the phosphodiester bond of 5′ ss by the hydroxyl group of adenosine at the branch point generating a free 5′ exon and intron-3′ exon lariat intermediate. The thus generated spliceosomal complex, comprised of U2, U6 and U5 snRNPs, undergoes further structural rearrangements leading to the second trans-esterification reaction. This reaction involves attack of phosphodiester bond at the 3′ ss by the 3′ hydroxyl of the 5′ exon. Following the second trans-esterification, the intron lariat is released with the spliced mRNA containing ligated exons (Figure 1.2). Once the splice cycle is completed, the released U snRNPs are recycled for the next round of splicing (Wahl et al., 2009).
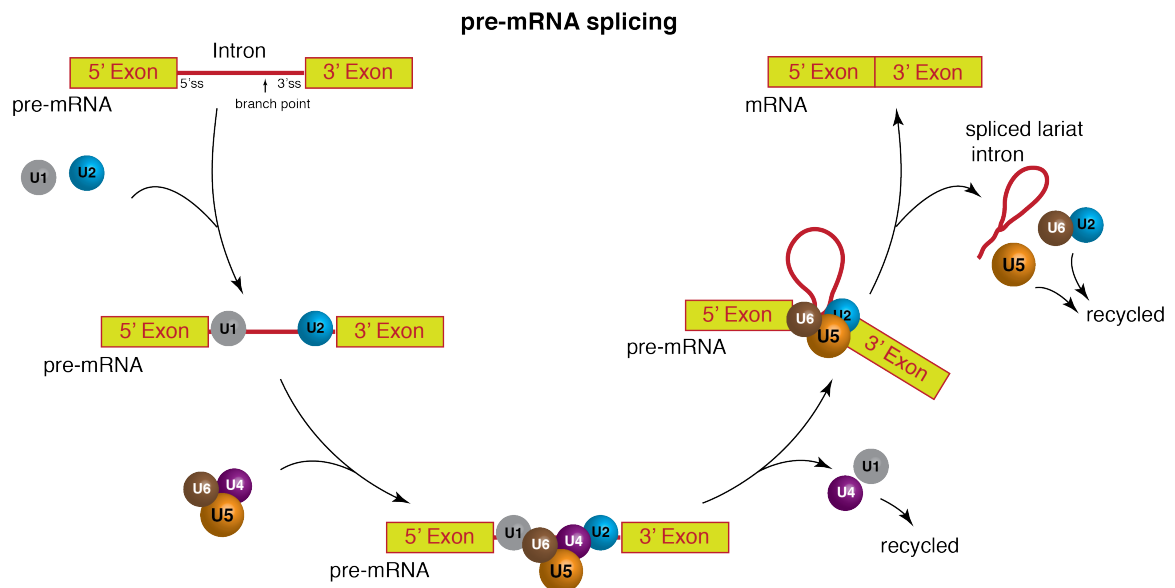


**Figure 1.2 Overview of pre-mRNA splicing by major spliceosomes**
Pre-mRNA splicing begins with the interaction of U1 and U2 snRNPs co-transcriptionally at the 5′ and 3′ splice sites (ss) of the introns, respectively. This is followed by the recruitment of U4/U6.U5 tri-snRNP resulting in first trans-esterification with the release U1 and U4 snRNPs. Then the second trans-esterification reaction occurs eventually releasing the intron lariat and the spliced exons, thus leading to the formation of mature mRNA. For the sake of simplicity, non-splicing factors and other intermediate complexes of the pathway are excluded from the schematics.

Of note, splicing of the rare introns by the minor spliceosomes also occurs in a similar

manner. They differ from major spliceosomes in the sequence that is recognized at the splice sites and the branch point site of the introns. During splicing, extensive remodeling of snRNA-snRNA, mRNA-snRNA and RNA-protein interactions occurs. These interactions are dependent on a group of spliceosome-associated DExD/H-type RNA helicases, ATP and GTP (Cordin et al., 2012; Small et al., 2006). Recent studies have also shown that divalent metal ions, like $Mg^{2+}$, participate in the catalytic removal of the introns (Bessonov et al., 2008; Fica et al., 2013; Valadkhan, 2010). The steady state level of the U snRNPs in eukaryotes is usually very high, at nearly 10 µM in a HeLa nucleus, in order to cope with the task of splicing all intron containing pre-mRNAs. Therefore, efficient production and maintenance of U snRNPs seems to be an indispensable task for eukaryotic cells.

## 1.3    Biogenesis of Sm-class of U snRNPs

Although the assembly of entire spliceosomes occurs in the nucleus on nascent pre-mRNAs, the biogenesis of U snRNPs spans different subcellular compartments. While the U snRNA is transcribed in the nucleus, the assembly of the Sm core of U snRNPs takes place in the cytoplasm. Further processing of U snRNPs and formation of higher order spliceosomal structures occurs again in the nucleus. Such a spatio-temporal organization of this pathway likely provides checkpoints for the quality control of the assembled U snRNPs.

The first step in the U snRNP assembly begins in the nucleus with the transcription of U snRNA by RNA polymerase II (for U1, U2, U4, U5, U11, U12 and U4atac snRNAs) or polymerase III (for U6 and U6atac snRNAs). The RNA polymerase II transcribed U snRNAs are subjected to co-transcriptional modifications. These include addition of 7-methyl guanosine ($m^7G$) cap at their 5' end and processing by integrator complex at 3' end (Baillat et al., 2005). The $m^7G$ cap facilitates the binding of the CBC (cap-binding complex) and ARS2 (arsenite resistance protein 2) to form the CBC-ARS2 or CBCA complex (Barth et al., 2003; Izaurralde et al., 1995). The CBCA complex then recruits PHAX (hyper-phosphorylated adaptor of RNA export protein) along with CRM1 (chromosome region maintenance 1) and RAN GTPase (RAs related nuclear protein in GTP-bound form) to the 5' cap resulting in the formation of the U snRNA export complex (Fornerod et al., 1997; Ohno et al., 2000). The addition of all these proteins on the 5' cap of the U snRNA probably occurs in sub-nuclear domains called Cajal bodies (CBs) (Frey and Matera, 2001; Lemm et al., 2006; Smith and Lawrence, 2000; Suzuki et al., 2010). The snRNA is then exported to the cytoplasm via the

nuclear pore complex (NPC). In contrast to the RNA polymerase II transcribed U snRNAs, the RNA polymerase III transcribed U6 snRNA attains a 5'-γ-methylphosphate cap and is retained in the nucleus where the rest of the assembly occurs (Singh and Reddy, 1989). As depicted in Figure 1.3, following the export into the cytoplasm, the proteins at the 5' cap of the U snRNA dissociate. This enables the onset of the cytoplasmic phase of the U snRNP assembly, which is assisted by a complex network of assembly factors and chaperones. The newly translated Sm proteins that are processed by the Protein Arginine Methyltransferase 5 (PRMT5) complex in the cytoplasm are assembled onto the Sm-site of the U snRNA to form the Sm core. The formation of the Sm core is catalyzed by the Survival Motor Neuron (SMN) complex.
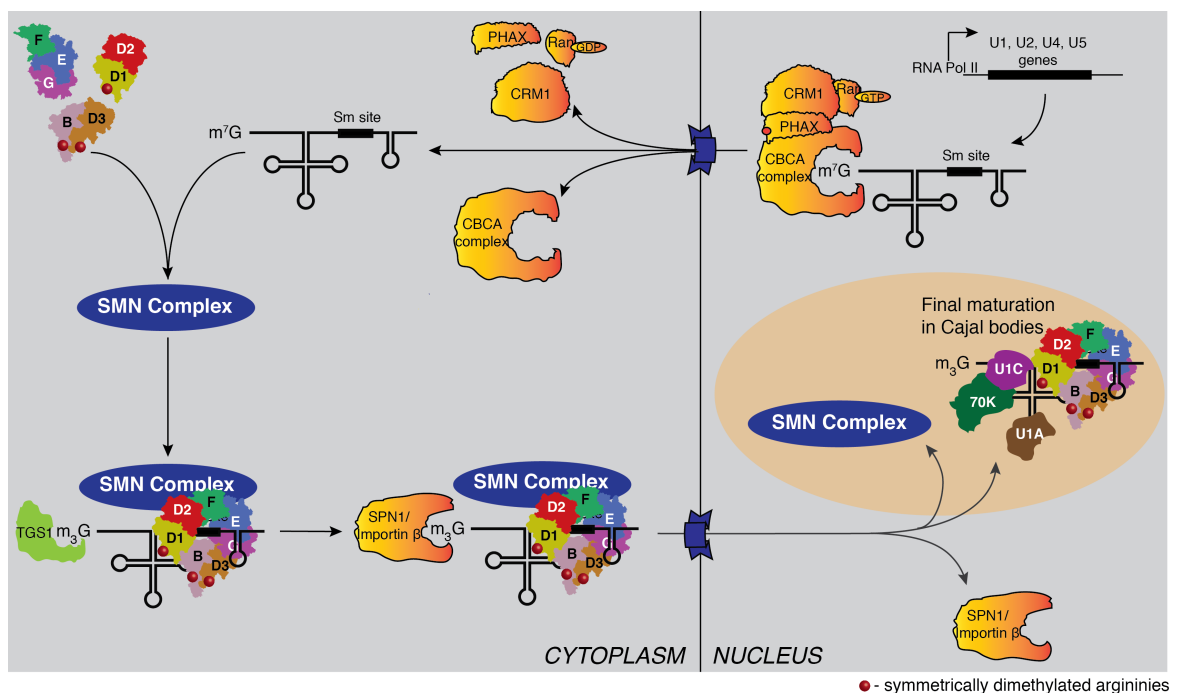


**Figure 1.3 Overview of the U snRNP biogenesis pathway**

The 5' end of the RNA polymerase II transcribed U snRNAs is co-transcriptionally modified to attain 7-methylguanosine (m⁷G) cap in the nucleus. The 5' cap recognized by the cap-binding complex in turn associates with ARS2, phosphorylated PHAX, CRM1 and Ran-GTP forming nuclear export complex. Once imported into the cytoplasm, the export complex is dissociated leading to the formation of the Sm core on the Sm site of the U snRNA with the help of the SMN complex. Following the hypermethylation of the 5' cap of the U snRNA by TGS1, SPN1/Importin β (nuclear import complex) recognizes the 5' cap. This eventually leads to the import of assembled snRNPs into the nucleus where they are targeted to Cajal bodies, resulting in the dissociation of the SMN complex from the snRNPs for final maturation.

Following the Sm core formation, hypermethylation of the m⁷G cap to 2, 2, 7-

trimethylguanosine cap (m$^{2,2,7}$G/m$_3$G/TMG cap) by trimethylguanosine synthase 1 (TGS1) occurs (Plessel et al., 1994)). The fully assembled Sm core and the TMG cap act as a bipartite signal for the nuclear import of the SMN complex loaded with the assembled U snRNPs where they are likely directed to the Cajal bodies (CBs). The nuclear import is mediated by binding of the import complex comprising of the import adaptor snurportin (SPN) and the import receptor importin β to the TMG cap of U snRNAs (Fischer et al., 1991; Fischer and Luhrmann, 1990; Hamm and Mattaj, 1990; Narayanan et al., 2002). U snRNPs undergo final maturation in Cajal bodies (CBs) (Neugebauer, 2002; Sleeman et al., 2001; Sleeman and Lamond, 1999). This includes the addition of U snRNP-specific proteins and introduction of site-specific pseudouridylation and 2'-O- methylation on the U snRNAs (Darzacq et al., 2002; Jady et al., 2003). The base modifications of the snRNAs are mediated by the small Cajal body RNAs (scaRNAs), which are a class of small non-coding nucleolar RNAs that significantly localize to Cajal bodies, for example U85 scaRNA (Kiss et al., 2004; Kiss et al., 2002)). The resulting mature snRNPs are finally targeted to nuclear speckles.

## 1.4     Cytoplasmic phase of U snRNP assembly

The assembly of Sm proteins onto the U snRNA occurs spontaneously *in vitro* (Raker et al., 1999; Raker et al., 1996). However, *in vivo*, the biogenesis of Sm-class of spliceosomal U snRNPs requires assistance from several trans-acting factors (Figure 1.4).
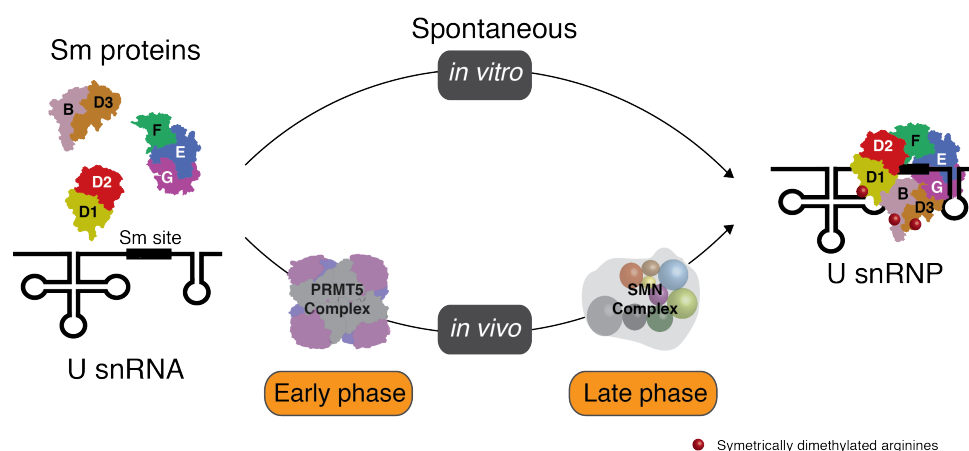


**Figure 1.4 U snRNP assembly *in vitro* and *in vivo***
The assembly of Sm proteins on the Sm site of the U snRNA occurs spontaneously *in vitro.* However, *in vivo,* while the PRMT5 complex assists the early phase, SMN complex catalyzes the late phase of the assembly pathway.

These factors are organized in two major complexes, namely, Protein arginine methyltransferase 5 (PRMT5) complex and Survival motor neuron (SMN) complex. The cytoplasmic assembly phase can be divided into two distinct temporal phases - the early and the late phase. While PRMT5 complex assists the early phase, SMN complex dominates the late phase (Buhler et al., 1999; Fischer et al., 1997; Meister and Fischer, 2002). However, whether the assembly of other LSm class of U snRNPs also requires the assistance of such factors is still elusive.

### 1.4.1 Early phase of cytoplasmic assembly

The early phase describes how the newly synthesized Sm proteins are safeguarded to prevent non-cognate protein-protein and protein-RNA interactions. The PRMT5 complex that orchestrates the early phase consists of the methyltransferase PRMT5, the assembly chaperone pICln (Meister et al., 2001b) and WD45 (WD repeat domain 45; also termed Methylosome protein 50 (MEP50)) (Friesen et al., 2002). It belongs to the type II class of methyltransferases that catalyzes the symmetric dimethylation of arginines (sDMA). The N-terminal pleckstrin homology (PH) domain of pICln consists of anti-parallel β strands (Grimm et al., 2013), which interacts with the Sm fold of the Sm proteins. This enables pICln to form distinct heteromers with Sm D1/D2 (via D1) and Sm B/D3 but not with Sm F/E/G (Chari et al., 2008; Friesen et al., 2001; Pu et al., 1999). The PRMT5 complex mainly performs two tasks, sequentially. Firstly, it catalyzes the methylation of the newly synthesized SmB/B', SmD1 and SmD3 on their C-terminal tails rich in arginine residues (Brahms et al., 2000; Friesen et al., 2001). Secondly, it forms a platform for stepwise formation of higher order Sm protein complexes. PRMT5 complex mainly mediates its functions in the assembly pathway via the assembly chaperone, pICln (Figure 1.5).

pICln by binding to Sm D1/D2 dimer, recruits it to PRMT5 complex for symmetrical dimethylation of SmD1. Following this, Sm F/E/G hetero-trimer is engaged by the PRMT5 complex, leading to the formation of a ring-shaped kinetically trapped 6S complex that is released while engaging the next set of Sm D1/D2 heteromer for methylation (Neuenkirchen et al., 2015). pICln simultaneously recruits Sm B/D3 for symmetrical dimethylation of both the proteins allowing the formation of the other assembly intermediate- pICln/Sm B/D3. Association of pICln with Sm proteins inhibits the formation of the Sm core thereby kinetically trapping and preventing the Sm proteins from binding to non-cognate RNAs

(Chari et al., 2008; Meister et al., 2001c; Pesiridis et al., 2009; Pu et al., 1999). The RNA-free Sm protein intermediates thus formed, are made available for binding to U snRNA by the SMN complex during the late assembly phase. In an isolated system, *in vitro*, non-sDMA Sm proteins can be assembled onto U snRNAs either spontaneously (Buhler et al., 1999; Raker et al., 1999; Raker et al., 1996) or in presence of the SMN complex. However, *in vivo* significance of Sm proteins' methylation in the biogenesis pathway and splicing requires further studies.
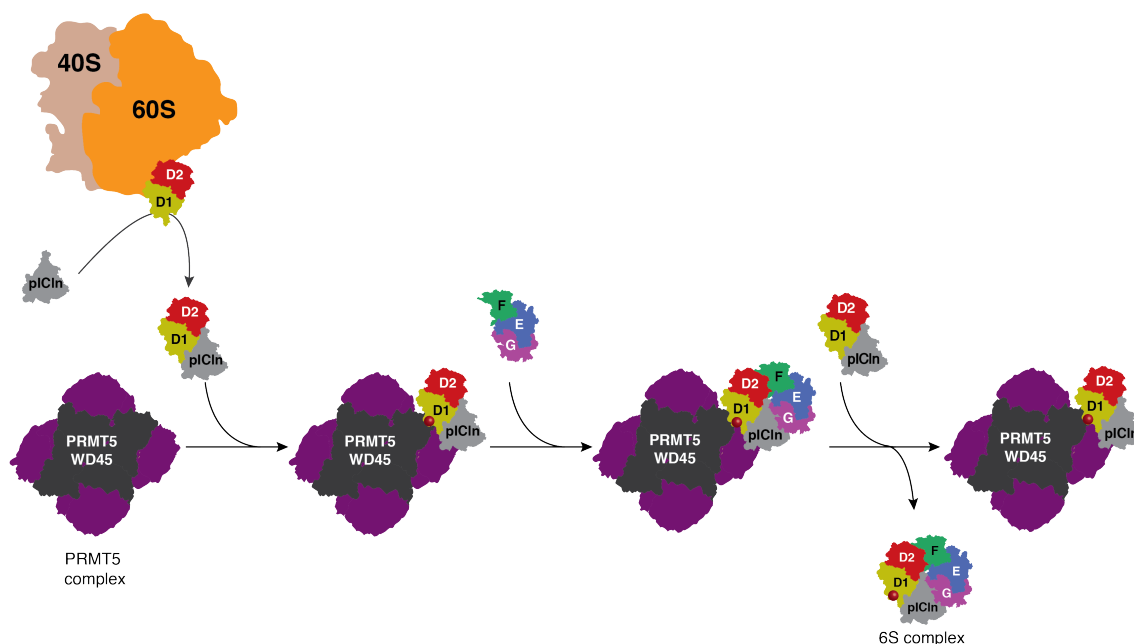


**Figure 1.5 Recruitment of newly synthesized Sm proteins by PRMT5 complex**
The newly synthesized Sm D1 and D2 are stalled at the ribosome exit tunnel until pICln, an assembly chaperone, recruits them onto the PRMT5 complex. The PRMT5 complex forms a platform by facilitating stepwise formation of a kinetically trapped, ring-shaped 6S complex composed of pICln and Sm D1, D2, E, F and G. The 6S complex is released in a feed-forward manner allowing the next round of recruitment of the newly translated Sm D1 and D2.

The biochemical dissection of the cytosolic assembly process and the identification of the assembly factors involved enabled detailed insight into the assisted RNP formation *in vivo*. However, how the newly translated Sm proteins are recruited into the assembly pathway has remained elusive for many years. Recent findings by Dr. Elham Paknia, in our group, suggested that the newly translated Sm proteins, particularly Sm D1/D2, are stalled at the ribosome exit tunnel awaiting the assembly chaperone, pICln, which then binds and channels these proteins into the U snRNP assembly via the PRMT5 complex (Paknia et al, submitted).

**1.4.2    Late phase of the cytoplasmic assembly**

In the late assembly phase, the kinetically trapped Sm proteins are made available for binding onto U snRNA by the SMN complex. This macromolecular machine consists of SMN, Gemins 2-8 and UNR interacting protein (UNRIP, also named STRAP) (Baccon et al., 2002; Carissimi et al., 2006; Charroux et al., 1999; Charroux et al., 2000; Gubitz et al., 2002; Liu and Dreyfuss, 1996; Liu et al., 1997; Pellizzoni et al., 2002) (see Figure 1.6 for the interaction map). SMN is a ubiquitous protein, which localizes to the cytoplasm and the nucleus. In the latter compartment, it is highly concentrated in the Cajal bodies (CBs). Based on the phylogenetic analysis, SMN and Gemin2 constitute a minimal entity that appeared first during evolution. Interestingly, this minimal entity is sufficient to perform the snRNP assembly *in vitro* (Battle et al., 2007; Chari et al., 2009; Fischer et al., 1997; Kroiss et al., 2008).
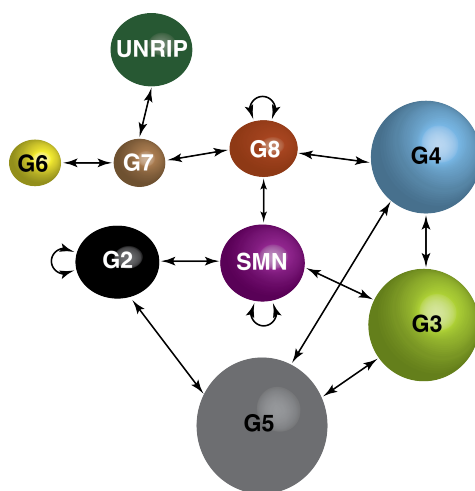


**Figure 1.6 The interaction map of the human SMN complex**
SMN complex consists of the name giving protein SMN, Gemins (G) 2 to 8 and UNRIP. SMN, Gemin2 and 8 have been demonstrated to self-oligomerize (Ogawa et al., 2009; Otter et al., 2007).

In the cytoplasm, SMN complex accepts the preassembled assembly intermediates, the 6S complex and the pICln/Sm B/D3 heteromer. The recognition of these intermediates was originally believed to be via the Tudor domain of SMN that can bind sDMA on Sm proteins (Buhler et al., 1999; Selenko et al., 2001; Tripsianes et al., 2011). However, structural studies implicated that the N-terminal arm of Gemin2 makes extensive contacts with Sm D1, D2, F, E, and G rather than the Tudor domain of SMN. This suggests the involvement of Gemin2 in docking the Sm proteins onto the SMN complex (Grimm et al., 2013; Zhang et al., 2011). After

the recruitment of the assembly intermediates, the next task for the SMN complex is to expel pICln leading to the formation of the Sm core. It is believed that the C-terminus of SMN and/or Gemin8 are likely to play a role in the expulsion of pICln from the kinetically trapped 6S complex (Chari et al., 2008). However, further structural insights are required to elucidate the plausible mechanistic role of the SMN complex in freeing the Sm proteins from pICln for U snRNA binding.

Apart from SMN and Gemin2, other proteins have also been described to play one or the other role in the pathway. Gemin5, through its N-terminal WD repeats, is reported to recruit the U snRNA by binding to the 3' end of the pre-snRNAs forming a scaffold that assists protein-RNA interactions (Battle et al., 2006a; Lau et al., 2009; Yong et al., 2004; Yong et al., 2010). Gemin5 has also been described as a cap-binding protein that can interact with the TMG cap of the assembled U snRNPs, to aid their nuclear import (Bradrick and Gromeier, 2009). Gemin3, having a putative ATPase/RNA helicase domain, has been hypothesized to assist the catalytic activity of the SMN complex (Charroux et al., 1999; Meister and Fischer, 2002). Gemins 6 and 7 seem to possess Sm-fold and can interact with the Sm proteins through the same interface as that between the Sm proteins, which might aid in the arranging of the Sm core on the U snRNA (Ma et al., 2005). UNRIP, by binding to Gemin7, influences the intracellular localization of SMN, as depletion of UNRIP leads to nuclear accumulation of SMN (Grimmler et al., 2005b). Several studies have shown the dependency of cellular snRNP assembly on ATP (Meister et al., 2001a; Meister and Fischer, 2002; Pellizzoni et al., 2002).

The cytosolic role of the SMN complex has now been understood in great detail. Much less, however, is known about the potential nuclear functions in particular in Cajal bodies (CBs). SMN complex along with the assembled U snRNPs is recruited to the CBs immediately after its import to the nucleus (Figure 1.7). Following the recruitment, U snRNPs are dissociated from the SMN complex for further modifications. The molecular mechanisms guiding these processes remain unclear till date. A few studies have hinted at the role of coilin in facilitating these processes, as it oligomerizes to provide a scaffold for the assembly of various proteins as well as non-coding RNAs (ncRNAs). It was shown that coilin interacts directly with SMN by competing with the binding site of SmB', thereby recruiting the SMN complex to the Cajal bodies, facilitating the subsequent release of the U snRNPs (Hebert et al., 2001). The C-terminus of coilin also interacts with Sm/Lsm proteins, which is different from its SMN binding site (Xu et al., 2005). In turn, SMN requires SIM-like motif in its Tudor domain for the

interaction with coilin and SmD1 (Tapia et al., 2014). Owing to differential methylation and phosphorylation states of coilin *in vivo,* it is possible that coilin dictates multiple mechanistic details of this pathway. A very recent study has shown that SMN might aid in protein-protein interactions necessary to recruit the U snRNP-specific proteins in the CBs (Bizarro et al., 2015).
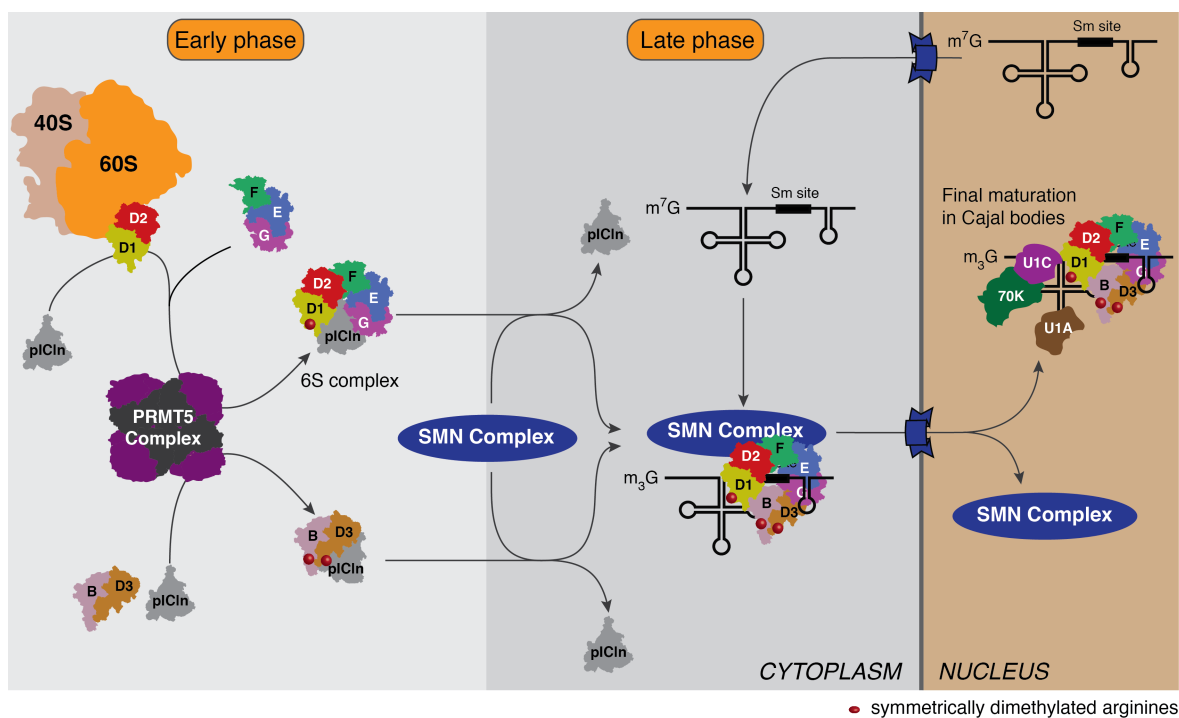


**Figure 1.7 Summary of the cytoplasmic assembly phase of U snRNP assembly**
In the cytoplasm during the early phase, pICln recruits the newly synthesized Sm D1/D2 (from the ribosome exit tunnel) and Sm B/D3 onto the PRMT5 complex for symmetric dimethylation of arginine residues (indicated by red sphere). The Sm F/E/G trimer binds to pICln/Sm D1/D2 leading to the formation of the kinetically trapped 6S complex. During the late phase of the assembly, SMN complex catalyzes the association of Sm proteins onto the U snRNA leading to the formation of the Sm core. Once imported into the nucleus, SMN complex is dissociated leading to the final maturation of the U snRNPs in Cajal bodies. For the sake of simplicity, the complexes involved in the import and export during the pathway individual subunits are not represented.

Apart from the hallmark role of SMN in U snRNP assembly, it was shown to be either directly or indirectly involved in cellular RNA metabolism, ranging from its direct role in splicing to aiding transcription termination (Table 7.1 and Table 7.2). However, the role of SMN in these cellular processes is less defined. It exists in hypophosphorylated state in the nucleus in comparison to the cytoplasm (Grimmler et al., 2005a). Not only SMN, but also other Gemins of the SMN complex have been shown to host several phosphorylation sites

(Table 7.2) (Husedzinovic et al., 2015). Although phosphorylation is dispensable for *in vitro* assembly, it is not known how the differential post-translational modification states of the SMN complex influences the snRNP assembly or any other functions that this complex might perform *in vivo*.

## 1.5    Spinal Muscular Atrophy

One of the major neurodegenerative disorders, Spinal Muscular Atrophy (SMA), is attributed to the loss and/or improper functioning of SMN. It is an autosomal recessive disorder that affects motor neurons resulting in atrophy of voluntary muscles in children and is known to be one of the most common causes of infant mortality. The *smn* gene exists in two copies, SMN1 (telomeric) and SMN2 (centromeric), on the long arm of chromosome 5 (5q13) (Lefebvre et al., 1995; Markowitz et al., 2012). Though both genes are nearly identical, only SMN1 gene encodes a fully functional SMN protein. A single nucleotide substitution in the exon7 of the SMN2 gene generates a weak splice site. This causes mis-splicing that results in SMN2 transcripts lacking exon7 (Cartegni and Krainer, 2002). Hence, around 80% of the SMN2 gene product obtained is truncated leading to its degradation (Cifuentes-Diaz et al., 2001). Homozygous knockout of SMN is embryonic lethal (Schrank et al., 1997). In *Xenopus sp.* and *Danio rerio*, reduced levels of SMN led to embryonic developmental and motor neuron defects that could be restored by supplementing with purified U snRNPs (Winkler et al., 2005). These experiments linked the motor neuron degeneration to U snRNP assembly defects. Even though 96% of the SMA patients constitute homozygous deletion of SMN1, 4% of the patients harbor intragenic mutations in the SMN1. Among these mutations is the most common E143K mutation in the Tudor domain that affects Sm protein binding (Buhler et al., 1999; Neuenkirchen et al., 2015; Tripsianes et al., 2011) and several other missense mutations in the C-terminus like S262I, Y272C, T274I (Hahnen et al., 1997; Wirth et al., 1999).

# 2    Aim

Albeit spontaneous assembly *in vitro*, cells employ specific assembly factors organized in PRMT5 and SMN complexes to orchestrate the early and late cytoplasmic phase of the U snRNP assembly. The Sm proteins have a tendency to bind non-specifically to RNA under physiological conditions suggesting that PRMT5-SMN system might render specificity to the assembly of U snRNPs. In this direction, two studies have shown that the presence of SMN complex prevents non-cognate interactions and allows specific binding of the Sm proteins to cognate RNAs (Neunkirchen et al., 2015, Pellizzoni, L., 2002). However, whether such plethora of assembly factors also serves other functions in the assembly is not known. Based on structural studies, the Sm proteins are prone to aggregation as they have solvent-exposed hydrophobic interaction surfaces (Grimm et al., 2013; Kambach et al., 1999a; Kambach et al., 1999b; Zhang et al., 2011). Therefore, shielding these surfaces until the incorporation of individual proteins into the functional Sm core formation seems to be a critical task for the cell. I want to address this issue in my thesis by asking how cells handle the aggregation-prone Sm proteins in the absence of the assisting factors. The strategy was to perform series of experiments like pulsed SILAC and metabolic labeling that would allow me to analyze the Sm protein pool upon the perturbation of the assembly pathway. Further, I wanted to explore the underlying cellular mechanisms that are responsible for the altered Sm protein levels under these conditions.

For the second aspect of my thesis, I planned to investigate the potential nuclear function of SMN. Despite being highly enriched in Cajal bodies (CBs), the precise role of SMN in this nuclear domain remains unclear. To gain insights into SMN's nuclear role, I intended to identify its interacting partners, particularly in CBs, via immunoprecipitation, mass spectrometric analysis and subsequent validation via biochemical approaches.

# 3    Materials and Methods

*Note:* Common chemicals were purchased from either Carl Roth or Sigma or Merck unless otherwise mentioned. Also, all cell lysis buffers were supplemented with a cocktail of protease inhibitors in 1:1000 dilution.

| Protease inhibitor | Stock |
|---|---|
| Leupeptin/Pepstatin A | 1 mg/mL |
| PMSF | 200 mM |
| AEBSF | 100 mM |
| Aprotinin | 1 mg/mL |

## 3.1    General Materials

### 3.1.1    List of antibodies

| Name | Dilution | | | Supplier |
|---|---|---|---|---|
| | WB | IF | IP | |
| Mouse α SMN | 1:1000 | 1:200 | 2 µg/µL | Clone 7B10, affinity purified from hybridoma supernatant (0176-01; immunoGlobe) |
| Mouse α sDMA Sm proteins | 1:1000 | 1:200 | 2 µg/µL | Clone Y12, Protein-G purified from hybridoma supernatant |
| Rabbit α pICln | 1:1000 | -- | 0.6 µg/µL | 1035; affinity purified from immunized bleed |
| Mouse α α-tubulin | 1:2000 | -- | -- | T5168;Sigma |
| Mouse α β-actin | 1:2000 | -- | -- | A5316; Sigma |
| Rabbit α Histone3 | 1:1000 | -- | -- | ab1791; Abcam |
| Rabbit α Prp4 | 1:50 | -- | -- | IG 519, serum, immunoaffinity purified |
| Rabbit α Coilin | 1:1000 | 1:200 | -- | H-300, SC-32860; Santa Cruz Biotechnology |
| Rat α MED15 | 1:25 | -- | 10 µL/µL | 6C9 Monoclonal Hybridoma supernatant (kind gift from Michael Meisterernst, Münster University) |
| Rat α MED25 | 1:25 | -- | 10 µL/µL | VC1 Monoclonal Hybridoma supernatant (kind gift from Michael Meisterernst, Münster University) |
| Mouse α β-catenin | 1:1000 | -- | -- | 610153; BD Transduction laboratories |
| Rabbit α LC3 | 1:100 | -- | -- | L7543; Sigma |

| | | | | |
|---|---|---|---|---|
| Rabbit α SmD3 | 1:500 | 1:100 | -- | PA5-26288; Thermo Scientific-Pierce |
| Rabbit α SmD1 | 1:1000 | 1:25 | -- | PA5-12459; Thermo Scientific-Pierce |
| Mouse α Gemin5 | 1:1000 | 1:200 | 0.6 μg/μL | Clone 10G11, 05-1535; EMD Millipore |
| Rabbit α SmF | 1:1000 | -- | -- | ab66895; Abcam |
| Mouse α TMG-cap | -- | 1:250 | 2 μg/μL | Clone H20, a kind gift from R. Lührmann, Max Planck Institute |
| Rat anti-Gemin3 | -- | 1:100 | -- | A kind gift from Friedrich Grässer |
| Mouse anti-FLAG M2 | -- | 1:200 | -- | F1804; Sigma |
| α -mouse | 1:5000 | -- | -- | A6154; Sigma |
| α –rabbit | 1:5000 | -- | -- | A5795; Sigma |
| α -rat | 1:10,000-1:50,000 | -- | -- | A5795; Sigma |
| Cy5 anti-mouse IgG | -- | 1:200 | -- | 115-175-146; Jackson Immuno Research Laboratories |
| Cy5 anti-rabbit IgG | -- | 1:200 | -- | 111-175-144; Jackson Immuno Research Laboratories |
| Cy5 anti-rat IgG | -- | 1:200 | -- | 712-175-150; Jackson Immuno Research Laboratories |
| Alexa488- goat anti-rabbit | -- | 1:500 | -- | A11070; Thermo Scientific |
| Alexa488- goat anti-mouse | -- | 1:500 | -- | A11017; Thermo Scientific |
| Alexa488- donkey anti-goat | -- | 1:500 | -- | A11055; Thermo Scientific |

### 3.1.2   List of RNAi sequences

| RNAi | Sequence |
|---|---|
| shSMN-1 | 5' TGCAGCTTCCTTACAACAGTGGAAAGTTG 3' |
| shSMN-2 | 5' TTCTGCCATTTGGTCAGAAGACGGTTGCA 3' |
| shSMN-3 | 5' GAAACCTGTGTTGTGGTTTACACTGGATA 3' |
| shSMN-4 | 5' CAACAGATGAAAGTGAGAACTCCAGGTCT 3' |
| siFirefly Luciferase | 5' CGUACGCGGAAUACUUCGA(dTdT) 3' |

### 3.1.3   List of RT-PCR primer sequences

| Target | Primer sequences |
|---|---|
| SmB | FP 5' CGGATCTTCATTGGCACCTT 3' |
| | RP 5' CGAGGACTCGCTTCTCTTCC 3' |
| SmD1 | FP 5' GCTGGAAACGCTGAGTATTCG 3' |
| | RP 5' GCCACGTCCTCTTCCTCTTC 3' |
| SmD2 | FP 5' ACCGGTCCACTCTCTGTGCT 3' |
| | RP 5' CACGTTCTCCAGCACCATGT 3' |
| SmD3 | FP 5' GAGACGAACACCGGTGAGG 3' |

| | RP 5' GCCACGGATGTATACCTGCTC 3' |
|---|---|
| SmE | FP 5' CCAGGGTCAGAAAGTGCAGA 3' |
| | RP 5' TGCTCATAGAGCCACACCTGA 3' |
| SmF | FP 5' CAGGAAAGCCAGTGATGGTG 3' |
| | RP 5' TCCTCTTCTTCCACACCTCTGA 3' |
| SmG | FP 5' CACCCTCCCGAGTTGAAAAA 3' |
| | RP 5' CGCCATCTCCACACATTCAT 3' |
| SMN | FP 5' CAAGCCCAAATCTGCTCCAT 3' |
| | RP 5' GAGGCAGCCAGCATGATAGTAA 3' |
| Gemin5 | FP 5' TGCCCAAATTCCAGTGTCTG 3' |
| | RP 5' TGTTTGGCTCTGGCTGAGAA 3' |
| pICln | FP 5' TGGAAGCACATGAACAAGGA 3' |
| | RP 5' TCCTGACCCCAGCCATATTA 3' |
| GAPDH | FP 5' CCAGAACATCATCCCTGCCT 3' |
| | RP 5' GGTCAGGTCCACCACTGACA 3' |
| U1 snRNA | FP 5' TACCTGGCAGGGGAGATACC 3' |
| | RP 5' GCAGTCCCCCACTACCACA 3' |
| U2 snRNA | FP 5' CGGCCTTTTGGCTAAGATCA 3' |
| | RP 5' CTGCAATACCAGGTCGATGC 3' |

## 3.2 Pulsed SILAC

### 3.2.1 Solutions

| Solutions | Stocks |
|---|---|
| $^{13}C$, $^{15}N$-Lysine or Lysine-8 (CNLM-291-H; Cambridge Isotope Laboratories) | 73 g/L in ddH$_2$O |
| $^{13}C$, $^{15}N$-Arginine or Arginie-10 (CNLM-539-H; Cambridge Isotope Laboratories) | 42 g/L in ddH$_2$O |
| $^{2}H$-Lysine or Lysine-4 (DLM-2640; Cambridge Isotope Laboratories) | 73 g/L in ddH$_2$O |
| $^{13}C$-Arginine or Argining-6 (CLM-2265-H; Cambridge Isotope Laboratories) | 42 g/L in ddH$_2$O |
| L-Glutamine (25030123; Life technologies) | 0.584 g/L; 200 mM |
| L-Proline (P5607-25g; Sigma) | 100 g/L |
| L-Lysine monohydrochloride (L-8662-25g; Sigma) | 73 g/L in ddH$_2$O |
| L-Arginine monohydrochloride (A-6969-25g; Sigma) | 42 g/L in ddH$_2$O |
| 1 % NP40 lysis buffer | 50 mM HEPES-NaOH pH 7.9 |
| | 150 mM NaCl |
| | 1 % NP40 |
| | 1 mM EDTA |
| | 0.8 U/μL murine RNase inhibitor (M0314S, NEB) |

### 3.2.2 pICln knockdown

HeLa WT cells were grown to 30 to 40 % confluency with normal DMEM media containing 10 % (v/v) FCS and no antibiotic in a 6-well plate. Cells were transfected with 90 pmol either the siRNA against Firefly Luciferase (control, 12US-N200T; Eurofins MWG Operon) or pICln

(Knockdown, L-012571-00-0005; Dharmacon RNAi Technologies) using Lipofectamine RNAiMAX transfection reagent (13778-150; Life Technologies) according to the vendor's protocol. Briefly, to 125 µL of OptiMEM medium (319.850.47; Gibco, Life Technologies), 7.5 µL of Lipofectamine RNAiMAX transfection reagent was added (Solution A). To another 125 µL of OptiMEM medium, 4.5 µL of 20 µM siRNA (for Firefly Luciferase or pICln) was added (Solution B). Both solutions were incubated separately at RT for 5 min. Subsequently, Solution B was added to Solution A and mixed well. This mixture was then incubated at RT for 15 min before adding to the cells. After 48 h, both control and knockdown cells were washed twice with 1xPBS and grown in DMEM medium  (high glucose and no glutamine, no arginine, no lysine; A14431-0; Invitrogen) containing light amino acids in 1:500 dilution from the stock and 10 % (v/v) dialyzed FCS (26400-036; Invitrogen). They were allowed to grow for 96 h. After this the cells were again washed twice with 1x PBS and both the control and knockdown cells were switched to media containing heavy isotope amino acids ($^{13}C$, $^{15}N$-lysine and $^{13}C$, $^{15}N$-arginine) and medium-heavy isotope amino acids ($^{2}H$-lysine and $^{13}C$-arginine) respectively in 1:500 dilution from stock and 10 % dialyzed FCS.  At around 120 h, cells were washed with 1xPBS and scraped in 100 µL of 1 % NP40 lysis buffer. The cell suspension was then incubated for 10 min on ice, passed through 26G syringe needle six times. Employing a water-bath sonicator, the cell suspension was sonicated at maximum output with 15 s pulse for six times with a cycle interval of 15 s. The lysates were then clarified by centrifuging at 13,200 rpm for 20 min at 4 °C. Finally, 100 µg of total protein each, from control and knockdown lysates, were mixed and analyzed by quantitative mass spectrometry.

### 3.2.3    SMN knockdown

For the knockdown of SMN, lentiviral-mediated HeLa cell line that is capable of doxycycline-inducible expression of shRNA against SMN mRNA was generated in collaboration with Dr. Bhupesh K Prusty, Department of Microbiology, University of Wuerzburg. The lentiviral constructs used are as described in Wiznerowicz and Trono, 2003 (Wiznerowicz and Trono, 2003). These shSMN cells were seeded in 6-well plate in the presence (for knockdown) and absence (for control) of doxycycline. Labeling for SMN knockdown with heavy and medium heavy amino acids was similar to pICln knockdown conditions but was performed from 120 to 144 h.

### 3.3 $^{35}$S Metabolic labeling and Autoradiography

#### 3.3.1 Buffers and solutions

| Buffers and Solutions | Composition |
| --- | --- |
| IP wash buffer I | 50 mM HEPES pH 7.5 |
| | 300 mM NaCl |
| | 0.01 % (v/v) NP40 |
| IP wash buffer II | 50 mM HEPES pH7.5 |
| | 300 mM NaCl |
| IP wash buffer III | 50 mM HEPES pH7 .5 |
| | 100 mM NaCl |

#### 3.3.2 $^{35}$S- metabolic labeling

Cells containing stably integrated SMARTpool of shSMN were seeded in 14x 10 cm cell culture dishes. Of these, 7 plates were treated with 1 µg/mL of Doxycycline (D9891; Sigma-Aldrich) for SMN knockdown over 120 h in DMEM media (41965062; Gibco, Life Technologies) supplemented with 10 % (v/v) FCS (Tetracycline negative, US origin), 1 % (v/v) Penicillin and Streptomycin (15140122; Gibco, Life Technologies) to 90-95 % confluency. For labeling with radiolabeled $^{35}$S-methionine, cells were initially starved for 30 min in seru and methionine-free media (1642254; MP Biomedicals) following which, they were grown in radioactive $^{35}$S-methionine (25 µCi; SCM-01; Hartmann Analytic) substituted methionine-free media containing 10 % (v/v) dialyzed FCS (26400-036; Invitrogen), 20 mM HEPES pH 7.4 for 3.5 h. The remaining 7 plates were treated as control plates and processed similarly.

#### 3.3.3 Cell lysis

Following $^{35}$S metabolic labeling, the cells were washed twice, thoroughly with 1xPBS and collected in 700 µL of 1 % NP40 cell lysis buffer per plate with the aid of a cell scrapper. Cell lysis was performed as mentioned in the section 3.2.2. The resulting supernatant was snap frozen in liquid nitrogen and stored at -80 °C until further processing.

#### 3.3.4 Immunoprecipitation and Autoradiography

50 µL slurry of Dynabeads (10004D; Life Technologies) was incubated with required antibody (against sDMA Sm proteins, pICln, Gemin5, m$^7$G/m$_3$G cap) in 1 mL 1xPBS on the HOT rotor for 1 h at RT. Meanwhile, $^{35}$S labeled control and SMN knockdown lysates were pre-cleared using 15 µL Dynabeads slurry for 1 h at 4 °C on head-over-tail (HOT) rotor.

Immunoprecipitation was performed with the pre-cleared lysates by incubating with 25 µL of antibody-coupled magnetic bead slurry for 3 h on HOT at 4 °C. Following this, beads were collected and washed thrice with IP wash buffer I. After a final wash with 1xPBS, IPed material was eluted by boiling the beads in 100 µL 1xSDS sample loading buffer for 10 min at 95 °C. 25 µL from each of the eluates were separated based on molecular weight on 13 % high TEMED Bis-Tris SDS-PAGE. The gels were stained with coomassie, de-stained and incubated with Amplify fluorographic reagent (NAMP100; Amersham) for 45 min. The gels were dried for 30 min and exposed to hypersensitive autoradiography films (28906843; Amersham, GE Healthcare Life Sciences).

## 3.4    RNA isolation and qRT-PCR

### 3.4.1    RNA isolation

Control and knockdown (pICln and SMN) HeLa cells were grown to 90-95 % confluency in a 10 cm dish. Cells were washed with 1xPBS and collected in 1 mL of TRIzol reagent (15596018; Ambion, Life Technologies). The trizolyzed cells were incubated at RT for 15 min. To this, 200 µL of chloroform was added and the tubes were shaken vigorously for 15 s and incubated at RT for 2 min. To enable phase separation, the solubilized cells were centrifuged at 12,000 $g$ for 15 min at 4 °C. The resulting aqueous phase was transferred to a new tube. To the aqueous phase, 1 µL of Glycoblue (AM9515; Ambion, Life Technologies) and equal volume of isopropanol were added and incubated for 30 min at 4 °C after mixing well. To precipitate the RNA, the above mixture was centrifuged at 12000 $g$ for 10 min at 4 °C. The concomitant RNA pellet was washed by adding 75 % EtOH and centrifuging at 7500 $g$ for 5 min at 4 °C. The washed pellet was then air dried before re-suspending in 20 µL of DEPC treated water. Prior to storage at -80 °C, the freshly resuspended RNA pelleted was incubated at 55 °C for 10 min. For 5-fluorouracil treatment, cells were incubated with 40 µM 5-FU in DMSO (F6627; Sigma) for 24 h prior to RNA isolation.

### 3.4.2    DNase treatment

Around 6 µg of the total RNA extracted as stated in the previous section was treated with 1 µL of Turbo DNAse (AM1907; Ambion, Life Technologies) and 1 µL of 10x Turbo DNase buffer in a 10 µl reaction for 30 min at 37 °C. Following this, 2 µL of the inactivation reagent was added incubated for 5 min at RT with occasional mixing and centrifuged at 10,000 $g$ for 90 s. The supernatant containing the total RNA was carefully collected and the concentration

was measured. To ascertain the quality of extracted RNA, 500 ng of the same was checked on agarose gel, before and after DNase treatment.

### 3.4.3   Reverse transcription

Roughly, 5 µg of total RNA was used for cDNA synthesis in a 20 µL reaction volume. First to 5 µg of total RNA, 1 µL of random hexamer primer, 1 µL of dNTP mix was added and the reaction volume was made upto 13 µL using DEPC H$_2$O. This reaction mix was incubated at 65 °C for 5 min and then on ice for 1 min. At this stage, 7 µL of master mix consisting of 4 µL 5xfirst-strand buffer, 1 µL 0.1M DTT, 1 µL RNaseOUT, 1 µL of Superscript reverse transcriptase III (18080-044; Life Technologies) RT was added to the reaction mix. The final reaction mix was thoroughly mixed by careful pipetting. The RT-PCR was carried out at following conditions on PCR machine.

| Temperature | Time |
|---|---|
| 25 °C | 5 min |
| 50 °C | 60 min |
| 70 °C | 15 min |

Finally, the cDNA obtained was treated with RNaseH for 20 min at 37 °C. The cDNA thus obtained was diluted to 200 µL with DEPC treated water.

### 3.4.4   qPCR

3 µL of diluted cDNA from both control and knockdown (pICln, SMN) conditions was used in estimating relative total RNA levels of Sm proteins and U snRNAs using iTaq Universal SYBR Green Supermix (172-5124SP; Bio-rad). To 3 µL of the cDNA, 3 µL of required 1 µM forward and reverse qPCR primer mix and 6 µL of iTaq Universal SYBR Green Supermix was added. The qPCR run was performed on BioRad CFX 2.0 RT-PCR detection machine and the conditions were as follows:

| Temperature | Time | |
|---|---|---|
| 95 °C | 30 s | |
| 95 °C | 5 s | |
| 60 °C | 30 s | x40 cycles |

The data was analyzed by BioRad CFX 2.0.

### 3.5 Polysome gradient and analysis of translational arrest

#### 3.5.1 Buffers and Solutions

| Buffers and solution | Composition |
|---|---|
| 10xgradient buffer | 1 M KCl |
| | 200 mM Tris pH 7.5 |
| | 50 mM $MgCl_2$ |
| 5 % Sucrose | 5 g of sucrose in 100 mL of 1xpolysome gradient buffer |
| 45 % Sucrose | 4.5 g of sucrose in 100 mL of 1xpolysome gradient buffer |
| Polysome lysis buffer | 20 mM Tris pH 7.5 |
| | 100 mM KCl |
| | 5 mM $MgCl_2$ |
| | 0.5 % NP40 |
| | 100 µg/mL Cyclohexamide |
| | 1 mM DTT |
| Cycloheximide | 5 mg in 1 mL of DMSO |

#### 3.5.2 Cell lysis

Control and pICln knockdown cells were grown for 120 h to 80 % confluency in a 14.5 cm cell culture dish. Cycloheximide (in DMSO) was added to the cells at a final concentration of 50 µg/mL and incubated at 37 °C for 30 min. After washing with 1xPBS containing 100 µg/mL cycloheximide, cells were collected in 200 µL of polysome lysis buffer with the help of a cell scraper. The resultant lysate was centrifuged at 10,000 rpm, 10 min, 4 °C after incubating on ice for 10 min.

#### 3.5.3 Polysome gradient

Initially, 5-45 % sucrose gradients made in 1xpolysome gradient buffer were pre-cooled. To these gradients, 350 µL of lysate was loaded after the removing an equal volume from the top of the gradient. The loaded gradients were centrifuged at 38,000 rpm, 90 min, 4 °C in SW40 rotor with maximum acceleration and minimum deceleration and no brake. Gradients were harvested using Biocomp gradient fractionator.

#### 3.5.4 RNA isolation and PCR from the gradient fractions

200 µL from consecutive fractions were pooled together. To each of these pooled fractions, equal amount of DEPC water was added followed by 400 µL of phenol. Thus obtained solution was mixed well, incubated at RT for 10 min and centrifuged at 13,000 rpm for 10 min at RT. Subsequently, to the obtained upper aqueous phase equal amount of isopropanol and 1 µL of GlycoBlue (AM9515; Ambion, Life Technologies) were added and stored overnight at -

20 °C. The precipitated RNA was collected by centrifuging at 13,000 rpm, 30 min, 4 °C. Pelleted RNA is washed with 70% EtOH, air-dried and dissolved in 20 µL of DEPC water. 10 µL of RNA was used for cDNA preparation as previously described. cDNA thus obtained was diluted by adding 90 µL of DEPC water. 5 µL of cDNA was further used to perform PCR using gene specific primers as per the conditions described in the qPCR section.

## 3.6 Analysis for Sm protein degradation upon pICln knockdown

### 3.6.1 Solutions

| Solutions | Stocks |
|-----------|--------|
| MG-132 | 14 mM in EtOH |
| Chloroquine | 50 mM in ddH$_2$O |

### 3.6.2 Procedure

HeLa cells were grown in a 6-well plate for control and pICln knockdown for 110 h. At this time point, cells were treated independently with 10 µM MG-132 (proteasome inhibitor; BML-PI102-0005; Enzo Life Sciences) 50 µM chloroquine (autophagy inhibitor; C6628; Sigma-Aldrich) for 10-12 h. EtOH and ddH$_2$O were used as solvent controls for MG-132 and chloroquine, respectively. Following this, cells were washed with 1xPBS and collected in 100 µL of 1xSDS sample loading buffer. Samples were boiled at 95 °C for 10 min. Part of the lysate from each fraction was used to analyze for recovery of SmD1, SmD3 via Western blot analysis. For analyzing the same in soluble fractions, similar drug treatment was carried out. Following the treatment, cells were collected in 100 µL of 1 % NP40 lysis buffer and cell lysis was performed as mentioned in the section 3.2.2. Total protein content was measured in the resulting lysates and an equal amount of protein from control and knockdown cells was analyzed via Western blotting.

## 3.7 Sm protein overexpression and Immunofluorescence

The Sm proteins, Sm D1 and D3 were cloned in between HindII and XbaI of pcDNA3 vector backbone, modified to contain a C- terminal Flag-tag between XbaI and ApaI restriction sites. The tagged constructs were transfected into HeLa control and pICln knockdown cells at an amount of 0.5 µg vector per 0.15 x 10$^6$ cells using polyethylenimine (PEI). Following transfection, the cells were allowed to grow for 48 h and analyzed via immunofluorescence. Cells were grown on coverslips, washed once with 1xPBS and fixed for 20 min using 4 %

(v/v) PFA. Fixed cells were washed thrice with 1xPBS and permeabilized using 0.2 % Triton X-100 in 1xPBS for 20 min. After three subsequent 1xPBS washes, cells were blocked with 10 % (v/v) FCS and incubated in primary antibody solution in a humidified chamber for 1 h each at RT. These coverslips were washed thrice in 1xPBS and incubated with secondary antibody solution containing DAPI for 1 h at RT in a humidified chamber, in the dark. Finally, cells were again washed thrice with 1xPBS and once with ddH$_2$O before being mounted on a glass slide using the Mowiol4-88 mounting medium. Images of the cells were taken using Lecia DM IRB epifluorescence microscope with a CCD camera or using a Leica SP5 confocal microscope with photomultiplier ocular acquisition. The images obtained were processed using FIJI/ Image J software.

## 3.8 Large-scale sub-cellular fractionation from HeLa S3 cells

### 3.8.1 Buffers and Solutions

| Buffers and solutions | Composition |
|---|---|
| Buffer A | 10 mM HEPES-KOH pH 7.9 |
| | 10 mM KCl |
| | 1.5 mM MgCl$_2$ |
| | 0.5 mM DTT |
| Buffer B | 300 mM HEPES-KOH pH 7.9 |
| | 1.4 M KCl |
| | 30 mM MgCl$_2$ |
| Buffer C | 20 mM HEPES-KOH pH 7.9 |
| | 420 mM KCl |
| | 1.5 mM MgCl$_2$ |
| | 0.2 mM EDTA |
| | 5 % Glycerol |
| Buffer D | 20 mM HEPES-KOH pH7.9 |
| | 100 mM KCl |
| | 1.5 mM MgCl$_2$ |
| | 0.5 mM DTT |
| | 20 % Glycerol |
| S1 solution | 0.25 M Sucrose |
| | 10 mM MgCl$_2$ |
| S2 solution | 0.35 M Sucrose |
| | 0.5 mM MgCl$_2$ |
| S3 solution | 0.5M Sucrose |
| 25 mM Tris-HCl pH 9.0 | 25 mM Tris-HCl pH 9.0 |
| Buffer N | 10 mM HEPES pH 7.5 |
| | 2 mM MgCl$_2$ |
| | 25 mM KCl |
| | 250 mM Sucrose |
| Hypotonic Buffer N | 10 mM HEPES pH 7.5 |
| | 2 mM MgCl$_2$ |
| | 25 mM KCl |
| Freezing medium | 70 % (v/v) Glycerol in buffer N |

| SP1 solution | 1 M sucrose |
| --- | --- |
| | 34.2 % (v/v) Percoll |
| | 22.2 mM Tris-HCl pH 7.4 |
| | 1.11 mM MgCl$_2$ |
| SP2 solution | 20 % (v/v) Percoll |
| | 10 mM Tris-HCl pH 7.4 |
| | 1 % (v/v) Triton X100 |
| | 0.5 mg/mL Heparin |
| 2.55 M Sucrose solution | 1710 g Sucrose added stepwise in three equal proportions to 900 mL ddH$_2$O |
| Heparin (20 mg/mL) | 20 mg of Heparin in 1 mL of ddH$_2$O |

### 3.8.2 Preparation of cytoplasmic and nuclear extracts

HeLa S3 cytoplasmic and nuclear extract preparation was adapted from (Dignam et al., 1983; Meister et al., 2000). Briefly, HeLa S3 cells were seeded at a density of $3x10^5$ cells/mL in DMEM media (41965062; Gibco, Life Technologies) supplemented with 10 % (v/v) FCS (10270106; Gibco, Life Technologies) and 1 % (v/v) Penicillin/Streptomycin (15140122; Gibco, Life Technologies). They were allowed to grow at 37 °C, 5 % CO$_2$ in cell culture stirring flasks to a density of not more than $10^6$ cells/mL (roughly corresponding to 9 litre culture). The subsequent steps were carried out on ice or at 4 °C. Cells were pelleted at 800 rpm for 10 min. Pelleted cells were washed once with 1xPBS (14190169, Gibco, Life Technologies) followed by a surface wash with 2 pellet volume (PV) Buffer A at 2000 rpm for 10 min using swing out rotor. Before proceeding for the lysis, cells were allowed to swell by soaking them in 5 PV of hypotonic Buffer A for 10 min on ice. Following this, the cells were pelleted, resuspended in 2 PV of the same buffer with cocktail of protease inhibitors and DTT. This suspension was homogenized using glass Dounce Tissue Grinder pestle S, approximately 8 times. To monitor the extent of cytoplasmic cell lysis with intact nuclei, a small fraction of the cell suspension was observed under light microscope at 63x magnification. Once the cells were lysed >98 %, the cell suspension was centrifuged in swing out rotor at 4500 $g$ for 20 min to pellet the nuclei. The resultant supernatant was mixed with 0.11 volumes of Buffer B and centrifuged at 40,000 rpm in Beckman Type 60 Ti for 1h. The thus obtained supernatant is the cytoplasmic extract.

To proceed with nuclear extract, the nuclei obtained during the process of cytoplasmic extraction were washed thoroughly with 30 mL Buffer A and pelleted at 25,000 $g$ in Beckman JA 25.5 rotor for 20 min to wash away cytoplasmic contaminants. Subsequently, the clean nuclei were resuspended at a concentration of $3x10^9$ nuclei/mL in Buffer C containing cocktail of protease inhibitors and DTT. The nuclei were then lysed as 3 mL aliquots by sonication using the Branson sonicator and 3 mm microtip. The extent of nuclear lysis was further

observed under light microscope. Once an efficient lysis of nuclei was achieved, the lysate was clarified by centrifugation at 25,000 $g$ in Beckman JA 25.5 rotor for 30 min. The cytoplasmic and nuclear extracts thus obtained were dialyzed against 20 column volumes (CV) and 50 CV of Buffer D respectively for 6-8 h. The precipitates formed during the process of dialysis were cleared off by centrifuging at 16,000 rpm in Backman JA 25.5 rotor for 20 min. Finally the extracts were snap frozen in liquid nitrogen prior to storing at -80 °C. 25 μg of cytoplasmic and nuclear extracts were analyzed by western blot for cross-contamination using antibodies against β-actin, α-tubulin as cytoplasmic markers and Histone3, Prp4 as nuclear markers.

### 3.8.3    Isolation of nuclei

In order to isolate intact nuclei, HeLa S3 cells were harvested and washed with 1xPBS as mentioned earlier. The cells were incubated for 30-60 min in 10 PV of ice-cold hypotonic buffer N containing 1 mM DTT and protease inhibitors (1:1000). The swollen cells were homogenized using a glass Dounce Tissue Grinder pestle S with 100 gentle strokes on ice. The extent of cell lysis was monitored as previously mentioned to ensure that all cells were lysed leaving the nuclei intact. At this stage, 125 μL of 2 M sucrose per mL of lysate was added and mixed well by inverting the tubes. Following this, the nuclei were collected by centrifugation at 3000 $g$ in 15 mL falcons for 15 min at 4 °C in a swinging bucket rotor. The resulting pellet was washed in 2 PV of ice-cold buffer N and centrifuged again. Finally, the pellet containing the nuclei was resuspended in the freezing medium at a concentration of $10^8$ nuclei/mL and stored at -80 °C in 3 mL aliquots.

### 3.8.4    Thawing and washing of frozen nuclei

The frozen nuclei (around $2.5 \times 10^9$ nuclei) were thawed at RT and diluted with ice-cold buffer N (for 500 μL of nuclei, 1 mL of ice-cold buffer N was added). This nuclei suspension was mixed well but gently before centrifuging at 3,000 rpm for 15 min in the swing-out rotor. The nuclei were again washed thoroughly to remove any glycerol left with ice-cold buffer N equivalent to the initial volume of nuclei. The thus obtained clean nuclei were resuspended in S1 solution to the desired concentration and stored on ice until further processing for Cajal body purification.

### 3.8.5 Large-scale isolation of Cajal Bodies

The protocol for large-scale isolation of Cajal bodies was adapted from (Lam et al., 2002). Briefly, the thawed and washed $2.5 \times 10^9$ nuclei were resuspended to a final volume of 30 mL in S1 solution. This suspension was divided into two equal portions and each was carefully overlayed on 15 mL S2 solution in a 50 mL falcon ensuring a sharp interface of the two solutions. The carefully overlayed suspensions were centrifuged without mixing at 1430 $g$ for 5 min at 4 °C in swing out rotor. Following one more surface wash with 20 mL of S2 solution, the nuclei were resuspended in 30 mL S2 solution. This suspension was aliquoted to 10x 3 mL portions in 15 mL falcons. These portions were subsequently sonicated using 3 mm micro-tip in Branson sonicator 250 (50 % duty cycle, output=5, 7.5 cycles of 6 s pulse with a 6 s interval). As previously mentioned, the lysate was monitored for extent of nuclear lysis by light microscopy. Eventually, the ten 3 mL aliquots were pooled and 0.42x volume of 2.55 M sucrose was added and mixed thoroughly. This mixture was divided into two portions of roughly 20 mL each and centrifuged at 3000 $g$ for 10 min at 4 °C to on a swing out rotor to pellet the nucleoli. The resulting supernatant was mixed thoroughly with 0.82xvolume of SP1, 0.05x of 20 % Triton X-100. The concomitant mixture was subjected to ultracentrifugation at 37,000 rpm for 2 h using SW41 rotor. The pellet resting on the dense percoll precipitate consists of enriched Cajal bodies entangled with chromatin. Hence all the pellets from the centrifuged tubes were pooled together (1P fraction) to free the Cajal bodies from chromatin. This was done by treating 5 mL of 1P fraction with 125 μl of Heparin (20 mg/mL) and 1200 units of DNaseI (D4527-40KU; Sigma-Aldrich) for 45 min at RT on a HOT rotor. It was noted that the solution turned transparent immediately after addition of Heparin. To separate the Cajal bodies in this mixture, yet again density based sucrose-percoll gradient centrifugation was used. For this, 1xvolume of the SP2 solution was added to the DNase digested mixture and mixed well. This suspension was loaded into pre-cooled tubes of the SW55 rotor and was ultracentrifuged at 45,000 rpm for 1 h. This allows the Cajal bodies to settle in the middle of the gradient. Hence, the gradient was thus harvested in 200 μL fractions. 30 μg of total protein from each fraction was analyzed by western blot using an antibody against coilin as a marker for Cajal bodies.

### 3.8.6 Immunoprecipitation

HeLa S3 cytoplasmic and nuclear extracts prepared as mentioned above were pre-cleared with 30 μL of Protein G Sepharose (17-0618-085; GE Healthcare) for 1 h at 4 °C on a HOT

rotor. The pre-cleared extracts were incubated with 100 µL of 7B10 covalently coupled Protein G Sepharose beads at 4 °C for 3 h on a HOT rotor. For MED15 and MED25 immunoprecipitations, 50 µL of the magnetic Dynabeads were coupled with 1 mL of the hybridoma supernatant for 1 h at RT on HOT rotor before proceeding with incubation with the extracts. The beads then were collected by centrifugation at 5000 rpm for 5 min at 4 °C. In the case of magnetic beads, centrifugation was avoided by using a magnetic separator to collect the beads. Either of the the IPed beads were washed twice with IP wash buffer I. Subsequently, washed again once each with IP wash buffers II and III. The final wash was performed in 1xPBS. RNase A treatment of IPed material was performed at a concentration of 100 µg/mL for 45 min at 4 °C. IPed material was eluted in 100 µL of 1xSDS sample loading buffer and subsequent boiling at 95 °C for 10 min. 25 µL from the obtained eluate was run on a SDS-PAGE and visualized by silver staining. 18 µL of the same was used for western blot analysis. Control (mock) IP was performed under similar conditions with beads lacking coupled antibody.

## 3.9    Immunoblotting

### 3.9.1   Buffers and Solutions

| Buffers and Solutions | Composition |
|---|---|
| 10xTowbin buffer | 0.25 M Tris |
| | 1.92 M Glycine |
| | 10 % (w/v) SDS |
| 1xTransfer buffer | 25 mM Tris |
| | 192 mM glycine |
| | 20 % (v/v) methanol |
| | 0.1 % (w/v) SDS |
| Amido black staining solution | 0.2 % (w/v) amido black |
| | 10 % (v/v) methanol |
| | 2 % (v/v) acetic acid |
| Destaining solution | 90 % (v/v) methanol |
| | 3 %(v/v) acetic acid |
| 10 % skimmed milk | 10 g of skimmed milk in 1xPBS-T |
| Luminol | 1.25 mM luminol |
| | 100 mM Tris-HCl, pH 8.5 |
| Coumaric acid | 6.8 mM coumaric acid in DMSO |
| 10xNET | 1.5 M NaCl |
| | 0.05 M NaEDTA, pH 8.0 |
| | 0.5 M Tris, pH 7.5 |
| | 0.5 % (v/v) Triton X-100 |
| 1xNET-Gelatin | 100 mL 10XNET |
| | 900 mL ddH$_2$O |
| | 0.25 % (w/v) gelatin |
| Primary antibody solution | 1xNET-Gelatin |
| | 0.02 % Sodium azide |

| | |
|---|---|
| Secondary antibody solution | (or)<br>3 %BSA<br>1xNET-Gelatin<br>(or)<br>3 %BSA |
| 10xPBS | 1.37 M NaCl<br>27 mM sodium phosphate dibasic (Na$_2$HPO$_4$)<br>20 mM potassium phosphate monobasic (KH$_2$PO$_4$) |
| 1xPBS-T | 1x PBS<br>0.05 % (v/v) Tween 20<br>0.2 % (v/v) Triton X-100 |

### 3.9.2 Procedure

25-100 µg total proteins from cellular extracts or 1/4th of the IPed material were separated by SDS-PAGE based on molecular weight and transferred onto 0.45/0.22 µm pore size Immobilon-P Polyvinylidene Fluoride (PVDF) membrane (625.3435; IPVH 00010, 100.185.43; org. IPVH 00010) using 1x Towbin buffer containing 20 % methanol. The transfer was performed at 0.8 mA/cm² of the membrane for 90 to 120 min. The transferred membrane was blocked with 10 % skimmed milk (T145.2 Carl Roth) for 1 h at RT and incubated with primary antibody over the night at 4 °C on a falcon roller. The membrane was washed thrice, 10 min each, with 1xPBS-T and incubated with HRP-conjugated secondary antibody for 2 h at RT. After the membrane was washed thrice in 1xPBS-T, it was developed using either Luminol reagent (A8511, Sigma-Aldrich) containing 0.068 mM coumaric acid (C9008; Sigma) and 0.03 % H$_2$O$_2$ or Chemiluminescence substrate (170-5060;Bio-Rad).

### 3.10 Mass spectrometry analysis

Samples from pSILAC experiments were analyzed similar to Küspert et al., 2015 in collaboration with Prof. Dr. Andreas Schlosser, Rudolf-Virchow- Center for Experimental Biomedicine, University of Wuerzburg. Heavy and medium pulse-labeled cell lysates were mixed in a 1:1 ratio (based on whole protein content, Bradford test using Bio-Rad protein assay dye reagent; 500-0006) before reduction/alkylation and SDS-PAGE. Samples from Co-IP experiments were analyzed label-free, i.e. control and Co-IP samples were analyzed sequentially. For reduction, samples were incubated in NuPAGE LDS sample buffer (Life Technologies) supplemented with 50 mM DTT and incubated for 10 min at 70 °C and subsequently alkylated by incubation with iodoacetamide (final concentration 120 mM) for 20

min at room temperature. Reduced and alkylated samples were loaded on NuPAGE Novex Bis-Tris 4-12 % gradient gels (Life Technologies) and stained with Coomassie (Simply Blue, Life Technologies). Whole lanes were cut into 15 bands. The bands were destained with 30% acetonitrile, shrunk with 100 % acetonitrile and dried in a vacuum concentrator. Digests with 0.1 µg trypsin (Promega) per gel band were performed overnight at 37 °C in 50 mM ammonium bicarbonate (ABC) buffer. Peptides were extracted from the gel slices with 5 % formic acid.

NanoLC-MS/MS analyses were performed on an LTQ-Orbitrap Velos Pro (2 pSILAC replicates and Co-IP experiments) or on an Orbitrap Fusion (1 replicate) mass spectrometer equipped with an EASY-Spray ion source and coupled to an EASY-nLC 1000 UHPLC system (all Thermo Scientific). Peptides were loaded on a trapping column (2 cm x 75 µm ID PepMap C18 3 µm particles, 100 Å pore size) and separated on an EASY-Spray column (25 cm x 75 µm ID, PepMap C18 2 µm particles, 100 Å pore size). pSILAC samples were analyzed with a 120 min (pSILAC) or a 30 min (Co-IP) linear gradient from 3 to 30 % acetonitrile, 0.1 % formic acid and 200 or 400 nL/min flow rate.

For pSILAC samples, MS scans were acquired in the Orbitrap analyzer with a resolution of 30.000 at m/z 400 (Orbitrap Velos) or 240.000 at m/z 200 (Fusion). For Orbitrap Velos data, MS/MS scans were acquired in the LTQ Velos analyzer using CID fragmentation with a TOP15 data-dependent MS/MS method. The minimum signal threshold for precursor selection was set to 10.000. Predictive AGC was used with an AGC target value of 1e6 for MS scans and 1e4 for MS/MS scans. Lock mass option was applied for internal calibration using background ions from protonated decamethylcyclopentasiloxane (m/z 371.10124). For Fusion runs, MS/MS scans were acquired in the ion trap (rapid scan rate) with a top speed method (cycle time: 3 sec) using HCD fragmentation. The minimal signal threshold was set to 5.000, predictive AGC targets were 2e5 (MS) and 1e4 (MS/MS). For all experiments, a dynamic exclusion was applied with a repeat count of 1 and exclusion duration of 60 s. Singly charged precursors were excluded from the selection.

For Co-IP samples, MS scans were acquired in the Orbitrap analyzer of an LTQ-Orbitrap Velos Pro with a resolution of 30.000 at 400 m/z. MS/MS scans were acquired Orbitrap analyzer HCD fragmentation with a TOP5 data-dependent MS/MS method and a minimum signal threshold of 50.000 and rejection of singly charged precursors. Predictive AGC targets

were 1e6 (MS) and 5e4 (MS/MS). Ions were dynamically excluded from selection for duration of 30 s.

## 3.11 MS data analysis

For protein identification and quantitation, MS raw data files were analyzed with MaxQuant version 1.5.2.8 (Kuspert et al., 2015) and database searches were performed with the integrated search engine Andromeda. UniProt human reference proteome database was used in combination with a database containing common contaminants as a reverse concatenated target-decoy database. Protein identification was under the control of the false-discovery rate (<1% FDR on protein and peptide level). In addition to MaxQuant default settings (e.g. at least 1 razor/unique peptide for identification, 2 allowed miscleavages), the search was performed against following variable modifications: Protein N-terminal acetylation, Gln to pyro-Glu formation and oxidation (on Met). For quantitation of pSILAC-labeled proteins, the median of the log2-transformed normalized peptide ratios heavy to median (H/M) for each protein was calculated. At least two ratio counts were required for protein quantitation. Protein ratios were normalized for each experiment in intensity bins (at least 300 proteins per bin) and outliers were identified by boxplot statistics as significantly altered, if their values were outside a 1.5x interquartile range (IQR) or 3x IQR (extreme outliers). For analysis of label-free data from Co-IP experiments, MaxQuant LFQ-intensities (Kuspert et al., 2015) were utilized. Missing values in the log10 transformed intensities of control samples were imputed from a random normal distribution around the 5 % lowest intensities (close to the detection limit) with a standard deviation of 0.1. Protein ratios between Co-IP and corresponding control experiment for each replicate were calculated. After normalization, significant outliers from the ratio distributions were identified basically as above, but using a mirrored distribution to account for the strong enrichment of proteins only present in the Co-IP samples.

# 4   Results

## 4.1   Regulation of Sm protein homeostasis

The cytoplasmic phase of the U snRNP assembly employs various trans-assisting factors organized in the PRMT5 and SMN complexes to facilitate the assembly of the Sm proteins with the U snRNAs. In this thesis, I investigated how cells regulate the expression of the U snRNP components (i.e. snRNP proteins and snRNA) in response to perturbations of the assembly machinery. I hypothesized that their production would be tightly controlled to avoid snRNP protein aggregation and/or malfunction. In the following sections, I will detail the experiments that address the fate of the Sm proteins upon perturbation of the early as well as the late assembly phase.

### 4.1.1   Tailback of Sm proteins on the assembly chaperone pICln under SMN limiting conditions

The SMN complex has a pivotal role in mediating the late phase of the U snRNP assembly and depletion of the key factor SMN has been shown to interfere with the U snRNP production *in vivo* (Boulisfane et al., 2011; Gabanella et al., 2007; Shpargel and Matera, 2005; Wan et al., 2005; Winkler et al., 2005; Zhang et al., 2008). Considering this along with the assumption that the unassembled Sm proteins have the tendency to aggregate, initial experiments were performed to address the fate of the newly synthesized Sm proteins upon depletion of SMN. For this purpose, a stable cell line that allowed doxycycline inducible expression of small hairpin RNAs (shRNAs) against SMN encoding mRNAs was generated (see materials and methods section 3.1.2, 3.2.3 for details). The shRNAs produced upon induction with doxycycline destabilized the SMN encoding mRNAs resulting in the knockdown of SMN protein. The efficiency of SMN knockdown was judged by comparing the induced and non-induced cells via immunoblotting using SMN-specific monoclonal antibody (7B10). Even though the SMN protein levels were reduced nearly by 50 % at 48 h, an efficient repression of SMN was observed only at 120 h of doxycycline treatment in comparison to the non-induced control cells (Figure 4.1). Hence, the time frame between 120 to 144 h following the induction with doxycycline was chosen to study the perturbations to snRNP homeostasis. Having established this inducible cell line, it was next investigated how SMN ablation affects the cellular snRNP production levels.

**a**

| | 48 h | 72 h | 96 h | 120 h | |
|---|---|---|---|---|---|
| | − + | − + | − + | − + | Doxycycline 1 µg/mL |

Tubulin

SMN

**b**
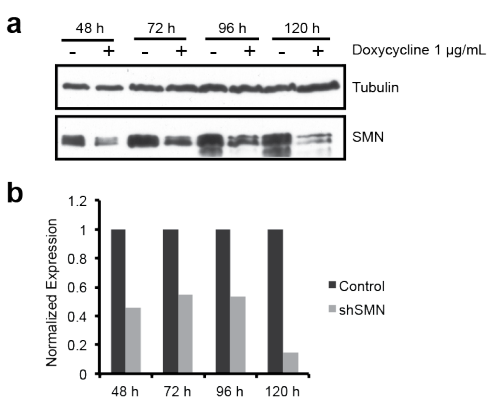
**Figure 4.1 shRNA-mediated knockdown of SMN**
**(a)** Immunoblot of SMN for total cellular lysates analyzed after the induction of shRNA with doxycycline (1µg/mL). Tubulin was used as a loading control. **(b)** Quantification of the immunoblot represented in (a) showing normalized fold expression of SMN in control and knockdown cells. At around 120 h post-induction with doxycycline, SMN was reduced by 90 %. (Figure contribution- AP- 35 %, BP- 65 %; refer Table 7.7)

I reasoned that the blockage of the late assembly phase would interfere with Sm protein flow through the assembly line and hence result either in Sm protein down-regulation or tailback on early assembly factors or their aggregation. To test for Sm protein down regulation upon SMN knockdown, pulsed SILAC approach was employed. In this approach, control (non-induced) and SMN knockdown cells were grown in media containing light amino acids (labeled $^{12}$C-Lysine and $^{12}$C-Arginine) for 120 h after addition of doxycycline. At this time point, SMN was down-regulated approximately by 90% as compared to the control cell line (Figure 4.1). The control cells were subsequently grown for further 24 h in the medium containing heavy amino acids ($^{13}$C, $^{15}$N-Lysine and $^{13}$C, $^{15}$N-Arginine) whereas the SMN knockdown cells in medium containing medium heavy amino acids ($^{2}$H-Lysine and $^{13}$C-Arginine). Equal amounts of total soluble proteins from both the cell populations were then analyzed by mass spectrometry (for experimental details see materials and methods section 3.2). This approach allows the detection of differences in the levels of newly synthesized proteins between the control and the SMN knockdown conditions. SMN knockdown resulted in down regulation of several proteins as compared to the proteins that are up-regulated. Figure 4.2 shows a comparison of detected proteins between two independent experiments whose expression levels were altered upon SMN knockdown. As expected, the most strongly de-regulated factor in the induced cell line was the SMN protein with more than 90% reduction as compared to the control. However, no significant alterations in the expression of the majority of the common- and specific-snRNP proteins could be identified. Also, the expression levels of proteins acting in various metabolic pathways were affected. As this

finding is most likely not relevant for the topic of this thesis, it was not pursued any further (refer Table 7.3 for the complete list of altered proteins under SMN knockdown).
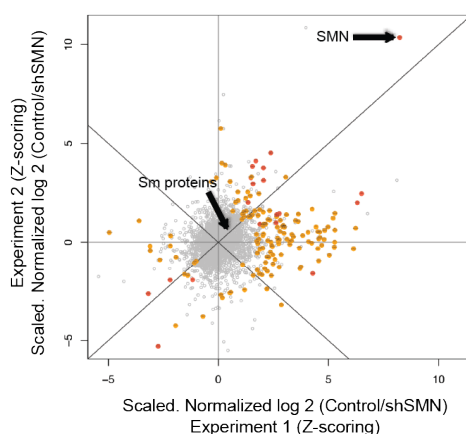


**Figure 4.2 Sm protein homeostasis remains unaltered under SMN paucity**
Correlation between the two independent pulsed SILAC experiments performed after shRNA-mediated knockdown of SMN. The right upper quadrant, showing the Z-scoring of scaled normalized log 2 values of control vs shSMN, represents the proteins that are significantly down-regulated in both the experiments. The left lower quadrant represents the proteins that are significantly up-regulated under the same conditions. The Sm proteins found in the grey zone indicate no significant changes during SMN knockdown. Note: Red- significantly altered, Orange- moderately altered, Grey- not significantly altered proteins. (Figure contribution- AP- 50 %, MS- 50 %; refer Table 7.7)

Based on the results described above, it could be excluded that the reduced expression of SMN alters the steady-state levels of Sm protein production. Next, I tested the hypothesis that Sm proteins become sequestered at early assembly complexes, particularly on pICln, the main Sm protein-binding factor of the early assembly phase. To test this, I investigated the path of the newly synthesized Sm proteins through the assembly pathway was investigated. Newly translated proteins of control and SMN knockdown cells were metabolically labeled with [$^{35}$S]-methionine for 3.5 h. Subsequently, immunoprecipitations from the soluble lysates of both cell lines were performed using antibodies that recognize specific factors of the snRNP biogenesis cycle and, hence help to monitor the fate of Sm proteins at different stages of the pathway (see Figure 4.3 for details). The Y12 antibody recognizes the sDMA on the C-terminal tails of Sm proteins thereby enables capturing of sDMA Sm proteins from all the different stages of the U snRNP assembly from as early as the PRMT5 complex to the final mature U snRNPs (Figure 4.3(i)). Next, to analyze the early assembly intermediates, pICln antibody was used. pICln majorly recognizes the assembly incompetent Sm protein intermediates (6S complex consisting of pICln, Sm D1, D2, F, E and G; pICln/SmB/D3) either

in free or PRMT5-bound state (Figure 4.3(ii)). Finally, to monitor the transfer of Sm proteins to the late and the final phases of the assembly, Gemin5 (a component of SMN complex) and H20 (for the $m_3G/m^7G$-cap of the snRNA) antibodies were used, respectively (Figure 4.3(iii) and (iv)). While the Gemin5 antibody immunoprecipitates the SMN complex, H20 antibody mainly pulls down the mature U snRNPs. The immunoprecipitates thus obtained were then analyzed by resolving them using SDS-PAGE and autoradiography (Figure 4.4(a) and (b)).
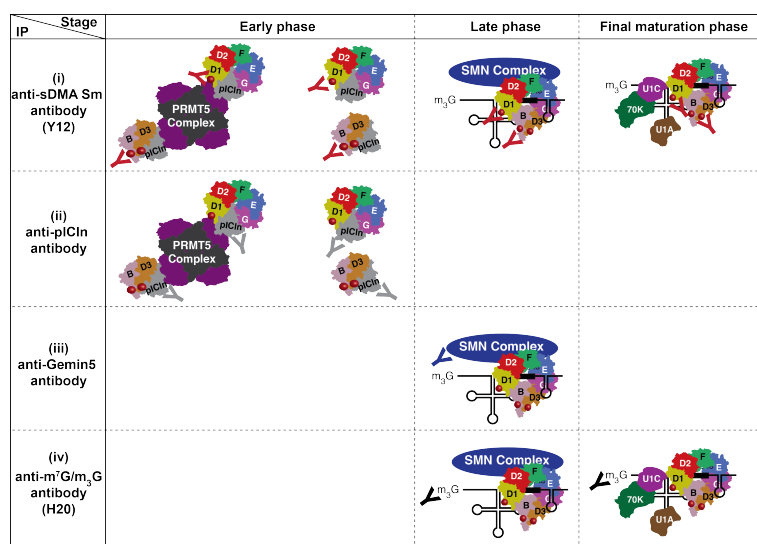


**Figure 4.3 List of assembly intermediates that are recognized by various antibodies**
**(i)** The monoclonal Y12 antibody against symmetrically dimethylated arginines of Sm proteins recognizes the 6S complex and the pICln/SmB/SmD3 heterotrimer associated with the PRMT5 complex from the early phase, the SMN complex bound to the U snRNA loaded with the Sm core. It also recognizes the fully assembled mature U snRNPs in the nucleus. **(ii)** The polyclonal antibody against pICln immunoprecipitates majorly the early assembly intermediates. **(iii)** But, the antibody against Gemin5 can recognize predominately the last phase intermediates involving the SMN complex from the cytoplasm as well as the nucleus. **(iv)** The H20 antibody against $m_3G/m^7G$-cap of the U snRNA immunoprecipitates majorly the mature U snRNPs that are in association with the specific proteins in the nucleus.

Immunoprecipitation of the extracts with monoclonal Y12 antibody precipitated equal amounts of [$^{35}$S]-labeled Sm proteins along with the U snRNP specific proteins, U1A and U1C, from control and SMN knockdown lysates (Figure 4.4(a) lane 5 and 6). This suggested that the absence of SMN has no effect on the total amount of newly translated Sm proteins that are directed into the U snRNP assembly pathway and is consistent with the results of pulsed SILAC experiment. However, the engagement of Sm proteins with the early assembly factor, pICln, was significantly changed as illustrated by the anti-pICln immunoprecipitation. Even though there was no alteration in the association of pICln with the core components of

the PRMT5 complex (i.e. WD45 and PRMT5), there was a pronounced enrichment of the newly translated Sm proteins over pICln in the absence of SMN. This enrichment was significant for Sm F/E/G but less pronounced for Sm B/D1/D2/D3 (Figure 4.4(a) lane 7 and 8). Such an accumulation of the Sm proteins on pICln observed during the depletion of SMN predominately constitutes the kinetically trapped 6S state (pICln, Sm D1, D2, F, E, G). This was inferred based on the specific accumulation of Sm E/F/G on pICln observed in this experiment and also the results demonstrated by Dr. Paknia, where Sm D1 and D2 are associated with pICln immediately after their translation.
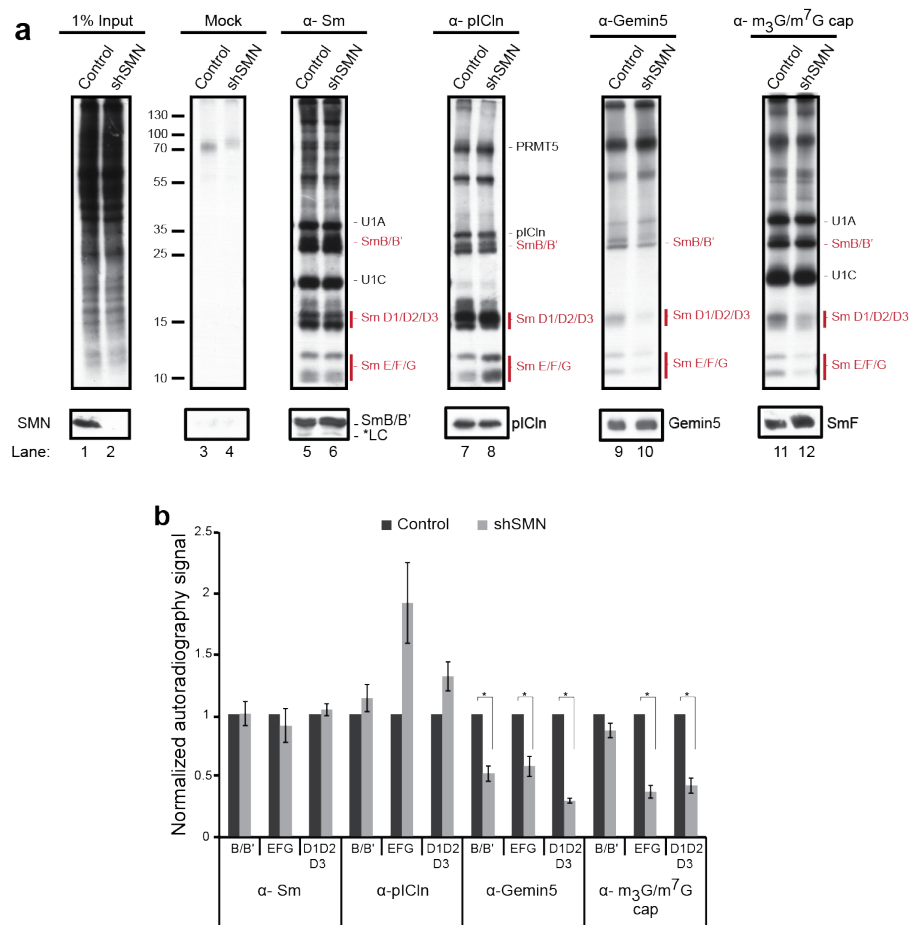


**Figure 4.4 Tailback of Sm proteins on pICln under SMN limiting conditions**
[35]S-metabolic labeling in control and SMN knockdown conditions. **(a)** Autoradiographs of mock (no antibody), sDMA-Sm proteins (Y12), pICln, Gemin5 and $m_3G/m^7G$ cap (H20) immunoprecipitations, from control and SMN knockdown lysates. Lower panels: corresponding western blots. **(b)** Quantification of the autoradiography signal from three independent biological experiments. Error bars - standard error; * represents $p \leq 0.05$ from Student's t-test. (Figure contribution- AP- 100 %; refer Table 7.7)

The accumulation of Sm proteins on pICln may be due to their inhibited transfer to the late assembly factors caused by SMN scarcity. To test this possibility, immunoprecipitations with antibodies against either Gemin5 (a component of SMN complex) or the $m_3G/m^7G$-cap (H-20) of the U snRNA was performed. Even though Gemin5 was equally enriched in the immunoprecipitations (as demonstrated by immunoblotting, Figure 4.4(a), lane 9 and 10 lower panel), the amount of co-precipitated Sm proteins was drastically reduced, showing an inefficient progression of the Sm proteins to the late assembly factors. As a consequence, significantly less incorporation of the newly translated Sm proteins into the assembled U snRNPs was observed during SMN paucity, as evidenced by the immunoprecipitation using H-20 monoclonal antibody (Figure 4.4(a) lane 11 and 12). However, incorporation of the newly synthesized snRNP-specific proteins such as U1A and U1C remained unaffected.

In sum, the aforementioned results confirm the previous findings of a unidirectional flow of the newly synthesized Sm proteins from the PRMT5 complex to the SMN complex. Perturbing the late phase of the assembly, results in the tailback of the newly translated Sm proteins on the assembly chaperone pICln, affecting the final U snRNP levels. However, there was no overall effect on the newly translated Sm proteins as evidenced by pulsed SILAC and Y12 immunoprecipitation.

### 4.1.2 Post-transcriptional regulation of Sm encoding transcripts during prolonged absence of SMN

The Sm proteins are accumulated over pICln in the absence of SMN. However, the cellular pICln levels are likely to be limiting in its ability to sequester Sm proteins during prolonged SMN deficiency. Hence, I wished to investigate whether there are other mechanisms that come into play when the system reaches beyond the capacity of pICln to sequester the Sm proteins. In such a condition, cells might respond either by regulating the synthesis or degrading the Sm proteins.

To explore whether the transcriptional or post-transcriptional events contribute to this scenario, transcripts encoding Sm proteins as well as the U snRNAs were analyzed by quantitative RT-PCR using cDNA samples prepared from the control and the SMN knockdown cells, 24 h post metabolic labeling analysis. In accordance with the earlier reports (Gabanella et al., 2007; Zhang et al., 2008), the U snRNA transcripts were down regulated by nearly 70 % (Figure 4.5(a)). Additionally, the mRNAs encoding Sm proteins were also down

regulated by 30 to 50 % (Figure 4.5(a)). These transcript levels were recovered to normal levels in the absence of SMN, upon treatment with 5-fluorouracil (5-FU), an anti-metabolite that inhibits ribonucleolytic activity of the exosome (Kammler et al., 2008) (Figure 4.5(b)). This finding strongly suggests post-transcriptional regulation of the Sm proteins under prolonged SMN paucity.
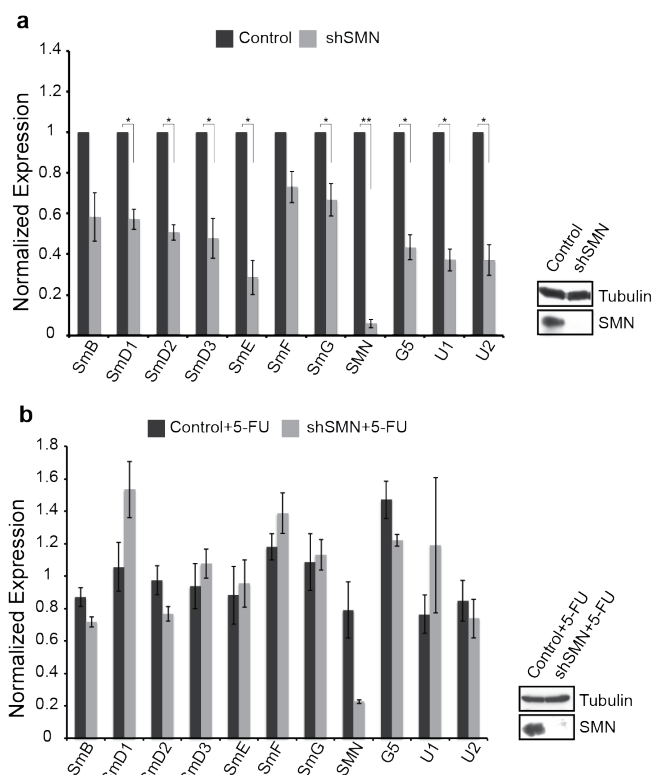


**Figure 4.5 Down regulation of Sm encoding transcripts during prolonged SMN deficiency**
Quantitative real-time PCR analysis of the Sm protein encoding mRNAs and U snRNAs in control and SMN knockdown conditions (at 144 h post doxycycline induction). **(a)** Sm protein encoding mRNAs and U snRNA transcripts are 30-50 % down-regulated under SMN knockdown. **(b)** The same transcripts levels are comparable in control and SMN knockdown cells, upon 5- FU treatment, suggesting exosome-mediated RNA degradation as the regulatory switch. Note that the RNAi-mediated degradation of SMN encoding transcript is unaffected upon 5-FU treatment confirming the specificity of the results obtained. Right panels of (a) and (b) show the efficiency of SMN knockdown at the protein level using immunoblotting. Error bars -standard error * = p≤0.05 and ** = p≤0.005 (Student's t-test). (Figure contribution- AP- 100 %; refer Table 7.7)

The results described in the sections 4.1.1 and 4.1.2 suggested that the cells respond in a bi-phasic manner when the late phase of the assembly is perturbed, by knocking down SMN. While the immediate response to SMN deficiency results in sequestering of the Sm proteins

by pICln, the exosome-mediated degradation of transcripts encoding the Sm proteins encompasses the regulation upon an extended period of SMN deficiency.

### 4.1.3 Down regulation of Sm proteins in the absence of the assembly chaperone pICln

Recent study by Dr. Elham Paknia from our lab revealed that the newly synthesized Sm D1 and D2 proteins are post-translationally retained at ribosomal exit tunnel until pICln picks up and guides them into the assembly pathway. These Sm proteins accumulate on the ribosome as an immediate response to the absence of pICln. Together with my finding of the crucial role of pICln in sequestering Sm proteins under SMN paucity, I next asked how cells regulate Sm protein homeostasis during prolonged perturbation of the early phase of the assembly. This question was addressed by the depletion of endogenous pICln using a smart pool of siRNAs targeting pICln-encoding mRNA. As a control knockdown for specificity and efficiency, a siRNA against Firefly Luciferase was used in parallel experiments (see materials and methods section 3.2.2 for details). Subsequently, the fate of the newly synthesized Sm proteins was analyzed by pulsed SILAC and mass spectrometry along the same lines as described in section 4.1.1.
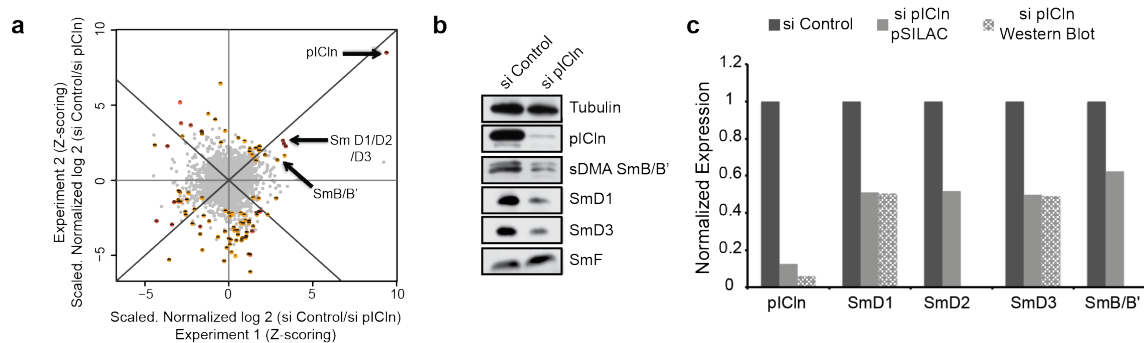


**Figure 4.6 Down regulation of Sm proteins after siRNA-mediated knockdown of pICln**
**(a)** Correlation between two independent pulsed SILAC experiments performed after siRNA-mediated knockdown of pICln. The right upper quadrant, showing the Z-scoring of scaled normalized log 2 values of si Control vs si pICln, represents the proteins that are significantly down-regulated in both experiments. The left lower quadrant represents proteins that are significantly up-regulated in the same. The Sm proteins can be seen in the right upper quadrant indicating significant down regulation during pICln knockdown. Note: Red- significantly altered, Orange- moderately altered, Grey- not significantly altered proteins. **(b)** Immunoblots using antibodies against Sm proteins to confirm the pSILAC results. **(c)** Graph showing a quantitative representation of the Sm protein levels in control and pICln deficient cells from pSILAC and immunoblotting. (Figure contribution- RM- 50 %, MS- 50 %; refer Table 7.7)

Figure 4.6(a) shows a comparison of cellular proteins detected by mass spectrometry that are regulated during pICln deficiency (refer Table 7.4 for details of proteins). These experiments, performed in duplicates, revealed a strong down regulation of pICln (i.e. the siRNA-targeted protein). In addition, a small but highly specific set of proteins was down regulated approximately by 40-50 %. Of note, these included the Sm proteins B, D1, D2, D3. However, Sm E, F, G and other U snRNP-specific protein levels remain less affected. These results were highly reproducible and were also validated by immunoblotting using antibodies against the respective Sm proteins (Figure 4.6(b)). Thus, prolonged down regulation of the assembly chaperone pICln, eventually leads to the down regulation of those Sm proteins that directly bind to pICln right after translation (Paknia et al., submitted).

### 4.1.4   Post-translational Sm protein degradation via autophagy

The decreased levels of Sm proteins upon pICln knockdown could be due to regulation at various levels including regulation of transcription, degradation of the transcript, translational arrest or protein degradation mechanisms. To test which of these mechanisms are involved, transcripts encoding Sm proteins were analyzed by quantitative RT-PCR in the control and pICln knockdown cells. In contrast to SMN knockdown, there was a noticeable increase in the Sm encoding transcripts upon pICln knockdown (Figure 4.7(a)). This finding ruled out any possible down-regulation at the level of transcription.

Next, I addressed whether regulation occurs through translational arrest. For this purpose, the control and pICln knockdown cells were treated with cycloheximide to inhibit translation elongation by arresting ribosomes on the translatable mRNA. Following this, the cytosolic extracts were subjected to sucrose density fractionation to allow the separation of monosomes and polysomes. There was no significant difference in the profiles of fractionated polyribosomes between the control and pICln knockdown conditions, thereby suggesting no alteration in the overall protein translation state of the cells (Figure 4.7(b)(i)). However, to monitor the translational arrest of Sm protein encoding mRNAs specifically, mRNAs associated with the separated monosome and polysome fractions was precipitated and cDNA was prepared. Following this, quantitative RT-PCR analysis was done to quantify the ribosomal association of transcripts encoding the Sm proteins. There was no apparent change in the association of the Sm encoding mRNAs with monosomes (fractions 3 to 5 in Figure 4.7(b)-(ii) to (vi)) and polysomes (fractions 6 to 9 in Figure 4.7(b)-(ii) to (vi)) in the absence of

pICln as compared to the control. Based on these results, it is unlikely that translational arrest is the cause for the observed down-regulation of the Sm proteins.
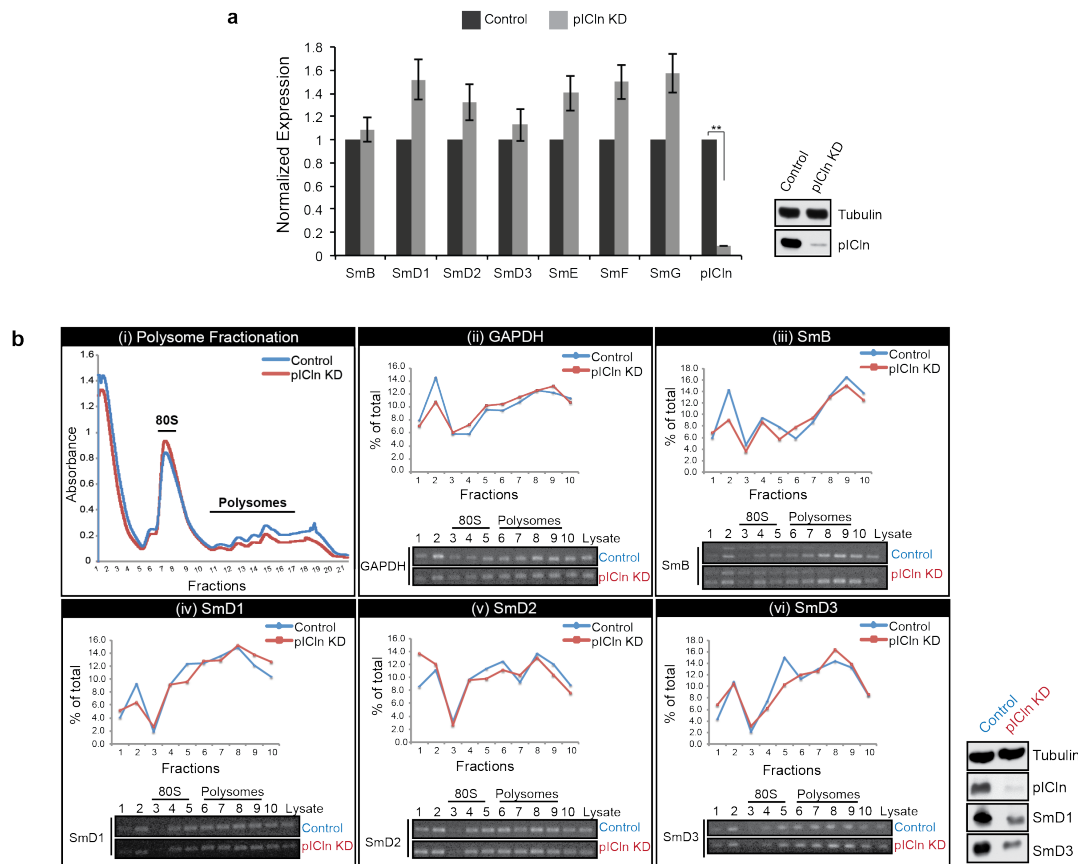


**Figure 4.7 No transcriptional or translational regulation of Sm proteins during the knockdown of pICln**

**(a)** Quantitative real-time PCR analysis showing no down regulation of Sm protein transcripts upon pICln knockdown. Error bars- standard errors, n=3, ** = p≤0.005 (Student's t-test) **(b) (i).** Polysome profile remains unaltered under pICln knockdown compared to the control. (**b) (ii) to (vi).** The graphs represent the normalized mRNA present in association with ribosomes in each fraction compared to the total mRNA associated with the ribosomes in all fractions. Lower panels: corresponding Ethidium bromide (EtBr) staining of the amplified cDNA that is quantified in the graph from each fraction. The association of any of the Sm B, D1, D3 and D2 mRNAs remain unaltered between the monosomes and polysomes during pICln knockdown. Right panels for (a) and (b) depict the immunoblots of the respective lysates showing efficiency of pICln knockdown and the down regulation of Sm proteins. (Figure contribution- RM- 95 %, AP- 5 %; refer Table 7.7)

Finally, I tested whether any of the known cellular protein degradation machineries are involved in the Sm proteins' modulation. There are two major pathways that are involved in protein degradation in general- proteasomal and autophagic pathways. To determine

whether the Sm proteins are degraded by any of these pathways, the control and pICln knockdown cells were treated for 10 h with MG-132 (an inhibitor of proteasomal degradation pathway) or chloroquine (an inhibitor of autophagy), prior to the total cellular lysis. To test for the efficiency of these drug treatments, a Western blot analysis was performed on the total cellular extracts with antibodies against β-catenin and LC3 II (microtubule-associated protein 1A/1B-light chain 3 I conjugated to phosphatidylethanolamine). While inhibition of the proteasomal degradation pathway leads to the stabilization of ubiquitinated β-catenin, inhibition of autophagy causes accumulation of LC3 II as a consequence of the decreased turnover of autophagosomes. Stabilization of the ubiquitinated β-catenin with MG132 treatment and the accumulation of LC3 II with the chloroquine treatment indicated a successful block of the proteasome and the autophagosome, respectively (Figure 4.8(a)).
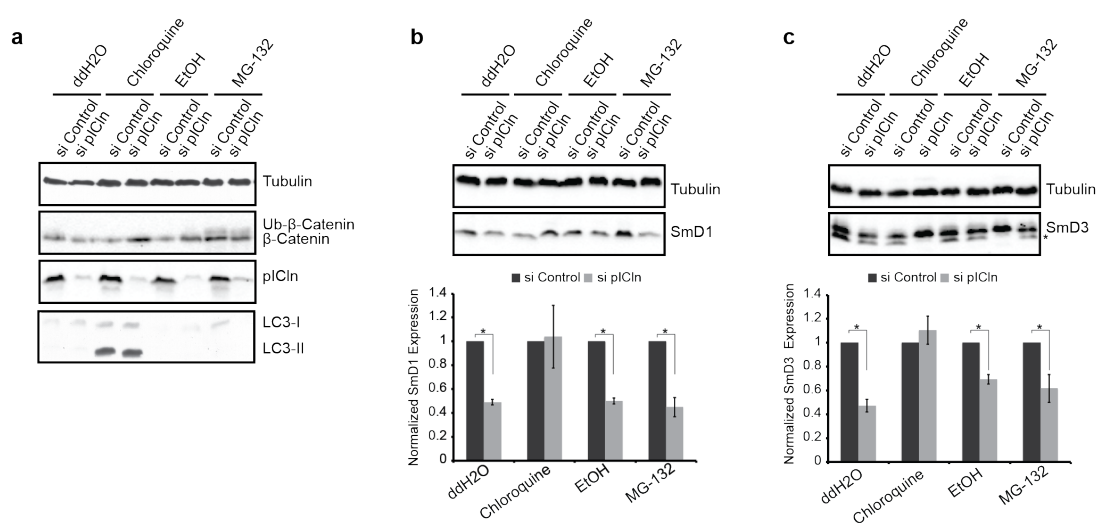


**Figure 4.8 Degradation of Sm proteins via autophagy in the absence of pICln**
Total lysates prepared in 1xSDS loading dye were analyzed by immunoblotting. **(a)** Stabilization of ubiquitinated β-catenin (upon MG-132 treatment) and accumulation of LC3-II (upon chloroquine treatment) show efficient inhibition of the proteasomal and autophagic pathways, respectively. **(b) and (c)** Immunoblots indicating the recovery of Sm D1 and D3 during pICln knockdown with the inhibition of autophagy. Lower panels- Quantification of normalized fold expression of Sm D1 and D3 from independent biological triplicates. Error bars -standard error * = $p \leq 0.05$ (Student's t-test). (Figure contribution- RM- 35 %, AP- 65 %; refer Table 7.7)

Having confirmed that the respective drugs work in a predicted manner, I next analyzed the cell extracts for the recovery of Sm protein levels upon pICln knockdown following the inhibition of either pathway. Stabilization of either ubiquitinated or non-ubiquitinated Sm proteins in the pICln knockdown cells compared to the controls was used as an indicative to

judge the pathway involved in Sm protein modulation. In this direction, it was shown that MG-132 treatment did not lead to the accumulation of either ubiquitinated or non-ubiquitinated Sm proteins upon pICln depletion. However, chloroquine stabilized SmD1 and SmD3 in the absence of pICln implicating autophagy as the mode of degradation (Figure 4.8(b) and (c); upper panels- Western blots, lower panels- quantification from biological triplicates).

The above-mentioned results demonstrate an elaborate post-translational surveillance mechanism for the Sm proteins upon depletion of pICln, the assembly chaperone, with the autophagy pathway coming into play to plausibly prevent the accumulation of Sm proteins.

### 4.1.5 Disruption of Sm protein homeostasis results in aggregation

The results above indicate an elaborate Sm protein surveillance system. I speculated that this system has evolved to prevent aggregation of this highly expressed and intrinsically hydrophobic protein class. This would imply that the newly synthesized Sm proteins that are neither protected by the assembly factors nor removed by autophagy, tend to aggregate. To investigate where the Sm proteins localize upon pICln knockdown, indirect immunofluorescence was performed. To this end, Flag-tagged SmD3 and SmD1 proteins were transiently over-expressed for 48 h and analyzed after blocking autophagy for 10 h in both the control and pICln deficient cells. FLAG-tagged SmD3 expressed by transient transfection localized to the Cajal bodies in control cells, where it co-localized with SMN and to nuclear speckles (i.e. interchromatin granular clusters and perichromatin fibrils). This is the typical pattern observed also for the endogenous Sm proteins (Figure 4.9(a)-(i) si Control). This pattern remained unaffected when cells were treated with chloroquine, indicating that this drug alone had no impact on the intracellular localization of Sm proteins (Figure 4.9(a)-(ii), si Control). However, removal of pICln (either +/- chloroquine) had a major impact on the intracellular localization of SmD3. In contrast to its speckled pattern observed under normal conditions, SmD3 now localized in large dispersed nuclear regions either within the nucleoli or as ring-like structures at the periphery of nucleoli (Figure 4.9(a)-(iii)&(iv) panels). A similar mis-localization pattern was observed with endogenous SmD3 as well, particularly with autophagy block (Figure 4.9(c)-(iii)&(iv)). Moreover, majority of these SmD3 aggregate-like nuclear structures co-stained very weakly with the $m^7G/m_3G$-cap detecting antibody showing impaired association with the capped U snRNA component (Figure 4.9(c)-(i) to (iv)).

Interestingly, SmD1-Flag accumulated in large cytoplasmic structures unlike the SmD3 nuclear structures (Figure 4.9(b)-(iii), (iv)). Apart from these observations, there was severe mis-localization of SMN (Figure 4.9(a)-(iii)) and other components of the SMN complex during pICln paucity (Figure 4.10). (Please refer Figure 7.1 for multichannel and Figure 7.2 for CUD immunofluorescence images).
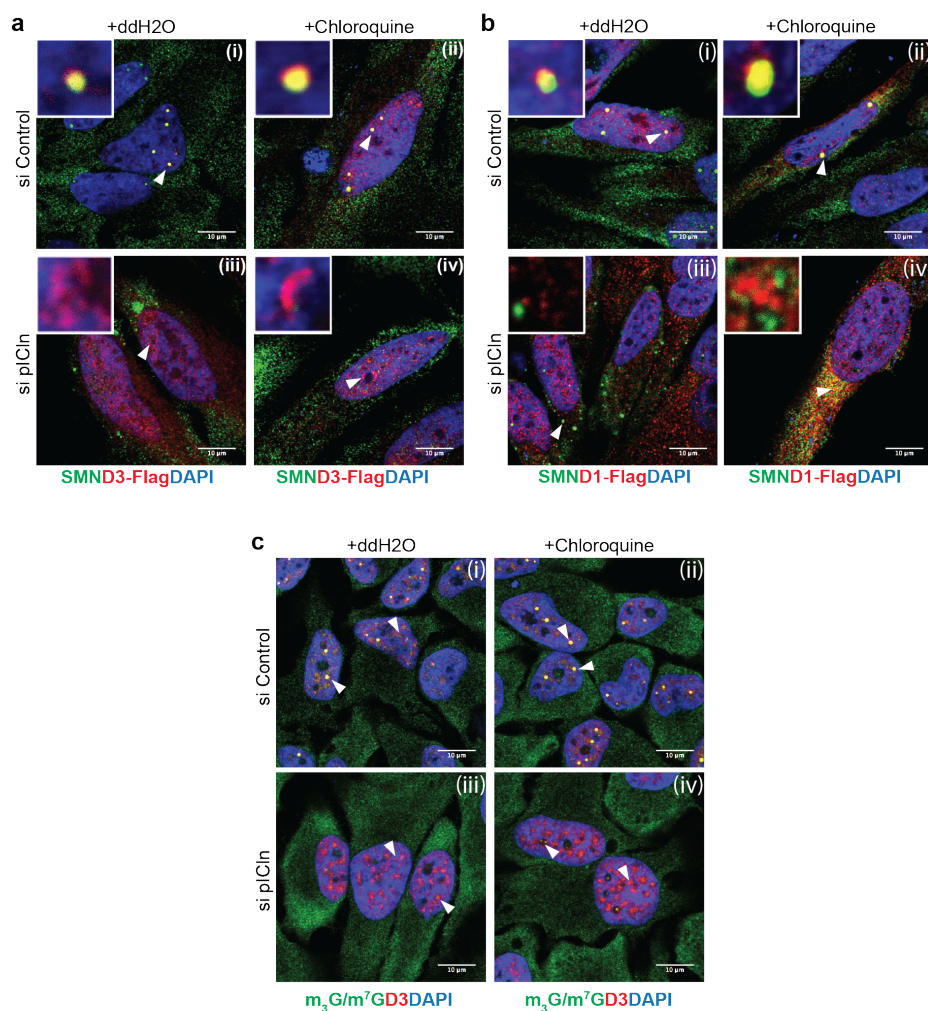


**Figure 4.9 Mis-localization of recovered newly translated Sm proteins in the absence of pICln**
Indirect immunofluorescence images showing **(a)** SmD3-Flag and SMN co-staining in control (upper panels) and pICln knockdown (lower panels) cells with water (ddH$_2$O) and chloroquine treatment. SmD3-Flag showed nuclear aggregates upon pICln depletion. **(b)** SmD1-Flag and SMN co-staining in control (upper panels) and pICln knockdown (lower panels) cells with water and chloroquine treatment. Sm D1-Flag showed cytoplasmic aggregates under pICln depletion. **(c)** co-staining of endogenous SmD3 and m$_3$G/ m$^7$G capped U snRNAs depicting very weak co-localization during pICln knockdown with water or chloroquine (lower panels). (Figure contribution- AP- 95 %, RM- 5 %; refer Table 7.7).
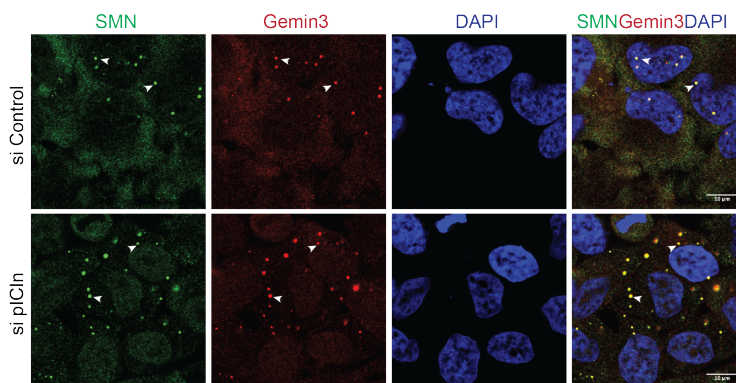
**Figure 4.10 Mis-localization of SMN complex during pICln deficiency**
SMN and Gemin3 formed numerous large cytoplasmic inclusions during pICln knockdown suggesting the mis-localization of SMN complex in the absence of pICln (lower last panel). (Figure contribution- AP-100 %; refer Table 7.7). Note: Please refer Figure 7.2(d) for CUD immunofluorescence images.

The indirect immunofluorescence experiments described above clearly demonstrate the accumulation and mis-localization of Sm proteins in the absence of pICln. There is a cause to believe that these mis-localized Sm proteins are unassembled and/or mis-assembled proteins as they are devoid of both U snRNA (Figure 4.9(c)-(i) to (iv)) and SMN (Figure 4.9(a)-(iii)). I next asked whether the accumulated Sm proteins indeed exist as insoluble aggregates. I wanted to address this by testing the solubility of the Sm proteins in extracts prepared from autophagy inhibited control and pICln deficient cells.

To this end, the soluble cell fractions prepared under these conditions were analyzed via Western blotting. There was no replenishment of SmD1 and D3 in the soluble fractions of the autophagy inhibited pICn deficient cells (Figure 4.11(b) and (c)). This was in contrast to the Sm protein recovery that was seen in total cell lysates, comprising of the soluble and the insoluble fractions of the cell (Figure 4.8(b) and (c); a comparison of Sm protein expression in soluble and total cell lysates is shown in Figure 4.11(d) and (e). Thus, it implicates that the unassembled or mis-assembled Sm proteins that are rescued from lysosomal degradation during pICln deficiency exist as insoluble aggregates. In summary, my results support a model in which pICln acts not only as an assembly chaperone but also as a ''classical chaperone'' in preventing the aggregation of the newly synthesized Sm proteins.
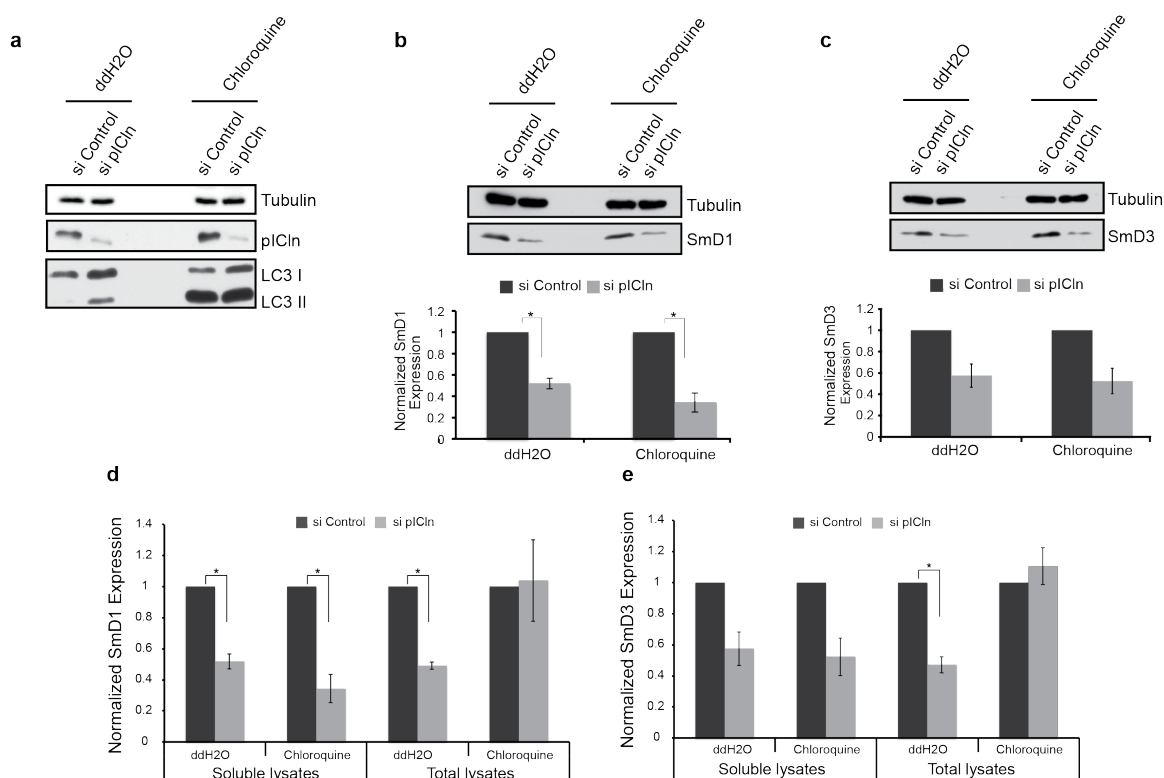
**Figure 4.11 No recovery of Sm proteins in soluble lysates upon autophagy inhibition during pICln paucity**

Soluble lysates prepared with 1% NP40 lysis buffer were analyzed by immunblotting. **(a)** Accumulation of LC3-II (after chloroquine treatment) shows efficient inhibition of the autophagy pathway. **(b) and (c)** Upper panel- No recovery of Sm D1 and D3 proteins in soluble lysates during pICln knockdown upon chloroquine treatment suggesting that the non-degraded Sm proteins result in insoluble aggregates. Lower panel- Quantification of normalized fold expression of Sm D1 and D3 from biological triplicates. **(d) and (e)** Comparison of soluble vs total lysates for the recovery of Sm proteins with chloroquine treatment. Error bars -standard error * = p≤0.05 (Student's t-test). (Figure contribution- RM-100%; refer Table 7.7)

## 4.2    A biochemical approach to identify new interactors of the SMN protein

Mediating the late assembly phase of the Sm class U snRNPs is certainly a major function of SMN. This activity is purely cytosolic and hence mediated by the SMN complex found in the same compartment. However, since the discovery of SMN in 1995, it has been known that SMN not only localizes to the cytoplasm but also to the nucleus, where the protein concentrates in Cajal bodies. Cajal bodies play a critical role in the final maturation of U snRNPs, as they are the sites where addition of the U snRNP-specific proteins and modifications of the U snRNAs occur.  SMN and the U snRNP biogenesis are crucial determinants of Cajal body number and integrity (Girard et al., 2006; Lemm et al., 2006). It is currently unclear whether Cajal bodies form merely a scaffold where snRNP assembly is enabled or whether this sub-nuclear domain also serves an active, probably even catalytic

role. Hence, the aim of this aspect of thesis was to gain insights into the potential role of SMN in the Cajal bodies (CBs). To this end, experiments were performed to analyze the nuclear and CB- interactome of SMN.

### 4.2.1 Identification of novel protein interacting proteins of SMN complex

To gain insight into the compartment-specific interactome of SMN, cytoplasmic and nuclear extracts were prepared from HeLa S3 cells (described in section 3.8.2). These extracts were first analyzed for cross-contamination from each other by analyzing equal amount of total protein from both the compartments via immunoblotting. Absence of tubulin and β-actin in nuclear extracts (Figure 4.12(a)) and Histone 3 and Prp4 (Figure 4.12(b)) in cytoplasmic extracts confirmed the successful separation of both compartments without significant cross-contamination. Interestingly, immunoblotting further revealed that SMN as well as the symmetrically dimethylated Sm proteins (Figure 4.12(c)) were more abundant in the nuclear fraction in comparison to the cytoplasm.
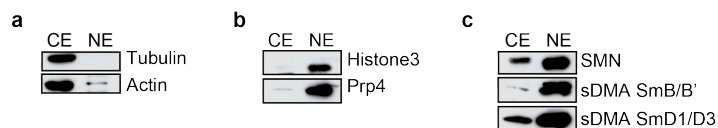


**Figure 4.12 Analysis of HeLa S3 cytoplasmic and nuclear extracts for cross-contamination**
Western blot of 25 μg cytoplasmic (CE) and nuclear (NE) HeLa S3 extracts using antibodies against α-Tubulin, β-Actin as cytoplasmic markers **(a)** and Histone H3, Prp4 as nuclear markers **(b)**. Enrichment of SMN and symmetrically dimethylated (sDMA) Sm proteins in cytoplasmic and nuclear extracts can be also seen **(c)**. (Figure contribution- RM- 100 %; refer Table 7.7)

Having established a protocol for the separation of nuclear and cytosolic fractions, I next aimed at a large-scale isolation of the Cajal bodies (CBs) from HeLa S3 (see section 3.8.5). This protocol started with the preparation of nuclear extract followed by the enzymatic degradation of chromatin. Subsequently, sucrose-percoll gradient was done to isolate the Cajal bodies. To detect which fractions of the gradient contained the Cajal bodies, they were analyzed via immunoblotting against coilin, the marker protein for CBs. Lanes 10-14 were found to contain the highest amounts of coilin indicating the presence of the Cajal bodies (Figure 4.13, lane 10 to 14). SMN was also detected in these fractions confirming SMN's association with Cajal bodies (Figure 4.13, lane 10 to 14). While these initial fractionation studies were successful, the protocol employed appeared to be not reproducible for unknown

technical reasons. Thus, I focused my studies on the isolation of the nuclear SMN complexes only.
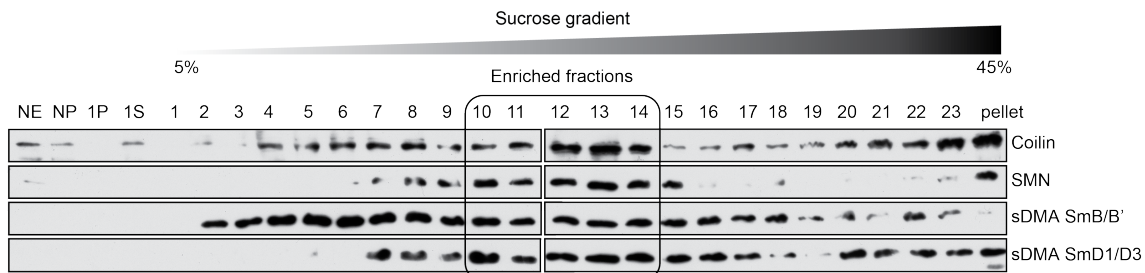


**Figure 4.13 Isolation of Cajal bodies**
30 µg of total protein from nuclear extract (NE), nucleoplasm (NP), pellet (1P) and supernatant (1S) from the first gradient along with the fractions harvested after the second gradient for Cajal body isolation were subjected to immunoblot analysis. Each fraction was analyzed for the presence of coilin, SMN, sDMA SmB/B' and sDMA SmD1, SmD3. Fractions 10 to 14 were highly enriched fractions for coilin, indicating the presence of Cajal bodies. (Figure contribution- RM- 100 %; refer Table 7.7)

Nuclear and cytoplasmic extracts were initially separated by a 5-45 % sucrose gradient centrifugation following which the sedimentation of SMN and the other key markers were analyzed by immunoblotting. Nuclear SMN sedimented consistently at higher S-values as compared to cytosolic SMN, suggesting differences in its interactome (Figure 4.14(a) and (b)). To gain insight into the biochemical composition of the nuclear SMN, an immunoaffinity purification using the monoclonal anti-SMN antibody (7B10) was performed and the interacting proteins were detected using gel electrophoresis followed by silver staining. Apart from the previously reported SMN complex members (indicated by black asterisks, Figure 4.15(a), lane 3, 4), novel putative interactors were also co-immunoprecipitated with both the cytoplasmic and nuclear SMN (indicated by blue and red asterisks; Figure 4.15(a), lane 3, 4). The co-purification of these interactors was found to be highly reproducible and hence were identified via mass spectrometry (MS).
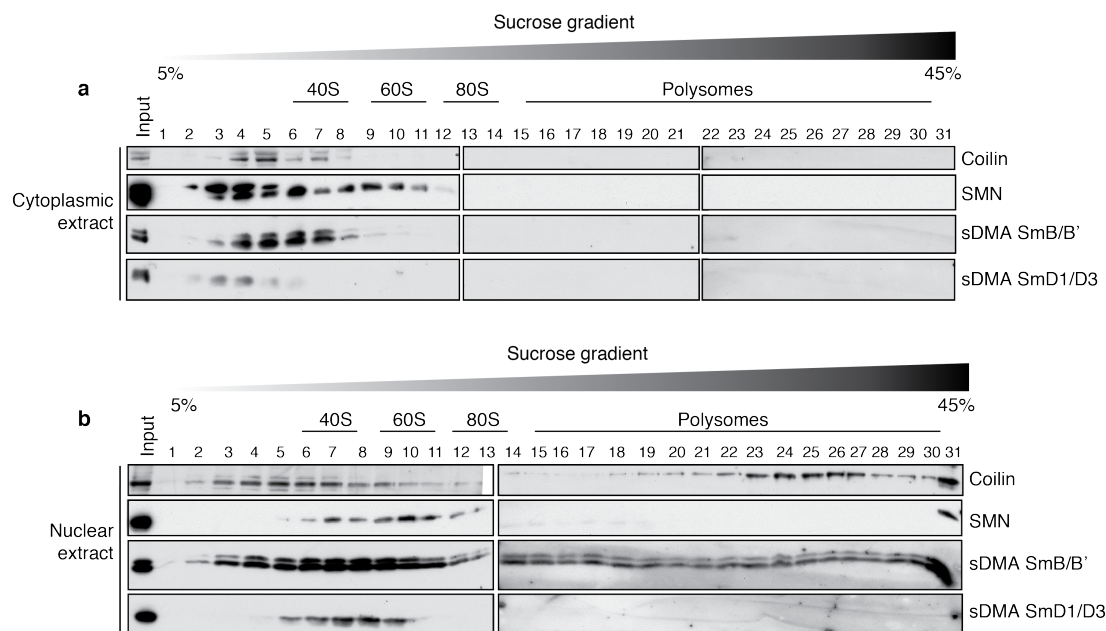
**Figure 4.14 Gradient centrifugation of HeLa S3 cytoplasmic and nuclear extracts**
Immunoblot analysis of gradient fractions obtained after subjecting HeLa S3 cytoplasmic **(a)** and nuclear **(b)** extracts to 5-45% sucrose gradient centrifugation. To have an overview about sedimentation coefficient of the migrating proteins, relative probable migration of ribosome subunits under these conditions is also depicted. Fractions 6 to 8 correspond to the sedimentation of 40S ribosome subunits, 9 to 11 correspond to 60S, 12 to 14 correspond to 80S and rest of the fractions correspond to the sedimentation of polysomes. (Figure contribution- RM- 100 %; refer Table 7.7)
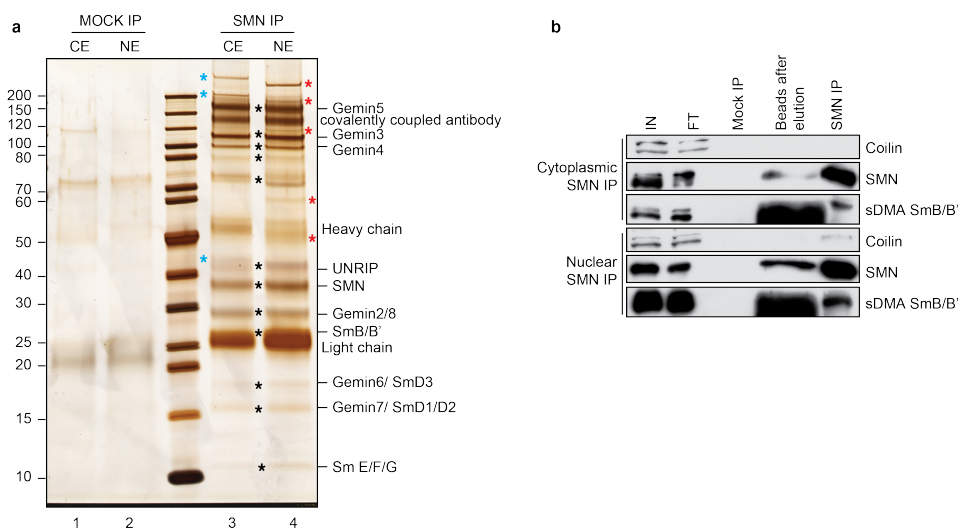


**Figure 4.15 Immunoprecipitation of endogenous SMN complex**
**(a)** Silver stained gel picture of SMN IP from cytoplasmic and nuclear extracts. Lanes 4 and 5 represent immunoprecipitated samples of SMN complex from cytoplasmic and nuclear fractions respectively. Lanes 1 and 2 represent corresponding mock controls without any antibody. **(b)** Western blot of SMN IP from cytoplasmic and nuclear extracts using antibodies against Coilin, SMN, SmB/B' and Sm D1/D3. Asterisks: putative novel proteins in cytosolic (blue) and nuclear (red) SMN IP; black- known interactors of SMN. (Figure contribution- RM- 70 %, MS- 30 %; refer Table 7.7)

As shown in Table 4.1, all known components of the SMN complex, namely SMN, Gemin2-8, and UNRIP were significantly enriched in purifications of both compartments. In addition, the Sm/LSm proteins B, D1, D2, D3, E, F G, LSm10 and 11 as well as the U1-specific protein SNRNP70 were co- purified (Table 4.1). However, Sm B and D1 were not as strongly enriched in nuclear SMN immunoprecipitates as compared to the cytoplasmic purifications (Table 4.1). Thus, the SMN complex with its known "substrate" proteins exists in both the compartments. I also noted interesting differences in the SMN purifications from both the compartments. The methyltransferase PRMT5, which acts as part of the PRMT5 complex upstream of the SMN complex was mostly enriched on the cytosolic SMN. In contrast, the CB marker protein coilin was found predominantly in nuclear SMN complexes (Table 4.1). These results validate the integrity of the SMN complexes in both the extracts and hence enabled the search for additional, yet unknown interactors of SMN. A detailed inspection of the list of identified polypeptides via mass spectrometry (Table 4.2) revealed several subunits of the Mediator complex (Table 4.2(b)) that appeared to co-immunoprecipitate specifically and exclusively with nuclear SMN. Mediator complex is a multi-subunit complex that orchestrates various steps involved in transcription. It consists of head (10 proteins), middle (6 proteins), tail (9 proteins), kinase (4) modules and other proteins that bind to nuclear transcription factors. This finding was interesting in the light of earlier reports where SMN was shown to interact with RNA polymerase and spliceosomal complexes (Makarov et al., 2012; Pellizzoni et al., 2001b).

**Table 4.1 List of well-known interactors of cytoplasmic and nuclear SMN obtained from MS data analysis**

Mean_CE, mean peptide intensities from cytoplasmic SMN IP; Mean_NE, mean peptide intensities from nuclear SMN IP; Sig. , Significance. The interactors that appeared in all three replicates were assigned significance 3, only in two experiments as 2 and so on.

| Gene Names | Sig._CE | Sig._NE | Mean_CE | Mean_NE | Score | Mol. Weight kDa |
|---|---|---|---|---|---|---|
| *Known interactors of SMN* | | | | | | |
| SMN1 | 3 | 3 | 7.95 | 5.59 | 323.31 | 31.689 |
| GEMIN2 | 3 | 3 | 10.22 | 7.80 | 254.1 | 29.931 |
| GEMIN3 | 3 | 3 | 8.01 | 6.56 | 323.31 | 92.239 |
| GEMIN4 | 3 | 3 | 8.67 | 6.85 | 323.31 | 120.04 |
| GEMIN5 | 3 | 3 | 11.34 | 10.28 | 323.31 | 168.59 |
| GEMIN6 | 3 | 3 | 9.61 | 7.78 | 323.31 | 18.824 |
| GEMIN7 | 3 | 3 | 8.47 | 9.50 | 127.64 | 14.536 |
| GEMIN8 | 3 | 3 | 9.60 | 7.65 | 323.31 | 28.636 |
| UNRIP | 3 | 3 | 8.90 | 8.64 | 323.31 | 38.438 |
| SNRPD2 | 3 | 3 | 8.56 | 6.74 | 290.69 | 13.527 |

| | | | | | |
|---|---|---|---|---|---|
| SNRPF | 3 | 3 | 6.93 | 5.93 | 71.377 | 9.7251 |
| SNRPG | 3 | 3 | 7.60 | 6.57 | 55.647 | 8.496 |
| LSM10 | 3 | 3 | 6.36 | 6.28 | 74.226 | 14.08 |
| LSM11 | 3 | 3 | 7.87 | 7.82 | 235.52 | 39.499 |
| SNRPD3 | 3 | 2 | 8.16 | 4.09 | 77.644 | 13.291 |
| SNRPE | 2 | 3 | 7.95 | 6.28 | 47.864 | 10.803 |
| SNRPB | 3 | 1 | 6.44 | 2.50 | 104.61 | 17.546 |
| SNRPD1 | 2 | 0 | 6.26 | Maybe | 50.279 | 13.281 |
| SNRNP70 | 3 | 3 | 10.29 | 7.08 | 323.31 | 51.556 |
| PRMT5 | 3 | 0 | 7.51 | N/A | 217.67 | 72.683 |
| COIL | 0 | 3 | N/A | 7.55 | 311.74 | 62.608 |

**Table 4.2 List of putative novel interactors of SMN from cytoplasmic (a), nuclear (b) and both (c) compartments obtained from MS data analysis**

Mean_CE, mean peptide intensities from cytoplasmic SMN IP; Mean_NE, mean peptide intensities from nuclear SMN IP; Sig. , Significance. The interactors that appeared in all three replicates were assigned significance 3, only in two experiments as 2 and so on.

| Gene Names | FDR.Sig. limma.CE | FDR.Sig. limma.NE | Mean_C E | Mean_ NE | Score | Mol. Weight kDa |
|---|---|---|---|---|---|---|
| *(a) Novel interactors that associate with SMN in the cytoplasm* | | | | | | |
| ARHGEF11 | 3 | 0 | 9.56 | N/A | 323.31 | 172.24 |
| ATXN1L | 3 | 0 | 6.01 | N/A | 167.15 | 73.305 |
| USP9X | 2 | 0 | 4.85 | N/A | 301.11 | 290.46 |
| *(b) Novel interactors that associate with SMN in the nucleus* | | | | | | |
| MED13 | 0 | 3 | N/A | 7.03 | 323.31 | 239.29 |
| MED1 | 0 | 3 | N/A | 6.05 | 323.31 | 168.48 |
| MED14 | 0 | 3 | N/A | 5.78 | 323.31 | 160.6 |
| MED17 | 0 | 3 | N/A | 5.71 | 311.55 | 72.889 |
| MED13L | 0 | 3 | N/A | 5.67 | 323.31 | 242.6 |
| ZBTB7A | 0 | 3 | N/A | 5.48 | 239.74 | 61.438 |
| MED11 | 0 | 3 | N/A | 5.18 | 38.458 | 13.129 |
| CDK8 | 0 | 3 | N/A | 4.87 | 139.38 | 53.155 |
| MED15 | 0 | 3 | N/A | 3.86 | 304.91 | 82.58 |
| MED22 | 0 | 2 | N/A | 4.39 | 89.866 | 12.853 |
| MED20 | 0 | 2 | N/A | 4.23 | 113.47 | 23.222 |
| MED30 | 0 | 2 | N/A | 4.16 | 159.39 | 16.279 |
| RBM4 | 0 | 2 | N/A | 3.91 | 199.81 | 40.313 |
| MED8 | 0 | 2 | N/A | 3.84 | 99.037 | 29.08 |
| MED23 | 0 | 2 | N/A | 3.83 | 323.31 | 155.55 |
| MED4 | 0 | 2 | N/A | 3.70 | 134.43 | 29.745 |
| MED27 | 0 | 2 | N/A | 3.61 | 56.329 | 31.351 |
| MED25 | 0 | 2 | N/A | 3.43 | 124.24 | 84.388 |
| MED6 | 0 | 2 | N/A | 3.35 | 140.57 | 28.723 |
| MED16 | 0 | 2 | N/A | 3.35 | 264.77 | 93.028 |
| ZNF326 | 0 | 2 | N/A | 3.20 | 96.2 | 65.653 |
| MED24 | 0 | 2 | N/A | 2.96 | 323.31 | 112.18 |
| MED29 | 0 | 2 | N/A | 2.91 | 203.75 | 23.472 |

| | | | | | | |
|---|---|---|---|---|---|---|
| TAF5L | 0 | 1 | N/A | 3.25 | 80.75 | 66.155 |
| MED18 | 0 | 1 | N/A | 3.23 | 43.548 | 23.662 |
| CCNC | 0 | 1 | N/A | 2.78 | 57.645 | 26.513 |
| *(c) Novel interactors that associate with SMN in both cytoplasm and nucleus* | | | | | | |
| ARHGEF5 | 3 | 3 | 10.29 | 6.85 | 323.31 | 176.8 |
| MED12 | 3 | 3 | 6.82 | 7.32 | 323.31 | 243.39 |
| ARNT | 3 | 3 | 7.65 | 5.35 | 323.31 | 86.636 |
| PKN2 | 2 | 3 | 6.66 | 7.02 | 323.31 | 112.03 |
| BCKDK | 2 | 3 | 4.03 | 8.52 | 218.98 | 46.36 |
| HOMEZ | 2 | 3 | 5.36 | 6.06 | 154.87 | 61.24 |
| MSH3 | 2 | 3 | 4.10 | 6.77 | 323.31 | 127.41 |
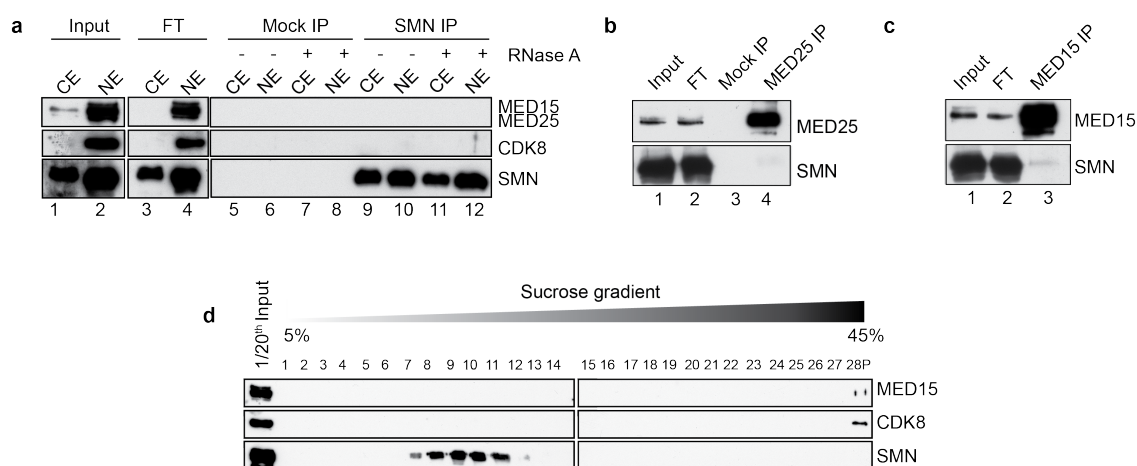


**Figure 4.16 Validation of Mediator complex as an interactor of SMN complex**
Immunoblot analysis of **(a)** SMN IP with MED 15, 25 and CDK 8 antibodies from cytosolic and nuclear extracts in the presence (Lane 9 and 10) and absence (Lane 11 and 12) of RNaseA treatment, respectively. **(b) and (c)** MED 25 (Lane 4) and MED 15(Lane 3) IPs with SMN antibody, respectively. **(d)** sucrose gradient fractions of nuclear extract with MED 15, CDK 8 and SMN antibodies to study co-migration. (Figure contribution- RM- 100 %; refer Table 7.7)

Next, I wished to confirm these interactions by independent biochemical approaches. To this end, two experiments were performed. Firstly, the immunoprecipitated SMN complexes were analyzed by Western blotting using monoclonal antibodies against the mediator subunits MED15, 25 and CDK8. As shown in Figure 4.16(a), neither of these components could be detected in the immunoprecipitates even though the antigens were easily detectable in the complete nuclear extracts (see input lane for nuclear extract). Likewise, SMN was also not detectable in the MED25 and MED15 immunoprecipitates (Figure 4.16(a), (b)). Secondly, I tested whether MED15 and/or CDK 8 co-migrate with the SMN complex in sucrose gradients. As shown in Figure 4.16(d), neither MED 15 nor CDK 8 co-migrated with SMN.

Thus, even though the mediator subunits were readily detectable by mass spectrometry, independent biochemical experiments could not confirm these observations. These results hinted at the possibility of SMN interaction with Mediator complex being either 'transient' or 'sub-stoichiometric'.

# 5    Discussion

## 5.1    Regulation of Sm protein homeostasis

The assembly of many macromolecular machines such as U snRNPs, ribosomes, nucleosomes etc., can occur spontaneously in dilute solutions *in vitro*. This indicates that the information for the formation of the respective particle lies within the individual components. However, the situation in cells is dramatically different: here, most of the intracellular space is occupied by macromolecules, metabolites etc., with the total concentration of biomolecules being as high as 400 mg/mL (Ellis and Minton, 2003). This "molecular crowding" within the cell often hinders diffusion driven, faithful self-assembly among cognate interactors making the assistance by assembly factors essential. Cells, therefore, engage a set of mostly un-related factors to assist assembly (or disassembly) and folding (or unfolding) of the individual components ultimately leading to the formation of macromolecular entities. The absence of these factors potentially pose a challenge to the cells, as the unassembled components often contain exposed hydrophobic surfaces that would lead to non-specific aggregation in a crowded cellular environment. This could result in cytotoxicity depending on the pathogenicity of the aggregates formed. Hence, it is an indispensable task for the cells to employ various defensive mechanisms to tightly control the production, assembly and turnover of all the aggregation-prone proteins. This would help in maintaining the cellular homeostasis.

In this thesis, I have described the cellular consequences of disturbed snRNP assembly *in vivo*. By using targeted inactivation of key components of the U snRNP assembly machinery, I demonstrated a crucial role of the assembly chaperone, pICln, in the Sm protein homeostasis. Furthermore, I revealed a complex multi-layered cellular regulatory mechanism when the intricate balance between the PRMT5-SMN system is affected. These mechanisms either prevent or clear Sm protein aggregates when they are not channeled into U snRNP assembly as in this case.

### 5.1.1    Inhibition of the late assembly phase causes tailback of Sm proteins over pICln followed by transcriptional down regulation of Sm encoding transcripts.

The late assembly assisting factor, SMN complex (Gemin 5, in particular) enables distinction between target and non-target RNAs (Battle et al., 2006b; Lau et al., 2009). This allows the

specific incorporation of the Sm proteins to only the target U snRNAs (Battle et al., 2006b; Lau et al., 2009), probably explaining the requirement of the SMN complex *in vivo*. Apart from this, I wanted to understand if there is any other potential relevance for the existence of SMN complex, particularly in handling the aggregation-prone Sm proteins. This was addressed by tracing the path of the Sm proteins in the assembly pathway upon perturbing the core component of the complex, SMN. Inactivation of this late assembly factor prevented, as expected from earlier studies, the delivery of Sm proteins onto snRNA (Figure 4.4(a), lane 11, 12, Figure 4.4(b)). I reasoned that this causes a potentially dangerous situation for the cell as it would lead to the accumulation of the unassembled and aggregation-prone free Sm proteins. It was shown in this thesis that under SMN paucity, the Sm proteins are tailing back on pICln in their kinetically trapped state, the 6S complex (Figure 4.4(a), lane 7, 8; Figure 4.4(b)). This most likely prevents the infidelities during U snRNP assembly posed by the uncontrolled release of the Sm proteins.

My results clearly have shown that the very abundant pICln protein buffers the uncontrolled deposition of the Sm proteins. However, the extent of buffering depends on the availability of the total cellular pool of pICln under steady state conditions. During prolonged SMN depletion, where the buffering capacity of pICln becomes saturated and there is risk of Sm proteins to overflow, degradation of the Sm protein encoding mRNAs occurred (Figure 4.5(a)). The degradation of these transcripts was mediated by exosome as the transcripts were recovered with the inhibition of exosome using 5- fluorouracil (Figure 4.5(b)). It has been demonstrated earlier that SMN deficiency results in lower levels of U snRNAs (Zhang et al., 2008). I could confirm these earlier findings and provide evidence that this down-regulation of U snRNAs was also a consequence of exosome-mediated degradation (Figure 4.5(b)).

The picture emerging from these studies uncovered an elaborate cellular response that is bi-phasic upon defects in the late assembly phase. In the initial phase, the emphasis is on safeguarding the already produced Sm proteins. This is achieved by pICln, which not only pre-arranges the Sm proteins into higher order complexes but also simultaneously shields, directly or indirectly the hydrophobic surfaces of the Sm proteins. By these measures, the aggregation of Sm proteins is efficiently prevented. In a later phase, with the prolonged absence of SMN, the cells successively emphasize to stop the production of the Sm proteins itself by the exosome-mediated destabilization of the Sm protein encoding transcripts. This

would ultimately add to decreased U snRNP biogenesis. Even though the U snRNP turnover deficits were reported, until now there is no account on the down-regulation of Sm proteins in SMA patients. I demonstrated an unprecedented scenario of Sm transcript down regulation via exosome in the absence of SMN. A similar situation could be speculated in Spinal Muscular Atrophy (SMA), wherein functional SMN levels are reduced.

### 5.1.2 Post-translational surveillance of Sm proteins in the absence of the early assembly factor pICln

Among the early assembly factors, the role of pICln is less understood. It is established that *in vivo* pICln segregates the early assembly phase into two distinct assembly lines where it pre-organizes Sm proteins into higher order structures (Neuenkirchen et al., 2015) for the later recruitment by the SMN complex. However, *in vitro*, pICln is not required for the recruitment of Sm proteins by the SMN complex. Considering the sequestration of the free unassembled Sm proteins by pICln in the absence of SMN, I wanted to study what happens to these unassembled Sm proteins when the buffering system offered by pICln itself is removed. The first line of evidence from previous studies in our lab demonstrated the arrest of Sm D1/D2 at the ribosome exit tunnel as an immediate response to the absence of pICln. This suggested that pICln assists controlled release of the Sm proteins into the assembly pathway right immediately after their synthesis.

In this dissertation, I could show that the prolonged absence of pICln resulted in a cellular response that caused the down-regulation of Sm proteins (Figure 4.6). Interestingly, this was neither a result of feedback regulation on the Sm gene transcription nor translational arrest (Figure 4.7(a),(b)). Therefore, I speculated that the protein degradation pathways could help in clearing the unassembled Sm proteins. This was indeed the case since prolonged absence of pICln led to the post-translational down regulation of Sm proteins via autophagy (Figure 4.8) in contrast to the post-transcriptional down-regulation of transcripts encoding Sm proteins upon SMN knockdown (Figure 4.5). The most affected Sm proteins were Sm D1, D2, D3 and B/B′ (Figure 4.6, Table 7.4) which are associated with pICln immediately after their synthesis. It is currently unclear why the Sm proteins E, F, G are less affected upon pICln knockdown (Figure 4.6(b), Table 7.4). One possible explanation is that they are capable of forming toroidal heterohexamers ($(FEG)_2$) independent of pICln (Xu et al., 2005). Since in this complex no hydrophobic surface is exposed, these three Sm proteins probably evade aggregation by protecting themselves. Further studies are needed to prove that this is indeed the case.

Considering the hydrophobic nature and the down regulation of the Sm proteins via autophagy in the absence of pICln, I reasoned that one of the major function of the "safety-belt" provided by pICln is to safeguard cells from the potential threat caused by the Sm protein aggregation. What happens to the Sm proteins when this safety-belt provided by pICln is absent? My findings have indeed shown that the Sm proteins form insoluble aggregates when pICln is removed (Figure 4.11). These insoluble aggregates could be non-functional as they showed mis-localization and absence of both SMN and U snRNA. The mis-localized Sm aggregates were either nuclear (for SmD3) or cytosolic (for SmD1) (Figure 4.9 and Figure 4.10). The nuclear diffusion of SmD3 forming aggregates was independent of SMN, which could be probably either via simple diffusion owing to its small size or because of the nuclear localization signal (NLS) in its binding partner SmB (Bordonne, 2000). On the other hand, the cytosolic SmD1 aggregates hint that during the prolonged absence of pICln, the stalled SmD1 is plausibly released from the ribosomes eventually forming cytosolic aggregates.

My findings identify pICln not only as an assembly chaperone but also as a "classical" chaperone by preventing the aggregation of Sm proteins and thereby acting as a master regulator of U snRNP biogenesis pathway. Search for mutations of pICln in the online databases has been not linked to any diseases. However, knockout of pICln results in the death of murine embryos at very early stages of development between E3.5 to E7.5 (Pu et al., 2000). Why is pICln such an essential gene? The significance of Sm proteins lies in the fact that they are inevitably required for splicing, a process that is indispensable for the survival of eukaryotic cells. The pivotal role played by pICln in preventing these Sm proteins from aggregation and their subsequent degradation described in this thesis allows speculating the plausible reason for the embryonic lethality in mice. The model summarizing my findings has been depicted in Figure 5.1.
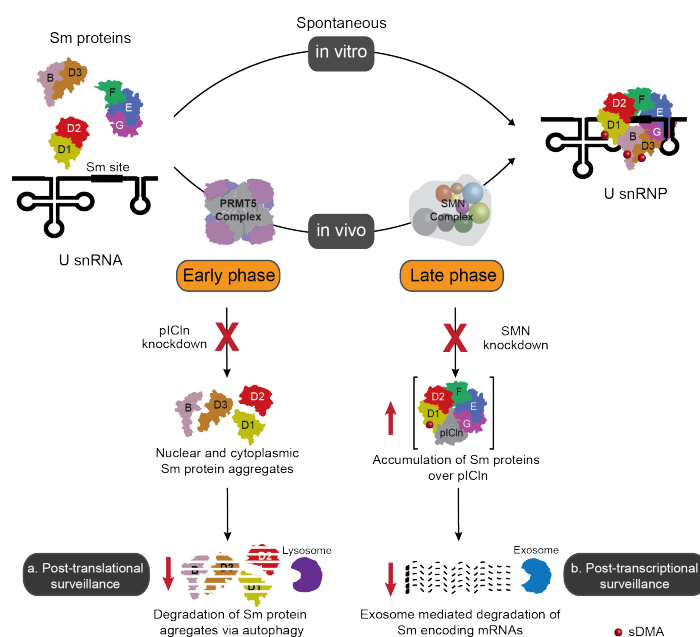
**Figure 5.1 Schematics showing the *in vitro* and *in vivo* assembly of U snRNPs**
**(a) Post-translational surveillance.** Disruption of early phase by the depletion of pICln results in aggregation of Sm proteins followed by their lysosomal degradation via autophagy. **(b) Post-transcriptional surveillance.** Disruption of late phase by the reduction of SMN results in initial accumulation of Sm proteins over pICln followed by the post-transcriptional degradation of Sm protein encoding transcripts via exosome. (sDMA- symmetrically dimethylated arginines)

### 5.1.3 pICln paucity leads to retention of SMN complex in the cytoplasm and Cajal body disintegration.

Absence of pICln would hamper the symmetrical dimethylation of the Sm proteins and hence their subsequent handover to the SMN complex. Supporting this view, I could show that the insoluble Sm aggregates formed during the absence of pICln lacked both SMN and U snRNA (Figure 4.9, Figure 4.10). So, U snRNP assembly being the main function of SMN, I reasoned that the main purpose of SMN to deliver the cargo (assembled U snRNPs) to the nucleus will not occur in the absence of pICln that will probably affect the nuclear localization of SMN. In this direction, I could show that the absence of pICln resulted in the cytoplasmic accumulation of SMN in the form of compact foci (Figure 4.10). These foci contain Gemin3 (but lack the Sm proteins, Figure 4.9(a)&(b)) suggesting the accumulation of not only SMN but also the other Gemins of the SMN complex (Figure 4.10). Cajal bodies (the sites for final maturation of U snRNPs) formation depends on the ongoing U snRNP biogenesis (Girard et al., 2006; Lemm et al., 2006). The retention of SMN complex in the cytoplasm coupled with the down regulation of the Sm proteins in the absence of pICln would affect the formation of new U snRNPs. This eventually led to the disintegration of the Cajal bodies substantiating the U snRNP formation defects in the absence of pICln (Figure 4.10, Figure 7.3).

The initial observations from the microscopy experiments performed in my thesis suggested that the cytoplasmic SMN foci could be stress granules (SGs) as they disappeared with the addition of chloroquine for 10 h. Earlier reports have shown similar disappearance pattern of the stress granules (SGs) during prolonged treatment either with MG-132 alone or along with chloroquine due to Hsp70 chaperone activity (Seguin et al., 2014). There was also another study addressing the localization of over-expressed SMN to SGs during cellular stress (Hua and Zhou, 2004b). Taken together these studies, one can hypothesize the probable presence of SMN in stress granules during pICln paucity. However, the exact mechanism of the formation and composition of these foci needs to be further investigated.

## 5.2    Compartment specific interactome analysis of SMN complex

Since the discovery of the involvement of SMN in SMA by Judith Melki's lab in 1995, several labs have worked on demonstrating the cytoplasmic role of SMN in the U snRNP assembly pathway. The ubiquitously expressed SMN is present in both the cytoplasm as well as nucleus. In the nucleus, the major fraction of the SMN is concentrated in sub-nuclear, non-membranous domains called Cajal bodies (CBs) (Sleeman and Lamond, 1999). SMN not only assists the assembly of U snRNPs in the cytoplasm but also in delivering the cargo to the nucleus, particularly to the CBs. CBs serve as the venue for further modifications of premature U snRNPs, namely, addition of several specific proteins and post-transcriptional modifications on the U snRNA. CB number and integrity is in turn dependent on the U snRNP biogenesis and the presence of SMN (Girard et al., 2006; Lemm et al., 2006).

Even though the cytoplasmic role of SMN in the U snRNP assembly pathway is well established, several open questions exist in understanding the nuclear role of SMN in general and also, the reasons for its significant enrichment in CBs. Firstly, how the assembled U snRNPs are dissociated from the SMN complex in Cajal bodies? U snRNPs need to be dissociated from SMN complex for further modifications to form higher order complexes in CBs before they are recruited for splicing. Recent studies reported that coilin, whose oligomerization is important for Cajal body framework, could be involved in the dissociation of U snRNPs (Hebert et al., 2001; Tapia et al., 2014; Xu et al., 2005). I wanted to study if there are any other factors that contribute to this process. Secondly, how the highly stable U snRNPs are disassembled? Given the high abundance of U snRNPs and also their essential

role in splicing, I made an assumption that their turnover and quality control needs to be tightly controlled. For this, I hypothesized the possible involvement of CBs in U snRNP turnover. I reasoned that the high concentrations of SMN in CBs probably play a role in disassembly of U snRNPs as it was shown that under certain *in vitro* conditions, SMN could reverse the U snRNP assembly reaction (Chari et al., 2008). Further, the disassembled U snRNPs could be either recycled for next round of the assembly or targeted for degradation.

Understanding the molecular mechanisms involved in the above-mentioned scenarios would explain the significant enrichment of SMN in Cajal bodies. For this purpose, I employed compartment-specific (cytoplasmic, nuclear and CBs) analysis of the SMN interactome to gain insight into the factors involved, if any, facilitating these processes. I reasoned that such an approach would enable to exclude non-specific interactors that would exist in disturbing cellular dynamics while analyzing total cellular lysates. Besides, as SMN complex is a multi-component system, over-expressing any of the components of the system alone might lead to non-stoichiometric populations *in vivo*. So isolation of the endogenous SMN complex using monoclonal antibody targeting SMN was employed. However, successful isolation of CBs could not be achieved considering the time frame of my thesis. Hence, I focused on the nuclear role of SMN in general.

Among the several interactors that have been reported for SMN over the past decades (see Table 7.1), only a few appeared consistent in their interaction with SMN. These include Gemin2-8, UNRIP, Sm proteins, Lsm10 and 11, PRMT5 and coilin. The same was also evident in the compartment-specific immunoprecipitations performed in this thesis work (Table 4.1). The ultra-centrifugation analysis of cytoplasmic and nuclear extracts revealed that SMN exists in the nucleus in higher order structures as compared to its cytoplasmic counterpart (Figure 4.14). Supporting this, the mass spectrometry (MS) data of the nuclear SMN, indicated the 1.2 MDa, 31 multi-subunit Mediator complex as a promising interactor, with many of the subunits from the head, middle, tail and the kinase modules of the Mediator complex being evident (Table 4.2(b)). Mediator complex, a part of the core transcription machinery, regulates various aspects of transcriptional initiation, elongation, termination and couples it to splicing. This hit was interesting as previous studies reported SMN associates with the spliceosomal E complex for stabilizing interactions of U1 and U2 snRNPs with pre-mRNA (Makarov et al., 2012) and also with RNA polymerase II (Pellizzoni et al., 2001b; Zhao et al., 2016). Although neither of the subunits from spliceosomal complex E nor RNA polymerase II were obtained in

the MS experiments performed in this thesis, the presence of Mediator complex subunits suggested the probable involvement of SMN in the co-transcriptional splicing process. However, all attempts to validate the interaction of SMN with MED15 and MED25 subunits failed (Figure 4.16). This suggests that the mediator is not a major interactor of SMN. However, one cannot exclude the possibility that this unit interacts either transiently or sub-stoichiometrically with SMN.
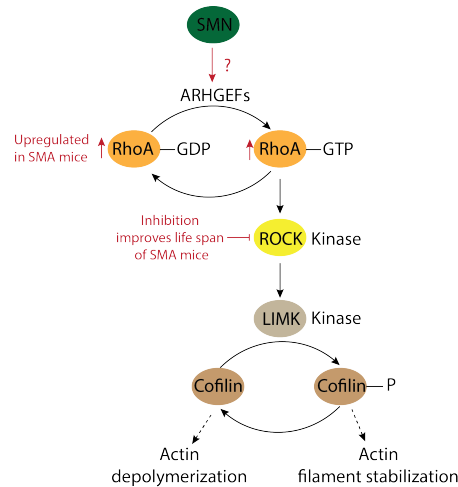


**Figure 5.2 Schematics showing the Rho-dependent pathway involved in regulating actin dynamics**
Rho guanine nucleotide exchange factors, ARHGEFs, promote the addition of GTP to RhoA proteins. The immediate downstream targets of RhoA proteins are Rho protein associated Kinases (ROCK). These kinases further activate LIM kinases (LIMK), which phosphorylate the Cofilin protein that leads to actin filament stabilization. An upregulation of RhoA protein in Spinal Muscular Atrophy (SMA) mice has been linked to change in actin dynamics. SMN's probable interaction with ARHGEFs hints towards its role in regulation of actin dynamics.

Apart from the Mediator complex, other plausible SMN interactors obtained were the Rho guanine nucleotide exchange factors (ARHGEFs; a class of Rho GTPases) that include ARHGEF 11 (in the cytoplasm; Table 4.2(a)) and ARHGEF5 (cytoplasm and nucleus; Table 4.2(c)). The ARHGEF family of proteins activates RhoA GTPase proteins by promoting their GTP-bound state and thus play an important role in the pathway regulating actin dynamics (Figure 5.2). The RhoA GTPase proteins are reported to be up-regulated in SMA mice (Bowerman et al., 2010). Also, the life span of SMA mice was improved by the treatment with inhibitors of the downstream effector proteins of this pathway (namely, Rho protein associated Kinases or ROCK) (Bowerman et al., 2010). The interaction with ARHGEF proteins is suggestive of SMN's probable involvement in actin dynamics. However these targets need to be validated by independent approaches and such experiments are ongoing.

# 6    Conclusion

Macromolecular crowding and cellular compartmentalization hinder the spontaneous self-assembly of macromolecular machines unlike *in vitro* conditions. Hence, cells employ not only molecular chaperones to protect individual subunits from aggregation but also a number of other factors that allow their specific unification to form functional complexes. But how the cells cope up with the assembly problem that becomes evident in the absence of these factors? The risk of formation of aggregation and dead-end non-functional complexes poses an extreme demand on the cell to stringently regulate the protein homeostasis. In this thesis, I studied the consequences arising because of the absence of assembly factors using U snRNP assembly pathway as an example. Amongst the assembly of several macromolecular machines, U snRNP biogenesis pathway is one of the very well studied pathways that use a complex PRMT5-SMN system for its assembly. It appears that these assembly factors united in the PRMT5-SMN system associates with the Sm proteins right immediately after their translation and drive them through the pathway until functional complexes are formed. I demonstrated an interesting model of complex cellular strategies involving post-transcriptional and post-translational surveillance mechanisms that are triggered in the absence of these assembly factors. The trigger of such mechanisms either prevented or cleared the Sm protein aggregates thereby safeguarding the cells from plausible cytotoxicity. The potential relevance of why cells employ such a macromolecular system for an essential task of association of the seven small Sm proteins with the U snRNA can be inferred from this thesis. Altogether, I believe that the insights gained into this pathway may also presumably help to understand the assembly of many other macromolecular complexes, for example ribosomes, nucleosomes etc.

# 7    Annexure

**Figure 7.1 Indirect immunofluorescence depicting mis-localization of unassembled Sm proteins during depletion of pICln**

Immunofluorescence images of control and pICln knockdown cells after water (ddH$_2$O) or chloroquine treatment. **(a)** co-staining of SmD3-Flag(red) , SMN(green), chromatin (DAPI) and overlay images (i)-(iv) showing nuclear inclusions of SmD3-Flag in pICln deficient cells (iii) and (iv). **(b)** co-staining of SmD1-FLAG (red) , SMN(green), chromatin (DAPI) and overlay images (i)-(iv) showing cytosolic inclusions of SmD1-Flag in pICln deficient cells (iii) and (iv). The zoomed region in the top left corner of each image represents the white arrowheads. **(c)** co-staining of endogenous SmD3 (red), m$_3$G/m$^7$G capped RNA (green), chromatin (DAPI) and overlay images (i)-(iv) showing nuclear inclusions of endogenous SmD3 in pICln deficient cells (iii) and (iv).
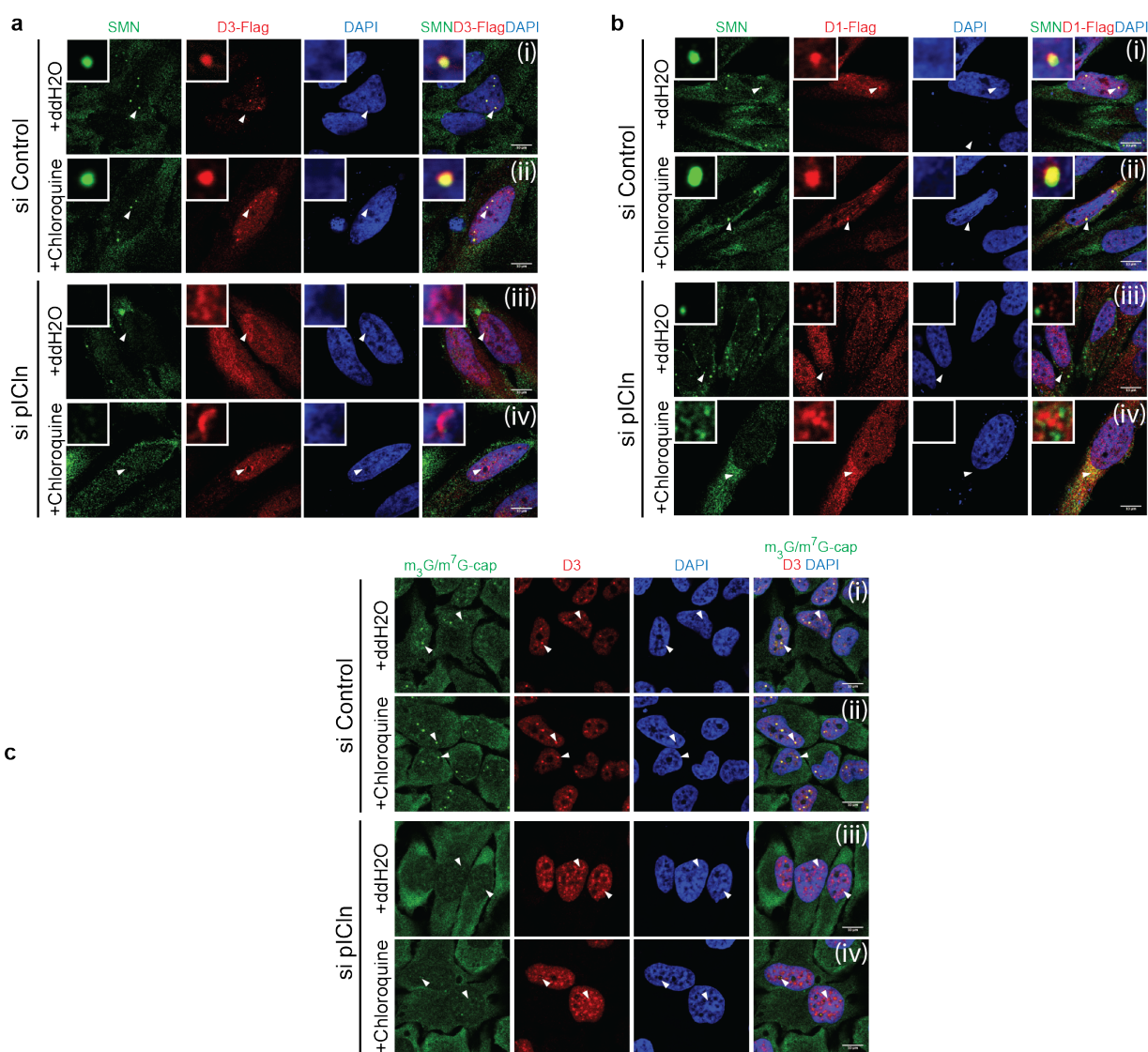
**Figure 7.2 Indirect immunofluorescence depicting mis-localization of unassembled Sm proteins during depletion of pICln (CUD images)**

Immunofluorescence images of control and pICln knockdown cells following water (ddH2O) or chloroquine treatment. **(a)** co-staining of SmD3-Flag(magenta) , SMN(green) and overlay images (i)-(iv) showing nuclear inclusions of SmD3-Flag in pICln deficient cells (iii) and (iv). **(b)** co-staining of SmD1-FLAG (magenta) , SMN(green) and overlay images (i)-(iv) showing cytosolic inclusions of SmD1-Flag in pICln deficient cells (iii) and (iv). The zoomed region in the top left corner of each image represents the white arrowheads. **(c)** co-staining of endogenous SmD3 (magenta), $m_3G/m^7G$ capped RNA (green) and overlay images (i)-(iv) showing nuclear inclusions of endogenous SmD3 in pICln deficient cells (iii) and (iv). **(d)** SMN (green) and Gemin3 (magenta) formed numerous large cytoplasmic inclusions during pICln knockdown.
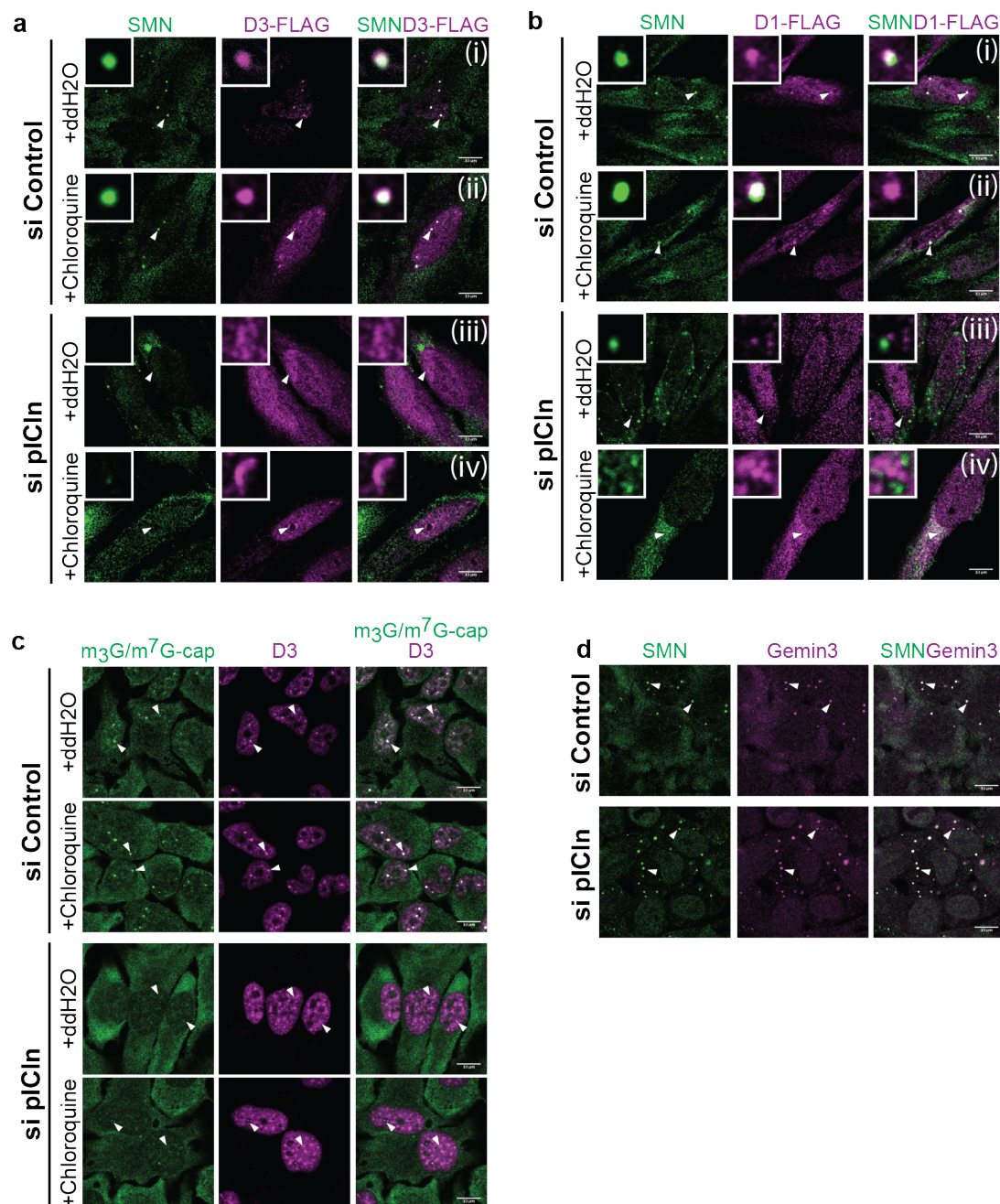
**Figure 7.3 Disintegration of Cajal bodies in the pICln deficient cells**

Indirect immunofluorescence images of control and pICln deficient cells. In the absence of pICln, SMN (red) and Gemin5 (red) are mis-localized forming compact foci in the cytoplasm (lower panel). Along with this, the Cajal bodies stained for coilin as red concentric spots in the nucleus (arrow heads in the nucleus) are disintegrated in pICln deficient cells suggestive U snRNP turnover deficits (third image of lower panel).
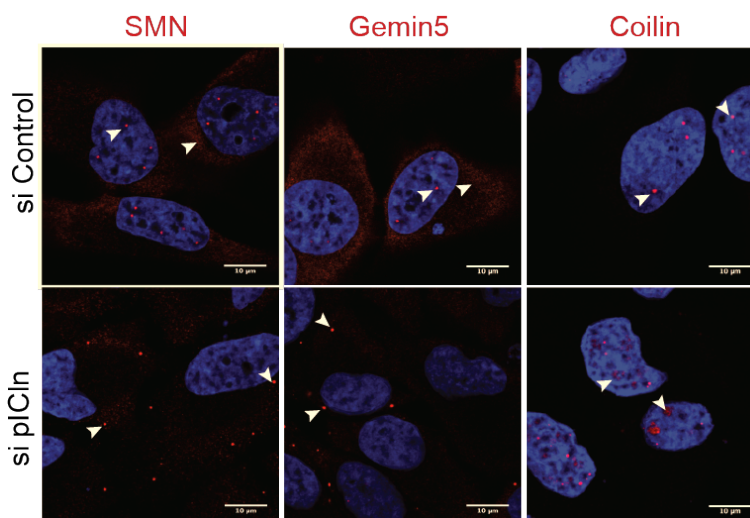


**Table 7.1 List of known SMN interactors and their probable roles in association with SMN other than the core SMN components**

(adopted and modified from the book chapter of Cell Biology of the Axon by Edward Koenig)

| Protein | Probable role | Reference |
|---|---|---|
| *RNA metabolism* | | |
| Snurportin, Importin | Nuclear import of U snRNPs | (Narayanan et al., 2002) |
| TGS1 | Hypermethylation of 5' cap of U snRNAs in cytoplasm | (Mouaikel et al., 2003) |
| hnRNP U, Q, R | Pre-mRNA splicing | (Liu and Dreyfuss, 1996; Mourelatos et al., 2001; Rossoll et al., 2002) |
| KH-type splicing regulatory protein | Neuro-specific alternative splicing, mRNA decay | (Tadesse et al., 2008; Williams et al., 2000) |
| U1-70K | Pre-mRNA splicing, Gem integrity | (Makarov et al., 2012) (Stejskalova and Stanek, 2014) |
| Nucleolin and B23 | rRNA metabolism | (Lefebvre et al., 2002) |
| Galectin 1 | Pre-mRNA splicing | (Park et al., 2001) |
| Fibrillarin and GAR1 | sno RNP assembly | (Jones et al., 2001; Liu and Dreyfuss, 1996; Pellizzoni et al., 2001a) |
| WRAP53 | Targeting SMN to Cajal bodies | (Mahmoudi et al., 2010) |
| Coilin | Cajal body formation | (Hebert et al., 2001) |
| Interferon stimulating gene 20 (ISG20) | Degradation of ssRNA, maturation of U snRNPs | (Espert et al., 2006) |
| Zinc finger protein R1 (ZPR1) | Protein translation and localization of SMN to nuclear bodies | (Gangwani et al., 2001) |

| | | |
|---|---|---|
| Hu antigen D (HuD) | For recruitment of HuD and its mRNA targets into neuronal RNA granules | (Hubers et al., 2011) |
| Fused In Sarcoma protein (FUS) | Connection between biochemical pathways leading to ALS and SMA diseases | (Yamazaki et al., 2012) (Sun et al., 2005) |
| Multiple Myeloma SET Domain Containing Protein Type III (MMSET) | Histone methyltransferase and role in pre-mRNA splicing | (Mirabella et al., 2014) |
| Insulin-Like Growth Factor 2 MRNA Binding Protein 1 (IMP1) | -actin mRNA binding protein and regulates its axonal localization | (Fallini et al., 2014) |
| NUFIP | U4 snRNP maturation | (Bizarro et al., 2015) |

*Stress granule-related role*

| | | |
|---|---|---|
| TIA-1- related protein (TIAR) | Stress granule formation | (Hua and Zhou, 2004b) |
| Rpp20 (Subunit of RNase P) | tRNA and rRNA metabolism | (Hua and Zhou, 2004a) |

*Transcriptional regulation*

| | | |
|---|---|---|
| Ewing's Sarcoma protein (EWS) | Transcriptional regulation | (Young et al., 2003) |
| Papilloma Virus E2 | Transcriptional regulation | (Strasswimmer et al., 1999) |
| Epstein-Barr Virus nuclear antigen2 and DP103 | Transcriptional regulation | (Voss et al., 2001) (Barth et al., 2003) |
| Minute Virus NS1 and NS2 | | (Young et al., 2002b) |
| RIF1 | Transcriptional repressor | |
| Nuclear factor associated with dsRNA (NFAR1/2) | Post-transcriptional regulation during viral infection | (Saunders et al., 2001) |
| RNA helicase A (RNA polymerase II) | Transcription | (Pellizzoni et al., 2001b) |
| Senataxin | Transcription termination | (Suraweera et al., 2009) (Zhao et al., 2016) |
| RNA polymerase II | Transcription termination | (Zhao et al., 2016) |

*Regulation of phosphorylation status of SMN complex*

| | | |
|---|---|---|
| Protein phosphatase 4(PPP4) | Ser/Thr protein phosphatase | (Carnegie et al., 2003) |
| Protein phosphatase 1 γ and PTPN3 | Effects phosphorylation state of SMN and Cajal body integrity | (Husedzinovic et al., 2015; Renvoise et al., 2012) |

*Apoptosis-related proteins*

| | | |
|---|---|---|
| p53 | Impaired association might lead to apoptosis | (Young et al., 2002a) |
| Bcl-2 | Anti-apoptotic role of SMN | (Iwahashi et al., 1997) |
| HLA-B associated transcript 3 (BAT3) | Regulation of p53 | (Stelzl et al., 2005) |

*Actin metabolism*

| | | |
|---|---|---|
| Profilin | Controls actin dynamics | (Giesemann et al., 1999) |
| T- Plastin | Actin binding | (Oprea et al., 2008) |
| FMRP | Actin filament organization, Dendrite and axon morphogenesis | (Piazzon et al., 2008) |
| Annexin II and Myosin | May help in understanding | (Shafey et al., 2010) |

| regulatory light chain protein (MRLC) | pathophysiology of SMA | |
|---|---|---|
| *Others* | | |
| Myb- binding protein 1a | Unknown function | (Fuller et al., 2010) |
| Osteoclast stimulating factor (OSF) | Src- related signaling | (Kurihara et al., 2001) |
| Ubiquitin-specific protease 9 (USP9X) | Deubiquitylating enzyme | (Trinkle-Mulcahy et al., 2008) |
| Fibroblast growth factor 2 (FGF-2) | Growth factor | (Claus et al., 2003) |
| Hsc70 | Protein folding/ trafficking | Meistel et al., 2001 |
| UNC119 | Photoreceptor synaptic protein | (Stelzl et al., 2005) |
| Growth differentiating factor 9 (GDF9) | Growth factor | (Stelzl et al., 2005) |
| COP9 signalosome subunit 6 (COPS6) | Regulation of Ubiquitin ligase | (Stelzl et al., 2005) |
| Pseudophosphorylated αB crystallin | Nuclear chaperone | (den Engelsman et al., 2013) |
| Telomerase holoenzyme (hTERT) | Telomerase biogenesis, Telomere maintenance | (Bachand et al., 2002) |

**Table 7.2 List of known posttranslational modifications of SMN complex members and Sm proteins**
(Brahms et al., 2000; Husedzinovic et al., 2014)

| Protein | Post-translational modifications |
|---|---|
| *Phosphorylation sites* | |
| SMN | Ser 4, 5, 8, 18, 28, 31, 88, 180 |
| | Thr 25, 62, 68, 69 |
| Gemin2 | Ser 81 |
| Gemin3 | Ser 48, 187, 268, 320, 505, 520, 522, 549, 557, 560, 672, 677, 687, 703, 714 |
| | Thr 552, 558, 705, 748 |
| Gemin4 | Ser 86 |
| | Thr 84 |
| Gemin5 | Ser 48, 624, 757, 765, 778, 847, 852 |
| | Thr 51, 751, 853 |
| Gemin6 | Ser 95, 166 |
| Gemin7 | None identified thus far |
| Gemin8 | None identified thus far |
| Unrip | None identified thus far |
| pICln | Ser144 |
| *Symmetrically dimethylated sites* | |
| Sm B/B' | Arg 108, 112, 147, 172, 181, 209 |
| SmD1 | Arg 98, 100, 102, 104, 106, 108, 110, 112, 114 |
| SmD3 | Arg 97, 110, 112, 114, 117 |

**Table 7.3 List of regulated proteins identified by pSILAC analysis in the absence of SMN**

The proteins that are represented in red (highly significant) and orange (moderately significant) in the graph plot are represented in the bold and regular font, respectively. **Note**- The percentage of proteins left during the knockdown from duplicate experiments (1 and 2) is represented.

| Gene.names | Full name | norm.med.log2.Ratio.H.M.normalized.SMN_1 | norm.med.log2.Ratio.H.M.normalized.SMN_2 | Percentage of protein left during SMN KD compared to control_1 | Percentage of protein left during SMN KD compared to control_2 |
|---|---|---|---|---|---|
| **SMN1** | **Survival motor neuron protein** | **2.72** | **2.12** | **15** | **23** |
| **VIM** | **Vimentin** | **2.15** | **0.50** | **23** | **70** |
| **HNRNPC** | **Heterogeneous nuclear ribonucleoproteins C1/C2** | **2.09** | **0.41** | **24** | **75** |
| **NPM1** | **Nucleophosmin** | **0.92** | **0.30** | **53** | **81** |
| **ITPR3** | **Inositol 1,4,5-trisphosphate receptor type 3** | **0.88** | **0.29** | **54** | **82** |
| **HNRNPU** | **Heterogeneous nuclear ribonucleoprotein U** | **0.87** | **0.20** | **55** | **87** |
| **DDX20** | **Probable ATP-dependent RNA helicase DDX20** | **0.79** | **0.93** | **58** | **53** |
| **L1CAM** | **Neural cell adhesion molecule L1** | **0.68** | **0.64** | **62** | **64** |
| **SUSD2** | **Sushi domain-containing protein 2** | **0.68** | **0.77** | **63** | **59** |
| **ASS1** | **Argininosuccinate synthase** | **0.62** | **0.19** | **65** | **88** |
| **ERLIN2** | **Erlin-2** | **0.56** | **0.84** | **68** | **56** |
| **TMEM43** | **Transmembrane protein 43** | **0.52** | **0.61** | **70** | **66** |
| **SOAT1** | **Sterol O-acyltransferase 1** | **0.51** | **0.79** | **70** | **58** |
| **LBR** | **Lamin-B receptor** | **0.49** | **0.67** | **71** | **63** |
| **NPEPPS** | **Puromycin-sensitive aminopeptidase** | **0.45** | **0.41** | **73** | **75** |
| H2AFY | Core histone macro-H2A.1;Histone H2A | 2.06 | 0.15 | 24 | 90 |
| RBMX | RNA-binding motif protein, X chromosome;RNA-binding motif protein, X chromosome, N-terminally processed | 1.75 | 0.30 | 30 | 81 |
| SIPA1 | Signal-induced proliferation-associated protein 1 | 1.75 | 0.13 | 30 | 92 |
| HIST1H4A | Histone H4 | 1.72 | 0.25 | 30 | 84 |
| SAP18 | Histone deacetylase complex subunit SAP18 | 1.65 | 0.16 | 32 | 89 |
| HIST2H2BE; HIST1H2BB; HIST1H2BO; HIST1H2BJ; HIST3H2BB | Histone H2B type 2-E;Histone H2B type 1-B;Histone H2B type 1-O;Histone H2B type 1-J;Histone H2B type 3-B | 1.60 | 0.12 | 33 | 92 |
| HIST1H3A | Histone H3.1 | 1.59 | 0.03 | 33 | 98 |
| HIST1H2BN; HIST1H2BM; HIST1H2BH; | Histone H2B;Histone H2B type 1-M;Histone H2B type 1-N;Histone H2B type 1-H;Histone H2B type 2-F;Histone H2B type 1-C/E/F/G/I;Histone H2B type 1-D;Histone H2B type 1-K;Histone H2B | 1.52 | 0.05 | 35 | 97 |

| | | | | | |
|---|---|---|---|---|---|
| HIST2H2BF; HIST1H2BC; HIST1H2BD; HIST1H2BK; HIST1H2BL; H2BFS | type 1-L;Histone H2B type F-S | | | | |
| ADAR | Double-stranded RNA-specific adenosine deaminase | 1.52 | 0.11 | 35 | 93 |
| HIST2H2AC; HIST2H2AA3 | Histone H2A type 2-C;Histone H2A type 2-A | 1.51 | 0.04 | 35 | 98 |
| RBM14 | RNA-binding protein 14 | 1.50 | 0.11 | 35 | 93 |
| PLEC | Plectin | 1.47 | 0.16 | 36 | 89 |
| PNN | Pinin | 1.41 | 0.35 | 38 | 79 |
| PLEC | Plectin | 1.35 | 0.10 | 39 | 93 |
| IFI44L | Interferon-induced protein 44-like | 1.27 | 0.07 | 42 | 95 |
| SP3 | Transcription factor Sp3 | 1.20 | 0.29 | 44 | 82 |
| THRAP3 | Thyroid hormone receptor-associated protein 3 | 1.20 | 0.22 | 44 | 86 |
| THOC6 | THO complex subunit 6 homolog | 1.16 | 0.23 | 45 | 86 |
| POLDIP3 | Polymerase delta-interacting protein 3 | 1.13 | 0.06 | 46 | 96 |
| BCLAF1 | Bcl-2-associated transcription factor 1 | 1.10 | 0.08 | 46 | 94 |
| ERH | Enhancer of rudimentary homolog | 1.03 | 0.03 | 49 | 98 |
| LAS1L | Ribosomal biogenesis protein LAS1L | 1.02 | 0.29 | 49 | 82 |
| FABP3 | Fatty acid-binding protein, heart | 1.01 | 0.68 | 50 | 63 |
| HNRNPM | Heterogeneous nuclear ribonucleoprotein M | 0.99 | 0.16 | 50 | 90 |
| NUMA1 | Nuclear mitotic apparatus protein 1 | 0.99 | 0.09 | 50 | 94 |
| DHX9 | ATP-dependent RNA helicase A | 0.98 | 0.18 | 51 | 89 |
| MKI67 | Antigen KI-67 | 0.96 | 0.16 | 51 | 89 |
| RBM3 | Putative RNA-binding protein 3 | 0.93 | 0.23 | 52 | 85 |
| FIP1L1 | Pre-mRNA 3-end-processing factor FIP1 | 0.93 | 0.11 | 53 | 92 |
| APOBEC3C | DNA dC->dU-editing enzyme APOBEC-3C | 0.89 | 0.04 | 54 | 97 |
| ILF2 | Interleukin enhancer-binding factor 2 | 0.89 | 0.16 | 54 | 90 |
| PPP1CC | Serine/threonine-protein phosphatase;Serine/threonine-protein phosphatase PP1-gamma catalytic subunit | 0.87 | 0.27 | 55 | 83 |
| POLR1A | DNA-directed RNA polymerase I subunit RPA1;DNA-directed RNA polymerase | 0.77 | 0.33 | 59 | 80 |
| ATP6V0A1 | V-type proton ATPase 116 kDa subunit a isoform 1 | 0.77 | 0.23 | 59 | 85 |
| SYNCRIP | Heterogeneous nuclear ribonucleoprotein Q | 0.75 | 0.24 | 60 | 85 |
| NUP153 | Nuclear pore complex protein Nup153 | 0.74 | 0.02 | 60 | 99 |

| WDR18 | WD repeat-containing protein 18 | 0.71 | 0.19 | 61 | 88 |
|---|---|---|---|---|---|
| RANBP2 | E3 SUMO-protein ligase RanBP2 | 0.68 | 0.19 | 62 | 88 |
| DEK | Protein DEK | 0.68 | 0.31 | 63 | 80 |
| NAT10 | N-acetyltransferase 10 | 0.67 | 0.17 | 63 | 89 |
| FAM98A | Protein FAM98A | 0.67 | 0.07 | 63 | 95 |
| CTH | Cystathionine gamma-lyase | 0.62 | 0.34 | 65 | 79 |
| COL6A1 | Collagen alpha-1(VI) chain | 0.61 | 0.50 | 66 | 70 |
| KHDRBS1 | KH domain-containing, RNA-binding, signal transduction-associated protein 1 | 0.61 | 0.03 | 66 | 98 |
| BAG2 | BAG family molecular chaperone regulator 2 | 0.60 | 0.28 | 66 | 82 |
| SRRM2 | Serine/arginine repetitive matrix protein 2 | 0.58 | 0.01 | 67 | 99 |
| LIMA1;TRMT1 | LIM domain and actin-binding protein 1 | 0.57 | 0.08 | 67 | 94 |
| TGM2 | Protein-glutamine gamma-glutamyltransferase 2 | 0.55 | 0.33 | 68 | 80 |
| RPRD1B | Regulation of nuclear pre-mRNA domain-containing protein 1B | 0.51 | 0.28 | 70 | 82 |
| LAPTM4A | Lysosomal-associated transmembrane protein 4A | 0.50 | 0.68 | 71 | 62 |
| NAPRT | Nicotinate phosphoribosyltransferase | 0.48 | 0.27 | 72 | 83 |
| SNTB2 | Beta-2-syntrophin | 0.48 | 0.48 | 72 | 72 |
| CAV1 | Caveolin-1;Caveolin | 0.46 | -0.01 | 73 | 101 |
| NUDT19 | Nucleoside diphosphate-linked moiety X motif 19, mitochondrial | 0.46 | 0.27 | 73 | 83 |
| ERLIN1 | Erlin-1 | 0.44 | 0.52 | 74 | 70 |
| ASPH | Aspartyl/asparaginyl beta-hydroxylase | 0.42 | 0.32 | 75 | 80 |
| LGALS1 | Galectin-1 | 0.41 | 0.46 | 75 | 73 |
| ALDH1A3 | Aldehyde dehydrogenase family 1 member A3 | 0.39 | 0.32 | 77 | 80 |
| DDAH1 | N(G),N(G)-dimethylarginine dimethylaminohydrolase 1 | 0.38 | 0.27 | 77 | 83 |
| UGP2 | UTP--glucose-1-phosphate uridylyltransferase | 0.37 | 0.29 | 78 | 82 |
| OAS3 | 2-5-oligoadenylate synthase 3 | 0.35 | 0.24 | 78 | 85 |
| FDFT1 | Squalene synthase | 0.30 | 0.43 | 81 | 74 |
| RPL7A | 60S ribosomal protein L7a | 0.29 | 0.52 | 82 | 70 |
| KRT18 | Keratin, type I cytoskeletal 18 | 0.26 | 0.42 | 84 | 75 |
| FDPS | Farnesyl pyrophosphate synthase | 0.22 | 0.32 | 86 | 80 |
| MT-CO2 | Cytochrome c oxidase subunit 2 | 0.18 | 0.63 | 88 | 65 |
| CENPH | Centromere protein H | 0.11 | 0.80 | 93 | 57 |
| POLR3H | DNA-directed RNA polymerase III subunit RPC8 | 0.05 | 0.82 | 96 | 57 |
| ACSL1 | Long-chain-fatty-acid--CoA ligase 1 | 0.04 | 1.18 | 98 | 44 |
| **CHD1** | **Chromodomain-helicase-DNA-binding protein 1** | **-1.05** | **-0.54** | **207** | **145** |
| **ADAM9** | **Disintegrin and metalloproteinase domain-containing protein 9** | **-0.90** | **-1.08** | **187** | **212** |
| **COL12A1** | **Collagen alpha-1(XII) chain** | **-0.72** | **-0.40** | **165** | **132** |

| | | | | | |
|---|---|---|---|---|---|
| **GSN** | **Gelsolin** | **-0.39** | **-0.39** | **131** | **131** |
| MACF1 | Microtubule-Actin Crosslinking Factor 1 | -1.03 | -0.04 | 204 | 103 |
| PARP1 | Poly [ADP-ribose] polymerase 1 | -1.02 | -0.09 | 203 | 106 |
| SUPT16H | FACT complex subunit SPT16 | -0.88 | -0.18 | 184 | 113 |
| DST | Dystonin | -0.72 | -0.04 | 165 | 103 |
| CTSL | Cathepsin L1;Cathepsin L1 heavy chain;Cathepsin L1 light chain | -0.64 | -0.87 | 156 | 183 |
| DPYD | Dihydropyrimidine dehydrogenase [NADP(+)] | -0.64 | -0.15 | 155 | 111 |
| CTSC | Dipeptidyl peptidase 1;Dipeptidyl peptidase 1 exclusion domain chain;Dipeptidyl peptidase 1 heavy chain;Dipeptidyl peptidase 1 light chain | -0.51 | -0.34 | 142 | 126 |
| S100A2 | Protein S100-A2 | -0.46 | -0.35 | 138 | 127 |
| TRIM16 | Tripartite motif-containing protein 16 | -0.36 | -0.21 | 128 | 116 |
| SNCG | Gamma-synuclein | -0.33 | -0.20 | 126 | 115 |
| S100A14 | Protein S100-A14 | -0.23 | -0.78 | 117 | 171 |

**Table 7.4 List of regulated proteins identified by pSILAC analysis in the absence of pICln**

The proteins that are represented in red (highly significant) and orange (moderately significant) in the graph plot are represented in bold and regular font, respectively. **Note-** The percentage of proteins left during the knockdown from duplicate experiments (1 and 2) is represented.

| Gene.names | Full name | norm.med.log2.Ratio.H.M.normalized.pICln_1 | norm.med.log2.Ratio.H.M.normalized.pICln_2 | Percentage of protein left during pICln KD compared to control_1 | Percentage of protein left during pICln KD compared to control_2 |
|---|---|---|---|---|---|
| **CLNS1A** | **Chloride Channel, Nucleotide-Sensitive, 1A** | **2.45** | **3.84** | **18** | **7** |
| **SNRPD2** | **Small Nuclear Ribonucleoprotein D1 Polypeptide 16kDa** | **0.88** | **1.02** | **54** | **49** |
| **SNRPD1** | **Small Nuclear Ribonucleoprotein D2 Polypeptide 16.5kDa** | **0.86** | **1.10** | **55** | **47** |
| **SNRPD3** | **Small Nuclear Ribonucleoprotein D3 Polypeptide 18kDa** | **0.84** | **1.19** | **56** | **44** |
| MDN1 | Midasin AAA ATPase 1 | 0.87 | 0.74 | 55 | 60 |
| SNRPN;SNRPB | Small Nuclear Ribonucleoprotein Polypeptides B And B1 | 0.75 | 0.61 | 59 | 66 |
| REEP5 | Receptor Accessory Protein 5 | 0.56 | 0.76 | 68 | 59 |
| SPC24 | SPC24, NDC80 Kinetochore Complex Component | 0.48 | 1.02 | 72 | 49 |
| SNCA | Synuclein, Alpha (Non A4 Component Of Amyloid Precursor) | 0.47 | 1.02 | 72 | 49 |
| HNRNPUL1 | Heterogeneous Nuclear Ribonucleoprotein U-Like 1 | 0.47 | 0.90 | 72 | 54 |

| | | | | | |
|---|---|---|---|---|---|
| DHFR | Dihydrofolate Reductase | 0.42 | 0.60 | 75 | 66 |
| C16orf13 | Chromosome 16 Open Reading Frame 13 | 0.42 | 0.97 | 75 | 51 |
| PHB | Prohibitin | 0.36 | 0.76 | 78 | 59 |
| PHB2 | Prohibitin 2 | 0.32 | 0.95 | 80 | 52 |
| KHSRP | KH-Type Splicing Regulatory Protein | 0.32 | 0.87 | 80 | 55 |
| ENO3 | Enolase 3 (Beta, Muscle) | 0.25 | 1.18 | 84 | 44 |
| KRT18 | Keratin 18, Type I | 0.15 | 1.28 | 90 | 41 |
| **COL5A1** | **Alpha 1 Type V Collagen** | **-1.12** | **-1.23** | **218** | **235** |
| **TGM2** | **Transglutaminase 2** | **-0.88** | **-1.33** | **184** | **252** |
| **GALNT2** | **Polypeptide N-Acetylgalactosaminyltransferase 2** | **-0.85** | **-0.66** | **180** | **158** |
| **DPYSL3** | **Dihydropyrimidinase-Like 3** | **-0.78** | **-0.64** | **172** | **156** |
| **CD59** | **CD59 Molecule, Complement Regulatory Protein** | **-0.44** | **-1.39** | **136** | **263** |
| SPTBN1 | Spectrin, Non-Erythroid Beta Chain 1 | -0.93 | -2.40 | 190 | 526 |
| ITGA11 | Integrin, Alpha 11 | -0.78 | -0.59 | 172 | 151 |
| MET | MET Proto-Oncogene, Receptor Tyrosine Kinase | -0.78 | -0.32 | 172 | 125 |
| PTPRF | Protein Tyrosine Phosphatase, Receptor Type, F | -0.76 | -0.36 | 169 | 128 |
| ITGA5 | Integrin, Alpha 5 (Fibronectin Receptor, Alpha Polypeptide) | -0.75 | -0.65 | 168 | 157 |
| PHLDA3 | Pleckstrin Homology-Like Domain, Family A, Member 3 | -0.67 | -0.95 | 160 | 193 |
| TIMP1 | Tissue Inhibitor Of Metalloproteinases 1 | -0.67 | -1.03 | 159 | 205 |
| GALNT1 | Polypeptide N-Acetylgalactosaminyltransferase 1 | -0.65 | -0.58 | 157 | 150 |
| ANXA3 | Annexin A3 (OR) Inositol 1,2-Cyclic Phosphate 2-Phosphohydrolase | -0.63 | -0.39 | 155 | 131 |
| PTGES | Prostaglandin E Synthase | -0.57 | -1.31 | 148 | 247 |
| NCEH1 | Neutral Cholesterol Ester Hydrolase 1 | -0.53 | -0.88 | 145 | 184 |
| GPRC5A | G Protein-Coupled Receptor, Class C, Group 5, Member A | -0.45 | -1.63 | 136 | 309 |
| SERPINB5 | Serpin Peptidase Inhibitor, Clade B (Ovalbumin), Member 5 | -0.42 | -0.54 | 133 | 145 |
| NT5E | 5'-Nucleotidase, Ecto (CD73) | -0.41 | -2.10 | 133 | 429 |
| CBX5 | Chromobox Homolog 5 | -0.39 | -1.06 | 131 | 209 |
| FOLR1 | Folate Receptor 1 (Adult) | -0.31 | -1.24 | 124 | 236 |

**Table 7.5 List of SMN interactome**

The complete list of proteins identified via Mass Spectrometry of the immunoprecipitated SMN from cytoplasmic (CE) and nuclear (NE) extracts (n=3). Based on false discovery rate (fdr), significance of various proteins was assigned as 3 (present in all triplicate sets), 2 (present in two sets), 1= (only one experiment).

| Gene. names | Protein.names | Mol. weightk Da | Score | mean CE | fdr.sig. limma. CE | mean NE | fdr.sig. limma. NE |
|---|---|---|---|---|---|---|---|
| GEMIN5 | Gem-associated protein 5 | 168.59 | 323.31 | 11.34 | 3 | 10.28 | 3 |
| GEMIN2 | Gem-associated protein 2 | 29.931 | 254.1 | 10.22 | 3 | 7.80 | 3 |
| GEMIN7 | Gem-associated protein 7 | 14.536 | 127.64 | 8.47 | 3 | 9.50 | 3 |
| STRAP | Serine-threonine kinase receptor-associated protein | 38.438 | 323.31 | 8.90 | 3 | 8.64 | 3 |
| GEMIN6 | Gem-associated protein 6 | 18.824 | 323.31 | 9.61 | 3 | 7.78 | 3 |
| SNRNP70 | U1 small nuclear ribonucleoprotein 70 kDa | 51.556 | 323.31 | 10.29 | 3 | 7.08 | 3 |
| GEMIN8 | Gem-associated protein 8 | 28.636 | 323.31 | 9.60 | 3 | 7.65 | 3 |
| ARHGEF5 | Rho guanine nucleotide exchange factor 5 | 176.8 | 323.31 | 10.29 | 3 | 6.85 | 3 |
| LSM11 | U7 snRNA-associated Sm-like protein LSm11 | 39.499 | 235.52 | 7.87 | 3 | 7.82 | 3 |
| GEMIN4 | Gem-associated protein 4 | 120.04 | 323.31 | 8.67 | 3 | 6.85 | 3 |
| SNRPD2 | Small nuclear ribonucleoprotein Sm D2 | 13.527 | 290.69 | 8.56 | 3 | 6.74 | 3 |
| DDX20 | Probable ATP-dependent RNA helicase DDX20 | 92.239 | 323.31 | 8.01 | 3 | 6.56 | 3 |
| SNRPG; SNRPGP15 | Small nuclear ribonucleoprotein G;Putative small nuclear ribonucleoprotein G-like protein 15 | 8.496 | 55.647 | 7.60 | 3 | 6.57 | 3 |
| MED12 | Mediator of RNA polymerase II transcription subunit 12 | 243.39 | 323.31 | 6.82 | 3 | 7.32 | 3 |
| SMN1 | Survival motor neuron protein | 31.689 | 323.31 | 7.95 | 3 | 5.59 | 3 |
| ARNT | Aryl hydrocarbon receptor nuclear translocator | 86.636 | 323.31 | 7.65 | 3 | 5.35 | 3 |
| SNRPF | Small nuclear ribonucleoprotein F | 9.7251 | 71.377 | 6.93 | 3 | 5.93 | 3 |
| LSM10 | U7 snRNA-associated Sm-like protein LSm10 | 14.08 | 74.226 | 6.36 | 3 | 6.28 | 3 |
| SNRPD3 | Small nuclear ribonucleoprotein Sm D3 | 13.291 | 77.644 | 8.16 | 3 | 4.09 | 2 |
| ARHGEF11 | Rho guanine nucleotide exchange factor 11 | 172.24 | 323.31 | 9.56 | 3 | NA | 0 |
| IGKV2D-29 | | 11.192 | 323.31 | 5.97 | 3 | 3.48 | 2 |
| SNRPN; SNRPB | Small nuclear ribonucleoprotein-associated proteins B and B;Small nuclear ribonucleoprotein-associated protein N | 17.546 | 104.61 | 6.44 | 3 | 2.50 | 1 |
| TRIM21 | E3 ubiquitin-protein ligase TRIM21 | 54.169 | 323.31 | 8.65 | 3 | 1.67 | 0 |
| NBEAL2 | Neurobeachin-like protein 2 | 299.34 | 323.31 | 8.52 | 3 | NA | 0 |
| PRMT5 | Protein arginine N-methyltransferase 5;Protein arginine N- | 72.683 | 217.67 | 7.51 | 3 | NA | 0 |

| | | | | | | | |
|---|---|---|---|---|---|---|---|
| | methyltransferase 5, N-terminally processed | | | | | | |
| ATXN1L | Ataxin-1-like | 73.305 | 167.15 | 6.01 | 3 | NA | 0 |
| NFIC | Nuclear factor 1 C-type | 55.674 | 323.31 | 5.62 | 2 | 8.95 | 3 |
| SNRPE | Small nuclear ribonucleoprotein E | 10.803 | 47.864 | 7.95 | 2 | 6.28 | 3 |
| PKN2 | Serine/threonine-protein kinase N2 | 112.03 | 323.31 | 6.66 | 2 | 7.02 | 3 |
| BCKDK | [3-methyl-2-oxobutanoate dehydrogenase [lipoamide]] kinase, mitochondrial | 46.36 | 218.98 | 4.03 | 2 | 8.52 | 3 |
| HOMEZ | Homeobox and leucine zipper protein Homez | 61.24 | 154.87 | 5.36 | 2 | 6.06 | 3 |
| MSH3 | DNA mismatch repair protein Msh3 | 127.41 | 323.31 | 4.10 | 2 | 6.77 | 3 |
| FN1 | Fibronectin;Anastellin;Ugl-Y1;Ugl-Y2;Ugl-Y3 | 222.97 | 158.24 | 5.45 | 2 | 3.89 | 1 |
| DTL | Denticleless protein homolog | 74.999 | 226.38 | 4.26 | 2 | 3.67 | 2 |
| SNRPD1 | Small nuclear ribonucleoprotein Sm D1 | 13.281 | 50.279 | 6.26 | 2 | NA | 0 |
| NCBP1 | Nuclear cap-binding protein subunit 1 | 91.838 | 296.76 | 6.21 | 2 | 2.73 | 0 |
| PHAX | Phosphorylated adapter RNA export protein | 44.402 | 126.64 | 5.57 | 2 | NA | 0 |
| TUBA1C; KLK9 | Tubulin alpha-1C chain | 57.73 | 51.259 | 4.98 | 2 | NA | 0 |
| USP9X | Probable ubiquitin carboxyl-terminal hydrolase FAF-X | 290.46 | 301.11 | 4.85 | 2 | NA | 0 |
| TUBB8 | Tubulin beta-8 chain | 49.775 | 70.7 | 4.10 | 2 | NA | 0 |
| SNRPA1 | U2 small nuclear ribonucleoprotein A | 28.415 | 72.228 | 3.70 | 2 | 0.37 | 0 |
| YWHAB | 14-3-3 protein beta/alpha;14-3-3 protein beta/alpha, N-terminally processed | 27.85 | 43.228 | 3.15 | 2 | NA | 0 |
| YWHAZ | 14-3-3 protein zeta/delta | 28.036 | 159.88 | 3.00 | 2 | NA | 0 |
| TACC2 | Transforming acidic coiled-coil-containing protein 2 | 296.74 | 323.31 | 6.41 | 1 | NA | 0 |
| YWHAG | 14-3-3 protein gamma;14-3-3 protein gamma, N-terminally processed | 28.302 | 73.845 | 3.29 | 1 | NA | 0 |
| YWHAQ | 14-3-3 protein theta | 27.764 | 93.578 | 2.97 | 1 | NA | 0 |
| TUBA1B | Tubulin alpha-1B chain | 50.151 | 323.31 | 2.38 | 1 | 0.57 | 0 |
| COIL | Coilin | 62.608 | 311.74 | NA | 0 | 7.55 | 3 |
| MED13 | Mediator of RNA polymerase II transcription subunit 13 | 239.29 | 323.31 | NA | 0 | 7.03 | 3 |
| MED1 | Mediator of RNA polymerase II transcription subunit 1 | 168.48 | 323.31 | NA | 0 | 6.05 | 3 |
| MED14 | Mediator of RNA polymerase II transcription subunit 14 | 160.6 | 323.31 | NA | 0 | 5.78 | 3 |
| MED17 | Mediator of RNA polymerase II transcription subunit 17 | 72.889 | 311.55 | NA | 0 | 5.71 | 3 |
| MED13L | Mediator of RNA polymerase II transcription subunit 13-like | 242.6 | 323.31 | NA | 0 | 5.67 | 3 |

| ZBTB7A | Zinc finger and BTB domain-containing protein 7A | 61.438 | 239.74 | NA | 0 | 5.48 | 3 |
|---|---|---|---|---|---|---|---|
| MED11 | Mediator of RNA polymerase II transcription subunit 11 | 13.129 | 38.458 | NA | 0 | 5.18 | 3 |
| CDK8 | Cyclin-dependent kinase 8 | 53.155 | 139.38 | NA | 0 | 4.87 | 3 |
| MED22 | Mediator of RNA polymerase II transcription subunit 22 | 12.853 | 89.866 | NA | 0 | 4.39 | 2 |
| ESRRA | Steroid hormone receptor ERR1 | 45.438 | 103.84 | NA | 0 | 4.32 | 1 |
| MED20 | Mediator of RNA polymerase II transcription subunit 20 | 23.222 | 113.47 | NA | 0 | 4.23 | 2 |
| MED30 | Mediator of RNA polymerase II transcription subunit 30 | 16.279 | 159.39 | NA | 0 | 4.16 | 2 |
| RBM4; RBM4B | RNA-binding protein 4;RNA-binding protein 4B | 40.313 | 199.81 | NA | 0 | 3.91 | 2 |
| MED15 | Mediator of RNA polymerase II transcription subunit 15 | 82.58 | 304.91 | NA | 0 | 3.86 | 3 |
| MED8 | Mediator of RNA polymerase II transcription subunit 8 | 29.08 | 99.037 | NA | 0 | 3.84 | 2 |
| MED23 | Mediator of RNA polymerase II transcription subunit 23 | 155.55 | 323.31 | NA | 0 | 3.83 | 2 |
| MED4 | Mediator of RNA polymerase II transcription subunit 4 | 29.745 | 134.43 | NA | 0 | 3.70 | 2 |
| MED27 | Mediator of RNA polymerase II transcription subunit 27 | 31.351 | 56.329 | NA | 0 | 3.61 | 2 |
| MED25 | Mediator of RNA polymerase II transcription subunit 25 | 84.388 | 124.24 | NA | 0 | 3.43 | 2 |
| MED6 | Mediator of RNA polymerase II transcription subunit 6 | 28.723 | 140.57 | NA | 0 | 3.35 | 2 |
| MED16 | Mediator of RNA polymerase II transcription subunit 16 | 93.028 | 264.77 | NA | 0 | 3.35 | 2 |
| TAF5L | TAF5-like RNA polymerase II p300/CBP-associated factor-associated factor 65 kDa subunit 5L | 66.155 | 80.75 | NA | 0 | 3.25 | 1 |
| MED18 | Mediator of RNA polymerase II transcription subunit 18 | 23.662 | 43.548 | NA | 0 | 3.23 | 1 |
| ZNF326 | DBIRD complex subunit ZNF326 | 65.653 | 96.2 | NA | 0 | 3.20 | 2 |
| MED24 | Mediator of RNA polymerase II transcription subunit 24 | 112.18 | 323.31 | NA | 0 | 2.96 | 2 |
| IXL;MED29 | Mediator of RNA polymerase II transcription subunit 29 | 23.472 | 203.75 | NA | 0 | 2.91 | 2 |
| CCNC | Cyclin-C | 26.513 | 57.645 | NA | 0 | 2.78 | 1 |
| MSH2 | DNA mismatch repair protein Msh2 | 104.74 | 323.31 | 2.33 | 0 | 2.66 | 1 |

**Table 7.6 List of acronyms, abbreviations and units**

| | |
|---|---|
| % | Percent |
| °C | Degree celsius |
| aDMA | Asymmetrical dimethyl-L-arginine |
| AEBSF | 4-(2-aminoethyl) benzenesulfonyl fluoride |
| ALS | Amyotrophic lateral sclerosis |
| ATP | Adenosine-5′-triphosphate |
| BisTris | 2-bis(2-hydroxyethyl)amino-2-(hydroxymethyl)-1,3-propanediol |
| BSA | Bovine serum albumin |
| C-terminal | Carboxy- terminal |
| CB(s) | Cajal body(s) |
| cDNA | Complementary DNA |
| Ci | Curie (1 Ci = 3.7 × 1010 Bq = 37 GBq) |
| cm | Centimeter |
| Co-IP | Coimmunoprecipitation |
| CUD | Color Universal Design |
| CV | Column volume |
| dd $H_2O$ | Double-distilled water |
| DEPC | Diethylpyrocarbonate |
| DMEM | Dulbecco's Modified Eagle Medium |
| DMSO | Dimethyl sulfoxide |
| DNA | Deoxyribonucleic acid |
| DNAse | Deoxyribonuclease |
| dNTP | Deoxyribonucleoside-5′-Triphosphosphate |
| DTT | Dithiothreitol |
| EDTA | Ethylenediaminetetraacetic acid |
| EtOH | Ethanol |
| FCS | Fetal calf serum |
| FP | Forward primer |
| $g$ | Gravity |
| G | Gemin |
| g | Gram |
| GTP | Guanosine-5′-triphosphate |
| h | Hour (s) |
| HCl | Hydrochloric acid |
| HeLa | Henrietta Lacks |
| HEPES | N-2-hydroxyethylpiperazine-N'-2-Ethane sulfonic acid |
| HOT | Head over tail |
| IP | Immunoprecipitation |
| IPed | Immunoprecipitated |
| k | Kilo |
| KCl | Potassium chloride |
| kDa | KiloDalton |
| L | Litre |
| M | Molar |
| m | Meter |
| $m_3G$ | 2,2,7- trimethylguanosine |
| $m^7G$ | 7- monomethylguanosine |
| mA | Milliampére |
| MeOH | Methanol |
| MES | 2-(N-morpholino)ethanesulfonic acid |
| mg | Milligram |
| $MgCl_2$ | Magnesium chloride |
| min | Minute |

| | |
|---|---|
| mL | Millilitre |
| mM | Millimolar |
| MS | Mass spectrometry |
| MW | Molecular weight |
| N-terminal | Amino-terminal |
| NaCl | Sodium chloride |
| NaOH | Sodium hydroxide |
| NP40 | Nonidet P40 |
| PAGE | Polyacrylamide gel electrophoresis |
| PBS | Phosphate buffered saline |
| PCR | Polymerase chain reaction |
| PEI | Polyethylenimine |
| PFA | Paraformaldehyde |
| pmol | Picomole |
| PMSF | Phenylmethylsulfonyl fluoride |
| PTM(s) | Post translational modification(s) |
| PV | Pellet volume |
| PVDF | Polyvinylidene Fluoride |
| RNase A | Ribonuclease A |
| RNAsin | RNase inhibitor |
| RP | Reverse primer |
| rpm | Revolutions per minute |
| RT | Room temperature |
| s | Seconds |
| sDMA | Symmetrical dimethyl-L-arginine (w-NG,N'G-Dimethyl-L-arginine) |
| SDS | Sodium dodecyl sulphate |
| SDS-PAGE | Sodium dodecyl sulphate polyacrylamide gel electrophoresis |
| SMA | Spinal muscular atrophy |
| ss | Splice sites |
| TCA | Trichloroacetic acid |
| TCEP | Tris(2-carboxyethyl)phosphine |
| TEMED | N,N,N',N',-tetramethylethylenediamine |
| v/v | Volume-volume percentage |
| w/v | Weight-volume percentage |
| α | Anti |
| β | Beta |
| μ | Micro |
| μg | Microgram |
| μL | Microlitre |
| μM | Micromolar |

**Table 7.7 Individual contributions for the final figures represented in the thesis work**
The background work that was not included in the thesis has been not considered for the analysis. RM-Rajyalakshmi Meduri, AP- Archana B. Prusty, BP- Bhupesh K. Prusty, MS- Mass Spectrometric analysis.

| Figure | RM | AP | BP | MS |
|---|---|---|---|---|
| Figure 4.1: shRNA-mediated knockdown of SMN. | | 35 % | 65 % | |
| Figure 4.2: Sm protein homeostasis remains unaltered under SMN paucity. | | 50 % | | 50 % |
| Figure 4.3: List of assembly intermediates that are recognized by various antibodies. | Schematics only for the ease of understanding | | | |
| Figure 4.4: Tailback of Sm proteins on pICln under SMN limiting conditions. | | 100 % | | |
| Figure 4.5: Down regulation of Sm encoding transcripts during prolonged SMN deficiency. | | 100 % | | |
| Figure 4.6: Down regulation of Sm proteins after siRNA-mediated knockdown of pICln. | 50 % | | | 50 % |
| Figure 4.7: No transcriptional or translational regulation of Sm proteins levels during the knockdown of pICln. | 95 % | 5 % | | |
| Figure 4.8: Down-regulated Sm proteins are recovered upon inhibition of autophagy during pICln knockdown. | 35 % | 65 % | | |
| Figure 4.9: Mis-localization of recovered newly translated Sm proteins by autophagy in the absence of pICln. | 5 % | 95 % | | |
| Figure 4.10: Mis-localization of SMN complex during pICln deficiency and Cajal body disintegration (annexure figure 7.3). | | 100 % | | |
| Figure 4.11: No recovery of Sm proteins in soluble lysates upon autophagy inhibition during pICln paucity | 100% | | | |
| Figure 4.12: Analysis of HeLa S3 cytoplasmic and nuclear extracts for cross-contamination. | 100 % | | | |
| Figure 4.13: Isolation of Cajal bodies. | 100 % | | | |
| Figure 4.14: Gradient centrifugation of HeLa S3 cytoplasmic and nuclear extracts. | 100 % | | | |
| Figure 4.15: Immunoprecipitation of endogenous SMN complex. | 70 % | | | 30 % |
| Figure 4.16: Validation of Mediator complex as an interactor of SMN complex. | 100 % | | | |

# 8 References

1. Achsel, T., Brahms, H., Kastner, B., Bachi, A., Wilm, M., and Luhrmann, R. (1999). A doughnut-shaped heteromer of human Sm-like proteins binds to the 3'-end of U6 snRNA, thereby facilitating U4/U6 duplex formation in vitro. EMBO J *18*, 5789-5802.
2. Baccon, J., Pellizzoni, L., Rappsilber, J., Mann, M., and Dreyfuss, G. (2002). Identification and characterization of Gemin7, a novel component of the survival of motor neuron complex. J Biol Chem *277*, 31957-31962.
3. Bachand, F., Boisvert, F.M., Cote, J., Richard, S., and Autexier, C. (2002). The product of the survival of motor neuron (SMN) gene is a human telomerase-associated protein. Molecular biology of the cell *13*, 3192-3202.
4. Baillat, D., Hakimi, M.A., Naar, A.M., Shilatifard, A., Cooch, N., and Shiekhattar, R. (2005). Integrator, a multiprotein mediator of small nuclear RNA processing, associates with the C-terminal repeat of RNA polymerase II. Cell *123*, 265-276.
5. Barth, S., Liss, M., Voss, M.D., Dobner, T., Fischer, U., Meister, G., and Grasser, F.A. (2003). Epstein-Barr virus nuclear antigen 2 binds via its methylated arginine-glycine repeat to the survival motor neuron protein. J Virol *77*, 5008-5013.
6. Battle, D.J., Kasim, M., Wang, J., and Dreyfuss, G. (2007). SMN-independent subunits of the SMN complex. Identification of a small nuclear ribonucleoprotein assembly intermediate. J Biol Chem *282*, 27953-27959.
7. Battle, D.J., Kasim, M., Yong, J., Lotti, F., Lau, C.K., Mouaikel, J., Zhang, Z., Han, K., Wan, L., and Dreyfuss, G. (2006a). The SMN complex: an assembly machine for RNPs. Cold Spring Harb Symp Quant Biol *71*, 313-320.
8. Battle, D.J., Lau, C.K., Wan, L., Deng, H., Lotti, F., and Dreyfuss, G. (2006b). The Gemin5 protein of the SMN complex identifies snRNAs. Mol Cell *23*, 273-279.
9. Bessonov, S., Anokhina, M., Will, C.L., Urlaub, H., and Luhrmann, R. (2008). Isolation of an active step I spliceosome and composition of its RNP core. Nature *452*, 846-850.
10. Bizarro, J., Dodre, M., Huttin, A., Charpentier, B., Schlotter, F., Branlant, C., Verheggen, C., Massenet, S., and Bertrand, E. (2015). NUFIP and the HSP90/R2TP chaperone bind the SMN complex and facilitate assembly of U4-specific proteins. Nucleic Acids Res *43*, 8973-8989.
11. Bordonne, R. (2000). Functional characterization of nuclear localization signals in yeast Sm proteins. Mol Cell Biol *20*, 7943-7954.
12. Boulisfane, N., Choleza, M., Rage, F., Neel, H., Soret, J., and Bordonne, R. (2011). Impaired minor tri-snRNP assembly generates differential splicing defects of U12-type introns in lymphoblasts derived from a type I SMA patient. Hum Mol Genet *20*, 641-648.
13. Bowerman, M., Beauvais, A., Anderson, C.L., and Kothary, R. (2010). Rho-kinase inactivation prolongs survival of an intermediate SMA mouse model. Hum Mol Genet *19*, 1468-1478.
14. Bradrick, S.S., and Gromeier, M. (2009). Identification of gemin5 as a novel 7-methylguanosine cap-binding protein. PloS one *4*, e7030.
15. Brahms, H., Raymackers, J., Union, A., de Keyser, F., Meheus, L., and Luhrmann, R. (2000). The C-terminal RG dipeptide repeats of the spliceosomal Sm proteins D1 and D3 contain symmetrical dimethylarginines, which form a major B-cell epitope for anti-Sm autoantibodies. J Biol Chem *275*, 17122-17129.
16. Buhler, D., Raker, V., Luhrmann, R., and Fischer, U. (1999). Essential role for the tudor domain of SMN in spliceosomal U snRNP assembly: implications for spinal muscular atrophy. Hum Mol Genet *8*, 2351-2357.
17. Carissimi, C., Saieva, L., Gabanella, F., and Pellizzoni, L. (2006). Gemin8 is required for the architecture and function of the survival motor neuron complex. J Biol Chem *281*, 37009-37016.
18. Carnegie, G.K., Sleeman, J.E., Morrice, N., Hastie, C.J., Peggie, M.W., Philp, A., Lamond, A.I., and Cohen, P.T. (2003). Protein phosphatase 4 interacts with the Survival of Motor Neurons complex and enhances the temporal localisation of snRNPs. J Cell Sci *116*, 1905-1913.

19. Cartegni, L., and Krainer, A.R. (2002). Disruption of an SF2/ASF-dependent exonic splicing enhancer in SMN2 causes spinal muscular atrophy in the absence of SMN1. Nat Genet *30*, 377-384.

20. Chari, A., Golas, M.M., Klingenhager, M., Neuenkirchen, N., Sander, B., Englbrecht, C., Sickmann, A., Stark, H., and Fischer, U. (2008). An assembly chaperone collaborates with the SMN complex to generate spliceosomal SnRNPs. Cell *135*, 497-509.

21. Chari, A., Paknia, E., and Fischer, U. (2009). The role of RNP biogenesis in spinal muscular atrophy. Curr Opin Cell Biol *21*, 387-393.

22. Charroux, B., Pellizzoni, L., Perkinson, R.A., Shevchenko, A., Mann, M., and Dreyfuss, G. (1999). Gemin3: A novel DEAD box protein that interacts with SMN, the spinal muscular atrophy gene product, and is a component of gems. J Cell Biol *147*, 1181-1194.

23. Charroux, B., Pellizzoni, L., Perkinson, R.A., Yong, J., Shevchenko, A., Mann, M., and Dreyfuss, G. (2000). Gemin4. A novel component of the SMN complex that is found in both gems and nucleoli. J Cell Biol *148*, 1177-1186.

24. Cifuentes-Diaz, C., Frugier, T., Tiziano, F.D., Lacene, E., Roblot, N., Joshi, V., Moreau, M.H., and Melki, J. (2001). Deletion of murine SMN exon 7 directed to skeletal muscle leads to severe muscular dystrophy. J Cell Biol *152*, 1107-1114.

25. Claus, P., Doring, F., Gringel, S., Muller-Ostermeyer, F., Fuhlrott, J., Kraft, T., and Grothe, C. (2003). Differential intranuclear localization of fibroblast growth factor-2 isoforms and specific interaction with the survival of motoneuron protein. J Biol Chem *278*, 479-485.

26. Cordin, O., Hahn, D., and Beggs, J.D. (2012). Structure, function and regulation of spliceosomal RNA helicases. Curr Opin Cell Biol *24*, 431-438.

27. Darzacq, X., Jady, B.E., Verheggen, C., Kiss, A.M., Bertrand, E., and Kiss, T. (2002). Cajal body-specific small nuclear RNAs: a novel class of 2'-O-methylation and pseudouridylation guide RNAs. EMBO J *21*, 2746-2756.

28. den Engelsman, J., van de Schootbrugge, C., Yong, J., Pruijn, G.J., and Boelens, W.C. (2013). Pseudophosphorylated alphaB-crystallin is a nuclear chaperone imported into the nucleus with help of the SMN complex. PloS one *8*, e73489.

29. Dignam, J.D., Lebovitz, R.M., and Roeder, R.G. (1983). Accurate transcription initiation by RNA polymerase II in a soluble extract from isolated mammalian nuclei. Nucleic Acids Res *11*, 1475-1489.

30. Ellis, R.J., and Minton, A.P. (2003). Cell biology: join the crowd. Nature *425*, 27-28.

31. Espert, L., Eldin, P., Gongora, C., Bayard, B., Harper, F., Chelbi-Alix, M.K., Bertrand, E., Degols, G., and Mechti, N. (2006). The exonuclease ISG20 mainly localizes in the nucleolus and the Cajal (Coiled) bodies and is associated with nuclear SMN protein-containing complexes. J Cell Biochem *98*, 1320-1333.

32. Fallini, C., Rouanet, J.P., Donlin-Asp, P.G., Guo, P., Zhang, H., Singer, R.H., Rossoll, W., and Bassell, G.J. (2014). Dynamics of survival of motor neuron (SMN) protein interaction with the mRNA-binding protein IMP1 facilitates its trafficking into motor neuron axons. Developmental neurobiology *74*, 319-332.

33. Fica, S.M., Tuttle, N., Novak, T., Li, N.S., Lu, J., Koodathingal, P., Dai, Q., Staley, J.P., and Piccirilli, J.A. (2013). RNA catalyses nuclear pre-mRNA splicing. Nature *503*, 229-234.

34. Fischer, U., Darzynkiewicz, E., Tahara, S.M., Dathan, N.A., Luhrmann, R., and Mattaj, I.W. (1991). Diversity in the signals required for nuclear accumulation of U snRNPs and variety in the pathways of nuclear transport. J Cell Biol *113*, 705-714.

35. Fischer, U., Liu, Q., and Dreyfuss, G. (1997). The SMN-SIP1 complex has an essential role in spliceosomal snRNP biogenesis. Cell *90*, 1023-1029.

36. Fischer, U., and Luhrmann, R. (1990). An essential signaling role for the m3G cap in the transport of U1 snRNP to the nucleus. Science *249*, 786-790.

37. Fornerod, M., Ohno, M., Yoshida, M., and Mattaj, I.W. (1997). CRM1 is an export receptor for leucine-rich nuclear export signals. Cell *90*, 1051-1060.

38. Frey, M.R., and Matera, A.G. (2001). RNA-mediated interaction of Cajal bodies and U2 snRNA genes. J Cell Biol *154*, 499-509.

39. Friesen, W.J., Paushkin, S., Wyce, A., Massenet, S., Pesiridis, G.S., Van Duyne, G., Rappsilber, J., Mann, M., and Dreyfuss, G. (2001). The methylosome, a 20S complex containing JBP1 and pICln, produces dimethylarginine-modified Sm proteins. Mol Cell Biol *21*, 8289-8300.

40. Friesen, W.J., Wyce, A., Paushkin, S., Abel, L., Rappsilber, J., Mann, M., and Dreyfuss, G. (2002). A novel WD repeat protein component of the methylosome binds Sm proteins. J Biol Chem *277*, 8243-8247.

41. Fuller, H.R., Man, N.T., Lam le, T., Thanh le, T., Keough, R.A., Asperger, A., Gonda, T.J., and Morris, G.E. (2010). The SMN interactome includes Myb-binding protein 1a. Journal of proteome research *9*, 556-563.

42. Gabanella, F., Butchbach, M.E., Saieva, L., Carissimi, C., Burghes, A.H., and Pellizzoni, L. (2007). Ribonucleoprotein assembly defects correlate with spinal muscular atrophy severity and preferentially affect a subset of spliceosomal snRNPs. PloS one *2*, e921.

43. Gangwani, L., Mikrut, M., Theroux, S., Sharma, M., and Davis, R.J. (2001). Spinal muscular atrophy disrupts the interaction of ZPR1 with the SMN protein. Nat Cell Biol *3*, 376-383.

44. Giesemann, T., Rathke-Hartlieb, S., Rothkegel, M., Bartsch, J.W., Buchmeier, S., Jockusch, B.M., and Jockusch, H. (1999). A role for polyproline motifs in the spinal muscular atrophy protein SMN. Profilins bind to and colocalize with smn in nuclear gems. J Biol Chem *274*, 37908-37914.

45. Girard, C., Neel, H., Bertrand, E., and Bordonne, R. (2006). Depletion of SMN by RNA interference in HeLa cells induces defects in Cajal body formation. Nucleic Acids Res *34*, 2925-2932.

46. Grimm, C., Chari, A., Pelz, J.P., Kuper, J., Kisker, C., Diederichs, K., Stark, H., Schindelin, H., and Fischer, U. (2013). Structural basis of assembly chaperone- mediated snRNP formation. Mol Cell *49*, 692-703.

47. Grimmler, M., Bauer, L., Nousiainen, M., Korner, R., Meister, G., and Fischer, U. (2005a). Phosphorylation regulates the activity of the SMN complex during assembly of spliceosomal U snRNPs. EMBO reports *6*, 70-76.

48. Grimmler, M., Otter, S., Peter, C., Muller, F., Chari, A., and Fischer, U. (2005b). Unrip, a factor implicated in cap-independent translation, associates with the cytosolic SMN complex and influences its intracellular localization. Hum Mol Genet *14*, 3099-3111.

49. Gubitz, A.K., Mourelatos, Z., Abel, L., Rappsilber, J., Mann, M., and Dreyfuss, G. (2002). Gemin5, a novel WD repeat protein component of the SMN complex that binds Sm proteins. J Biol Chem *277*, 5631-5636.

50. Hahnen, E., Schonling, J., Rudnik-Schoneborn, S., Raschke, H., Zerres, K., and Wirth, B. (1997). Missense mutations in exon 6 of the survival motor neuron gene in patients with spinal muscular atrophy (SMA). Hum Mol Genet *6*, 821-825.

51. Hamm, J., and Mattaj, I.W. (1990). Monomethylated cap structures facilitate RNA export from the nucleus. Cell *63*, 109-118.

52. Hebert, M.D., Szymczyk, P.W., Shpargel, K.B., and Matera, A.G. (2001). Coilin forms the bridge between Cajal bodies and SMN, the spinal muscular atrophy protein. Genes Dev *15*, 2720-2729.

53. Hermann, H., Fabrizio, P., Raker, V.A., Foulaki, K., Hornig, H., Brahms, H., and Luhrmann, R. (1995). snRNP Sm proteins share two evolutionarily conserved sequence motifs which are involved in Sm protein-protein interactions. EMBO J *14*, 2076-2088.

54. Hua, Y., and Zhou, J. (2004a). Rpp20 interacts with SMN and is re-distributed into SMN granules in response to stress. Biochem Biophys Res Commun *314*, 268-276.

55. Hua, Y., and Zhou, J. (2004b). Survival motor neuron protein facilitates assembly of stress granules. FEBS Lett *572*, 69-74.

56. Hubers, L., Valderrama-Carvajal, H., Laframboise, J., Timbers, J., Sanchez, G., and Cote, J. (2011). HuD interacts with survival motor neuron protein and can rescue spinal muscular atrophy-like neuronal defects. Hum Mol Genet *20*, 553-579.

57. Husedzinovic, A., Neumann, B., Reymann, J., Draeger-Meurer, S., Chari, A., Erfle, H., Fischer, U., and Gruss, O.J. (2015). The catalytically inactive tyrosine phosphatase HD-PTP/PTPN23 is a novel regulator of SMN complex localization. Molecular biology of the cell *26*, 161-171.

58. Husedzinovic, A., Oppermann, F., Draeger-Meurer, S., Chari, A., Fischer, U., Daub, H., and Gruss, O.J. (2014). Phosphoregulation of the human SMN complex. Eur J Cell Biol *93*, 106-117.

59. Iwahashi, H., Eguchi, Y., Yasuhara, N., Hanafusa, T., Matsuzawa, Y., and Tsujimoto, Y. (1997). Synergistic anti-apoptotic activity between Bcl-2 and SMN implicated in spinal muscular atrophy. Nature *390*, 413-417.

60. Izaurralde, E., Lewis, J., Gamberi, C., Jarmolowski, A., McGuigan, C., and Mattaj, I.W. (1995). A cap-binding protein complex mediating U snRNA export. Nature *376*, 709-712.

61. Jady, B.E., Darzacq, X., Tucker, K.E., Matera, A.G., Bertrand, E., and Kiss, T. (2003). Modification of Sm small nuclear RNAs occurs in the nucleoplasmic Cajal body following import from the cytoplasm. EMBO J *22*, 1878-1888.

62. Jones, K.W., Gorzynski, K., Hales, C.M., Fischer, U., Badbanchi, F., Terns, R.M., and Terns, M.P. (2001). Direct interaction of the spinal muscular atrophy disease protein SMN with the small nucleolar RNA-associated protein fibrillarin. J Biol Chem *276*, 38645-38651.

63. Kambach, C., Walke, S., and Nagai, K. (1999a). Structure and assembly of the spliceosomal small nuclear ribonucleoprotein particles. Curr Opin Struct Biol *9*, 222-230.

64. Kambach, C., Walke, S., Young, R., Avis, J.M., de la Fortelle, E., Raker, V.A., Luhrmann, R., Li, J., and Nagai, K. (1999b). Crystal structures of two Sm protein complexes and their implications for the assembly of the spliceosomal snRNPs. Cell *96*, 375-387.

65. Kammler, S., Lykke-Andersen, S., and Jensen, T.H. (2008). The RNA exosome component hRrp6 is a target for 5-fluorouracil in human cells. Mol Cancer Res *6*, 990-995.

66. Kiss, A.M., Jady, B.E., Bertrand, E., and Kiss, T. (2004). Human box H/ACA pseudouridylation guide RNA machinery. Mol Cell Biol *24*, 5797-5807.

67. Kiss, A.M., Jady, B.E., Darzacq, X., Verheggen, C., Bertrand, E., and Kiss, T. (2002). A Cajal body-specific pseudouridylation guide RNA is composed of two box H/ACA snoRNA-like domains. Nucleic Acids Res *30*, 4643-4649.

68. Kroiss, M., Schultz, J., Wiesner, J., Chari, A., Sickmann, A., and Fischer, U. (2008). Evolution of an RNP assembly system: a minimal SMN complex facilitates formation of UsnRNPs in Drosophila melanogaster. Proceedings of the National Academy of Sciences of the United States of America *105*, 10045-10050.

69. Kurihara, N., Menaa, C., Maeda, H., Haile, D.J., and Reddy, S.V. (2001). Osteoclast-stimulating factor interacts with the spinal muscular atrophy gene product to stimulate osteoclast formation. J Biol Chem *276*, 41035-41039.

70. Kuspert, M., Murakawa, Y., Schaffler, K., Vanselow, J.T., Wolf, E., Juranek, S., Schlosser, A., Landthaler, M., and Fischer, U. (2015). LARP4B is an AU-rich sequence associated factor that promotes mRNA accumulation and translation. RNA *21*, 1294-1305.

71. Lam, Y.W., Lyon, C.E., and Lamond, A.I. (2002). Large-scale isolation of Cajal bodies from HeLa cells. Molecular biology of the cell *13*, 2461-2473.

72. Lau, C.K., Bachorik, J.L., and Dreyfuss, G. (2009). Gemin5-snRNA interaction reveals an RNA binding function for WD repeat domains. Nat Struct Mol Biol *16*, 486-491.

73. Lefebvre, S., Burglen, L., Reboullet, S., Clermont, O., Burlet, P., Viollet, L., Benichou, B., Cruaud, C., Millasseau, P., Zeviani, M., *et al.* (1995). Identification and characterization of a spinal muscular atrophy-determining gene. Cell *80*, 155-165.

74. Lefebvre, S., Burlet, P., Viollet, L., Bertrandy, S., Huber, C., Belser, C., and Munnich, A. (2002). A novel association of the SMN protein with two major non-ribosomal nucleolar proteins and its implication in spinal muscular atrophy. Hum Mol Genet *11*, 1017-1027.

75. Lemm, I., Girard, C., Kuhn, A.N., Watkins, N.J., Schneider, M., Bordonne, R., and Luhrmann, R. (2006). Ongoing U snRNP biogenesis is required for the integrity of Cajal bodies. Molecular biology of the cell *17*, 3221-3231.

76. Liu, Q., and Dreyfuss, G. (1996). A novel nuclear structure containing the survival of motor neurons protein. EMBO J *15*, 3555-3565.

77. Liu, Q., Fischer, U., Wang, F., and Dreyfuss, G. (1997). The spinal muscular atrophy disease gene product, SMN, and its associated protein SIP1 are in a complex with spliceosomal snRNP proteins. Cell *90*, 1013-1021.

78. Ma, Y., Dostie, J., Dreyfuss, G., and Van Duyne, G.D. (2005). The Gemin6-Gemin7 heterodimer from the survival of motor neurons complex has an Sm protein-like structure. Structure *13*, 883-892.

79. Mahmoudi, S., Henriksson, S., Weibrecht, I., Smith, S., Soderberg, O., Stromblad, S., Wiman, K.G., and Farnebo, M. (2010). WRAP53 is essential for Cajal body formation and for targeting the survival of motor neuron complex to Cajal bodies. PLoS Biol *8*, e1000521.

80. Makarov, E.M., Owen, N., Bottrill, A., and Makarova, O.V. (2012). Functional mammalian spliceosomal complex E contains SMN complex proteins in addition to U1 and U2 snRNPs. Nucleic Acids Res *40*, 2639-2652.

81. Markowitz, J.A., Singh, P., and Darras, B.T. (2012). Spinal muscular atrophy: a clinical and research update. Pediatric neurology *46*, 1-12.

82. Meister, G., Buhler, D., Laggerbauer, B., Zobawa, M., Lottspeich, F., and Fischer, U. (2000). Characterization of a nuclear 20S complex containing the survival of motor neurons (SMN) protein and a specific subset of spliceosomal Sm proteins. Hum Mol Genet *9*, 1977-1986.

83. Meister, G., Buhler, D., Pillai, R., Lottspeich, F., and Fischer, U. (2001a). A multiprotein complex mediates the ATP-dependent assembly of spliceosomal U snRNPs. Nat Cell Biol *3*, 945-949.

84. Meister, G., Eggert, C., Buhler, D., Brahms, H., Kambach, C., and Fischer, U. (2001b). Methylation of Sm proteins by a complex containing PRMT5 and the putative U snRNP assembly factor pICln. Curr Biol *11*, 1990-1994.

85. Meister, G., and Fischer, U. (2002). Assisted RNP assembly: SMN and PRMT5 complexes cooperate in the formation of spliceosomal UsnRNPs. EMBO J *21*, 5853-5863.

86. Meister, G., Hannus, S., Plottner, O., Baars, T., Hartmann, E., Fakan, S., Laggerbauer, B., and Fischer, U. (2001c). SMNrp is an essential pre-mRNA splicing factor required for the formation of the mature spliceosome. EMBO J *20*, 2304-2314.

87. Mirabella, F., Murison, A., Aronson, L.I., Wardell, C.P., Thompson, A.J., Hanrahan, S.J., Fok, J.H., Pawlyn, C., Kaiser, M.F., Walker, B.A., *et al.* (2014). A novel functional role for MMSET in RNA processing based on the link between the REIIBP isoform and its interaction with the SMN complex. PloS one *9*, e99493.

88. Mouaikel, J., Narayanan, U., Verheggen, C., Matera, A.G., Bertrand, E., Tazi, J., and Bordonne, R. (2003). Interaction between the small-nuclear-RNA cap hypermethylase and the spinal muscular atrophy protein, survival of motor neuron. EMBO reports *4*, 616-622.

89. Mourelatos, Z., Abel, L., Yong, J., Kataoka, N., and Dreyfuss, G. (2001). SMN interacts with a novel family of hnRNP and spliceosomal proteins. EMBO J *20*, 5443-5452.

90. Narayanan, U., Ospina, J.K., Frey, M.R., Hebert, M.D., and Matera, A.G. (2002). SMN, the spinal muscular atrophy protein, forms a pre-import snRNP complex with snurportin1 and importin beta. Hum Mol Genet *11*, 1785-1795.

91. Neuenkirchen, N., Englbrecht, C., Ohmer, J., Ziegenhals, T., Chari, A., and Fischer, U. (2015). Reconstitution of the human U snRNP assembly machinery reveals stepwise Sm protein organization. EMBO J *34*, 1925-1941.

92. Neugebauer, K.M. (2002). On the importance of being co-transcriptional. J Cell Sci *115*, 3865-3871.

93. Ogawa, C., Usui, K., Ito, F., Itoh, M., Hayashizaki, Y., and Suzuki, H. (2009). Role of survival motor neuron complex components in small nuclear ribonucleoprotein assembly. J Biol Chem *284*, 14609-14617.

94. Ohno, M., Segref, A., Bachi, A., Wilm, M., and Mattaj, I.W. (2000). PHAX, a mediator of U snRNA nuclear export whose activity is regulated by phosphorylation. Cell *101*, 187-198.

95. Oprea, G.E., Krober, S., McWhorter, M.L., Rossoll, W., Muller, S., Krawczak, M., Bassell, G.J., Beattie, C.E., and Wirth, B. (2008). Plastin 3 is a protective modifier of autosomal recessive spinal muscular atrophy. Science *320*, 524-527.

96. Otter, S., Grimmler, M., Neuenkirchen, N., Chari, A., Sickmann, A., and Fischer, U. (2007). A comprehensive interaction map of the human survival of motor neuron (SMN) complex. J Biol Chem *282*, 5825-5833.

97. Park, J.W., Voss, P.G., Grabski, S., Wang, J.L., and Patterson, R.J. (2001). Association of galectin-1 and galectin-3 with Gemin4 in complexes containing the SMN protein. Nucleic Acids Res *29*, 3595-3602.

98. Patel, A.A., and Steitz, J.A. (2003). Splicing double: insights from the second spliceosome. Nat Rev Mol Cell Biol *4*, 960-970.

99. Pellizzoni, L., Baccon, J., Charroux, B., and Dreyfuss, G. (2001a). The survival of motor neurons (SMN) protein interacts with the snoRNP proteins fibrillarin and GAR1. Curr Biol *11*, 1079-1088.

100. Pellizzoni, L., Charroux, B., Rappsilber, J., Mann, M., and Dreyfuss, G. (2001b). A functional interaction between the survival motor neuron complex and RNA polymerase II. J Cell Biol *152*, 75-85.

101. Pellizzoni, L., Yong, J., and Dreyfuss, G. (2002). Essential role for the SMN complex in the specificity of snRNP assembly. Science *298*, 1775-1779.

102. Pesiridis, G.S., Diamond, E., and Van Duyne, G.D. (2009). Role of pICLn in methylation of Sm proteins by PRMT5. J Biol Chem *284*, 21347-21359.

103. Piazzon, N., Rage, F., Schlotter, F., Moine, H., Branlant, C., and Massenet, S. (2008). In vitro and in cellulo evidences for association of the survival of motor neuron complex with the fragile X mental retardation protein. J Biol Chem *283*, 5598-5610.

104. Plessel, G., Fischer, U., and Luhrmann, R. (1994). m3G cap hypermethylation of U1 small nuclear ribonucleoprotein (snRNP) in vitro: evidence that the U1 small nuclear RNA-(guanosine-N2)-methyltransferase is a non-snRNP cytoplasmic protein that requires a binding site on the Sm core domain. Mol Cell Biol *14*, 4160-4172.

105. Pu, W.T., Krapivinsky, G.B., Krapivinsky, L., and Clapham, D.E. (1999). pICln inhibits snRNP biogenesis by binding core spliceosomal proteins. Mol Cell Biol *19*, 4113-4120.

106. Pu, W.T., Wickman, K., and Clapham, D.E. (2000). ICln is essential for cellular and early embryonic viability. J Biol Chem *275*, 12363-12366.

107. Raker, V.A., Hartmuth, K., Kastner, B., and Luhrmann, R. (1999). Spliceosomal U snRNP core assembly: Sm proteins assemble onto an Sm site RNA nonanucleotide in a specific and thermodynamically stable manner. Mol Cell Biol *19*, 6554-6565.

108. Raker, V.A., Plessel, G., and Luhrmann, R. (1996). The snRNP core assembly pathway: identification of stable core protein heteromeric complexes and an snRNP subcore particle in vitro. EMBO J *15*, 2256-2269.

109. Renvoise, B., Querol, G., Verrier, E.R., Burlet, P., and Lefebvre, S. (2012). A role for protein phosphatase PP1gamma in SMN complex formation and subnuclear localization to Cajal bodies. J Cell Sci *125*, 2862-2874.

110. Rossoll, W., Kroning, A.K., Ohndorf, U.M., Steegborn, C., Jablonka, S., and Sendtner, M. (2002). Specific interaction of Smn, the spinal muscular atrophy determining gene product, with hnRNP-R and gry-rbp/hnRNP-Q: a role for Smn in RNA processing in motor axons? Hum Mol Genet *11*, 93-105.

111. Sakharkar, M.K., Chow, V.T., and Kangueane, P. (2004). Distributions of exons and introns in the human genome. In Silico Biol *4*, 387-393.

112. Saunders, L.R., Perkins, D.J., Balachandran, S., Michaels, R., Ford, R., Mayeda, A., and Barber, G.N. (2001). Characterization of two evolutionarily conserved, alternatively spliced nuclear phosphoproteins, NFAR-1 and -2, that function in mRNA processing and interact with the double-stranded RNA-dependent protein kinase, PKR. J Biol Chem *276*, 32300-32312.

113. Schrank, B., Gotz, R., Gunnersen, J.M., Ure, J.M., Toyka, K.V., Smith, A.G., and Sendtner, M. (1997). Inactivation of the survival motor neuron gene, a candidate gene for human spinal muscular atrophy, leads to massive cell death in early mouse embryos. Proceedings of the National Academy of Sciences of the United States of America *94*, 9920-9925.

114. Seguin, S.J., Morelli, F.F., Vinet, J., Amore, D., De Biasi, S., Poletti, A., Rubinsztein, D.C., and Carra, S. (2014). Inhibition of autophagy, lysosome and VCP function impairs stress granule assembly. Cell Death Differ *21*, 1838-1851.

115. Selenko, P., Sprangers, R., Stier, G., Buhler, D., Fischer, U., and Sattler, M. (2001). SMN tudor domain structure and its interaction with the Sm proteins. Nat Struct Biol *8*, 27-31.

116. Seraphin, B. (1995). Sm and Sm-like proteins belong to a large family: identification of proteins of the U6 as well as the U1, U2, U4 and U5 snRNPs. EMBO J *14*, 2089-2098.

117. Shafey, D., Boyer, J.G., Bhanot, K., and Kothary, R. (2010). Identification of novel interacting protein partners of SMN using tandem affinity purification. Journal of proteome research *9*, 1659-1669.

118.Shpargel, K.B., and Matera, A.G. (2005). Gemin proteins are required for efficient assembly of Sm-class ribonucleoproteins. Proceedings of the National Academy of Sciences of the United States of America *102*, 17372-17377.

119.Singh, R., and Reddy, R. (1989). Gamma-monomethyl phosphate: a cap structure in spliceosomal U6 small nuclear RNA. Proceedings of the National Academy of Sciences of the United States of America *86*, 8280-8283.

120.Sleeman, J.E., Ajuh, P., and Lamond, A.I. (2001). snRNP protein expression enhances the formation of Cajal bodies containing p80-coilin and SMN. J Cell Sci *114*, 4407-4419.

121.Sleeman, J.E., and Lamond, A.I. (1999). Newly assembled snRNPs associate with coiled bodies before speckles, suggesting a nuclear snRNP maturation pathway. Curr Biol *9*, 1065-1074.

122.Small, E.C., Leggett, S.R., Winans, A.A., and Staley, J.P. (2006). The EF-G-like GTPase Snu114p regulates spliceosome dynamics mediated by Brr2p, a DExD/H box ATPase. Mol Cell *23*, 389-399.

123.Smith, K.P., and Lawrence, J.B. (2000). Interactions of U2 gene loci and their nuclear transcripts with Cajal (coiled) bodies: evidence for PreU2 within Cajal bodies. Molecular biology of the cell *11*, 2987-2998.

124.Stejskalova, E., and Stanek, D. (2014). The splicing factor U1-70K interacts with the SMN complex and is required for nuclear gem integrity. J Cell Sci *127*, 3909-3915.

125.Stelzl, U., Worm, U., Lalowski, M., Haenig, C., Brembeck, F.H., Goehler, H., Stroedicke, M., Zenkner, M., Schoenherr, A., Koeppen, S., *et al.* (2005). A human protein-protein interaction network: a resource for annotating the proteome. Cell *122*, 957-968.

126.Strasswimmer, J., Lorson, C.L., Breiding, D.E., Chen, J.J., Le, T., Burghes, A.H., and Androphy, E.J. (1999). Identification of survival motor neuron as a transcriptional activator-binding protein. Hum Mol Genet *8*, 1219-1226.

127.Sun, Y., Grimmler, M., Schwarzer, V., Schoenen, F., Fischer, U., and Wirth, B. (2005). Molecular and functional analysis of intragenic SMN1 mutations in patients with spinal muscular atrophy. Hum Mutat *25*, 64-71.

128.Suraweera, A., Lim, Y., Woods, R., Birrell, G.W., Nasim, T., Becherel, O.J., and Lavin, M.F. (2009). Functional role for senataxin, defective in ataxia oculomotor apraxia type 2, in transcriptional regulation. Hum Mol Genet *18*, 3384-3396.

129.Suzuki, T., Izumi, H., and Ohno, M. (2010). Cajal body surveillance of U snRNA export complex assembly. J Cell Biol *190*, 603-612.

130.Tadesse, H., Deschenes-Furry, J., Boisvenue, S., and Cote, J. (2008). KH-type splicing regulatory protein interacts with survival motor neuron protein and is misregulated in spinal muscular atrophy. Hum Mol Genet *17*, 506-524.

131.Tapia, O., Lafarga, V., Bengoechea, R., Palanca, A., Lafarga, M., and Berciano, M.T. (2014). The SMN Tudor SIM-like domain is key to SmD1 and coilin interactions and to Cajal body biogenesis. J Cell Sci *127*, 939-946.

132.Thore, S., Mayer, C., Sauter, C., Weeks, S., and Suck, D. (2003). Crystal structures of the Pyrococcus abyssi Sm core and its complex with RNA. Common features of RNA binding in archaea and eukarya. J Biol Chem *278*, 1239-1247.

133.Trinkle-Mulcahy, L., Boulon, S., Lam, Y.W., Urcia, R., Boisvert, F.M., Vandermoere, F., Morrice, N.A., Swift, S., Rothbauer, U., Leonhardt, H., *et al.* (2008). Identifying specific protein interaction partners using quantitative mass spectrometry and bead proteomes. J Cell Biol *183*, 223-239.

134.Tripsianes, K., Madl, T., Machyna, M., Fessas, D., Englbrecht, C., Fischer, U., Neugebauer, K.M., and Sattler, M. (2011). Structural basis for dimethylarginine recognition by the Tudor domains of human SMN and SPF30 proteins. Nat Struct Mol Biol *18*, 1414-1420.

135.Urlaub, H., Raker, V.A., Kostka, S., and Luhrmann, R. (2001). Sm protein-Sm site RNA interactions within the inner ring of the spliceosomal snRNP core structure. EMBO J *20*, 187-196.

136.Valadkhan, S. (2010). Role of the snRNAs in spliceosomal active site. RNA Biol *7*, 345-353.

137.Voss, M.D., Hille, A., Barth, S., Spurk, A., Hennrich, F., Holzer, D., Mueller-Lantzsch, N., Kremmer, E., and Grasser, F.A. (2001). Functional cooperation of Epstein-Barr virus nuclear

antigen 2 and the survival motor neuron protein in transactivation of the viral LMP1 promoter. J Virol *75*, 11781-11790.

138. Wahl, M.C., Will, C.L., and Luhrmann, R. (2009). The spliceosome: design principles of a dynamic RNP machine. Cell *136*, 701-718.

139. Wan, L., Battle, D.J., Yong, J., Gubitz, A.K., Kolb, S.J., Wang, J., and Dreyfuss, G. (2005). The survival of motor neurons protein determines the capacity for snRNP assembly: biochemical deficiency in spinal muscular atrophy. Mol Cell Biol *25*, 5543-5551.

140. Williams, B.Y., Hamilton, S.L., and Sarkar, H.K. (2000). The survival motor neuron protein interacts with the transactivator FUSE binding protein from human fetal brain. FEBS Lett *470*, 207-210.

141. Winkler, C., Eggert, C., Gradl, D., Meister, G., Giegerich, M., Wedlich, D., Laggerbauer, B., and Fischer, U. (2005). Reduced U snRNP assembly causes motor axon degeneration in an animal model for spinal muscular atrophy. Genes Dev *19*, 2320-2330.

142. Wirth, B., Herz, M., Wetter, A., Moskau, S., Hahnen, E., Rudnik-Schoneborn, S., Wienker, T., and Zerres, K. (1999). Quantitative analysis of survival motor neuron copies: identification of subtle SMN1 mutations in patients with spinal muscular atrophy, genotype-phenotype correlation, and implications for genetic counseling. Am J Hum Genet *64*, 1340-1356.

143. Wiznerowicz, M., and Trono, D. (2003). Conditional suppression of cellular genes: lentivirus vector-mediated drug-inducible RNA interference. J Virol *77*, 8957-8961.

144. Xu, H., Pillai, R.S., Azzouz, T.N., Shpargel, K.B., Kambach, C., Hebert, M.D., Schumperli, D., and Matera, A.G. (2005). The C-terminal domain of coilin interacts with Sm proteins and U snRNPs. Chromosoma *114*, 155-166.

145. Yamazaki, T., Chen, S., Yu, Y., Yan, B., Haertlein, T.C., Carrasco, M.A., Tapia, J.C., Zhai, B., Das, R., Lalancette-Hebert, M., *et al.* (2012). FUS-SMN protein interactions link the motor neuron diseases ALS and SMA. Cell reports *2*, 799-806.

146. Yong, J., Golembe, T.J., Battle, D.J., Pellizzoni, L., and Dreyfuss, G. (2004). snRNAs contain specific SMN-binding domains that are essential for snRNP assembly. Mol Cell Biol *24*, 2747-2756.

147. Yong, J., Kasim, M., Bachorik, J.L., Wan, L., and Dreyfuss, G. (2010). Gemin5 delivers snRNA precursors to the SMN complex for snRNP biogenesis. Mol Cell *38*, 551-562.

148. Young, P.J., Day, P.M., Zhou, J., Androphy, E.J., Morris, G.E., and Lorson, C.L. (2002a). A direct interaction between the survival motor neuron protein and p53 and its relationship to spinal muscular atrophy. J Biol Chem *277*, 2852-2859.

149. Young, P.J., Francis, J.W., Lince, D., Coon, K., Androphy, E.J., and Lorson, C.L. (2003). The Ewing's sarcoma protein interacts with the Tudor domain of the survival motor neuron protein. Brain research Molecular brain research *119*, 37-49.

150. Young, P.J., Jensen, K.T., Burger, L.R., Pintel, D.J., and Lorson, C.L. (2002b). Minute virus of mice NS1 interacts with the SMN protein, and they colocalize in novel nuclear bodies induced by parvovirus infection. J Virol *76*, 3892-3904.

151. Zhang, R., So, B.R., Li, P., Yong, J., Glisovic, T., Wan, L., and Dreyfuss, G. (2011). Structure of a key intermediate of the SMN complex reveals Gemin2's crucial function in snRNP assembly. Cell *146*, 384-395.

152. Zhang, Z., Lotti, F., Dittmar, K., Younis, I., Wan, L., Kasim, M., and Dreyfuss, G. (2008). SMN deficiency causes tissue-specific perturbations in the repertoire of snRNAs and widespread defects in splicing. Cell *133*, 585-600.

153. Zhao, D.Y., Gish, G., Braunschweig, U., Li, Y., Ni, Z., Schmitges, F.W., Zhong, G., Liu, K., Li, W., Moffat, J., *et al.* (2016). SMN and symmetric arginine dimethylation of RNA polymerase II C-terminal domain control termination. Nature *529*, 48-53.

# 9     Publication list

1. Archana B. Prusty*, **Rajyalakshmi Meduri***, Bhupesh K. Prusty, Jens Vanselow, Andreas Schlosser, & Utz Fischer. 2016. *An elaborate safeguarding system prevents Sm protein aggregation and ensures UsnRNP homeostasis.* (* shared equal authors; to be submitted)

2. Maritta Küspert, **Rajyalakshmi Meduri**, Andria Pelava, Loren Gibson, Zhao Zhao, Raissa Schor, Mario Amend, Andreas Schlosser, Nicholas Watkins and Utz Fischer. 2016. *Inhibition of ribosome production by the sequestration of the ribosome biogenesis factor GRWD1.* (to be submitted)

3. Rajanikanth V, Sharma AK, **Rajyalakshmi M**, Chandra K, Chary KV, Sharma Y. 2015. *Liaison between myristoylation and cryptic EF-hand motif confers Ca(2+) sensitivity to neuronal calcium sensor-1.* Biochemistry. 54(4): 1111-22.

4. Rajanikanth V, Srivastava SS, Singh AK, **Rajyalakshmi M**, Chandra K, Aravind P, Sankaranarayanan R, Sharma Y. 2012. *Aggregation-prone near-native intermediate formation during unfolding of a structurally similar nonlenticular βγ-crystallin domain.* Biochemistry. 51(43): 8502-13.

# 10   Curriculum Vitae

Rajyalakshmi Meduri
B130, RG Fischer
Department of Biochemistry
Biocenter, University of Wuerzburg
Am Hubland
Wuerzburg, 97074
mail: meduri.rajyalakshmi@stud-mail.uni-wuerzburg.de, raji070986@gmail.com

## CURRENT POSITION

PhD student in Department of Biochemistry under the supervision of Prof. Dr. Utz Fischer at University of Wuerzburg, Germany.

*Topic of research:* Assembly of macromolecular machines *in vivo*

## RESEARCH EXPERIENCE AND TRAINING ACQUIRED

*Molecular and Cell Biology:* Cloning and purification of plasmids, recombinant protein expression (bacterial and mammalian cells), purification of tagged proteins via chromatographic or immunoprecipitation approaches, subcellular fractionation, *in vitro* and *in vivo* protein-RNA cross-linking, Western blotting, metabolic labeling, gradient centrifugation; *Biophysical techniques:* Fluorescence Spectroscopy, Circular Dichroism Spectroscopy.

## FELLOWSHIPS AWARDED AND ACHIEVEMENTS

- GSLS career development fellowship, University of Wuerzburg *(2016)*.
- GSLS fellowship for persuing PhD in Department of Biochemistry under RG Fischer, University of Würzburg *(2012)*.
- Awarded **CSIR Junior Research Fellowship** an all over India rank of 45 and was declared eligible for Lectureship in the subject of Life Sciences *(2011)*.
- **GATE** qualified with **92.74 percentile** and eligible for availing assistantship governed by MHRD, GOI for doing research in life sciences *(2010)*.
- Received 'Shikshana Shilpi Shri P. Mallikarjunappa Memorial **Gold Medal** for having secured the highest marks in Physical Chemistry, Bachelors degree exams held during May 2007, Bangalore University, India.
- Awarded **sixth rank** in Bachelors degree by the Bangalore University, India.
- Awarded prize for standing **first in Preliminary Masters degree** and in **Physiology** in the University examination held in July 2008 by Kasturba Medical College, Manipal, India.
- Received **'Certificate of Merit'** for reasons of outstanding academic performance and for being the top **0.1%** of successful candidates of Delhi Secondary School Examination 2002.

## PAPERS PUBLISHED

1. Rajanikanth V, Sharma AK, **Rajyalakshmi M**, Chandra K, Chary KV, Sharma Y. 2015. *Liaison between myristoylation and cryptic EF-hand motif confers Ca(2+) sensitivity to neuronal calcium sensor-1*. Biochemistry.  54(4): 1111-22.
2. Rajanikanth V, Srivastava SS, Singh AK, **Rajyalakshmi M**, Chandra K, Aravind P, Sankaranarayanan R, Sharma Y. 2012. *Aggregation-prone near-native intermediate*

*formation during unfolding of a structurally similar nonlenticular βγ-crystallin domain.* Biochemistry. 51(43): 8502-13.

## MANUSCRIPTS UNDER PREPARATION

1. Archana B. Prusty\*, **Rajyalakshmi Meduri\***, Bhupesh K. Prusty, Jens Vanselow, Andreas Schlosser, & Utz Fischer. 2016. *An elaborate safeguarding system prevents Sm protein aggregation and ensures UsnRNP homeostasis.* (\* shared equal authors; to be submitted)
2. Maritta Küspert, **Rajyalakshmi Meduri**, Andria Pelava, Loren Gibson, Zhao Zhao, Raissa Schor, Mario Amend, Andreas Schlosser, Nicholas Watkins and Utz Fischer. 2016. *Inhibition of ribosome production by the sequestration of the ribosome biogenesis factor GRWD1.*

## ACADEMIC AND RESEARCH BACKGROUND

- ➢ **Doctor of Philosophy** in the Department of Biochemistry under RG Fischer funded by GSLS, University of Würzburg, Germany. (*2012- present*)
- ➢ **Project Junior Research Fellow** in Biophysics Unit at Center for Cellular and Molecular Biology, Hyderabad, India. (*2010-12*)
- ➢ **Master of Science** in **Medical Biochemistry** with an aggregate of **74.25**% from Kasturba Medical College, Manipal University, Manipal, India. (*2007-10*)
- ➢ **Bachelor of Science** in Chemistry, Botany, Zoology with an aggregate of **93.4**% from Mount Carmel College, Bangalore University, Bangalore, India. *(2004-07)*
- ➢ **AISSCE (10+2)** with an aggregate of **84.2**% from Andhra Education Society Senior secondary School, Janakpuri, New Delhi. *(2002-04)*
- ➢ **AISSE (10)** with an aggregate of **88.4**% from Andhra Education Society Senior secondary School, Janakpuri, New Delhi. *(2001-02)*

## CONFERENCES ATTENDED

- ➢ Presented a speed talk and poster on *'Mechanistic dissection of the early phase of UsnRNP biogenesis uncovers a role of ribosomes in assembly and RNP homeostasis'* at 40th FEBS Congress in Berlin, Germany (2015).
- ➢ Presented poster on *'UsnRNP riddles resolved: An elaborate interplay of a macromolecular machine and an assembly chaperone'* at 10th Eureka GSLS Symposium in Wuerzburg, Germany (2015).
- ➢ Presented poster on *'The SMN interactome - Novel interactors of the Survival Motor Neuron protein'* at 9th Eureka GSLS Symposium in Wuerzburg, Germany (2014).

## PERSONAL DETAILS

Gender              Female
Nationality         Indian
Date of birth       7th, September, 1986
Marital status      Single


Date, Place:
Signature: